



**Analytical Models for Probabilistic Detection Coverage and Sink  
Connectivity in Wireless Sensor Networks**

**Pakpoom Hoyingcharoen**

**A Thesis Submitted in Fulfillment of the Requirements for the  
Degree of Doctor of Philosophy in Electrical Engineering  
Prince of Songkla University**

**2020**

**Copyright of Prince of Songkla University**



**Analytical Models for Probabilistic Detection Coverage and Sink  
Connectivity in Wireless Sensor Networks**

**Pakpoom Hoyingcharoen**

**A Thesis Submitted in Fulfillment of the Requirements for the  
Degree of Doctor of Philosophy in Electrical Engineering**

**Prince of Songkla University**

**2020**

**Copyright of Prince of Songkla University**

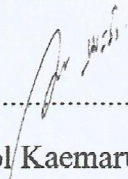
**Thesis Title** Analytical Models for Probabilistic Detection Coverage and Sink Connectivity in Wireless Sensor Networks

**Author** Mr. Pakpoom Hoyingcharoen

**Major Program** Electrical Engineering

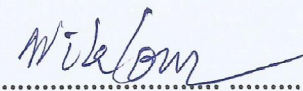
**Major Advisor**


.....  
(Assoc. Prof. Dr. Wiklom Teerapabkajorndet)

**Examining Committee :**



.....Chairperson

(Dr. Kamol Kaemarungsi)



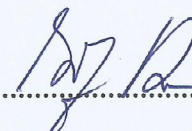
.....Committee

(Assoc. Prof. Dr. Wiklom Teerapabkajorndet)



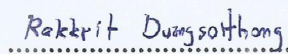
.....Committee

(Assoc. Prof. Dr. Nattha Jindapetch)



.....Committee

(Asst. Prof. Dr. Kusumal Chalermyanont)



.....Committee

(Asst. Prof. Dr. Rakkrut Duangsoithong)

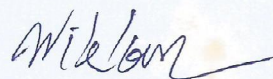
The Graduate School, Prince of Songkla University, has approved this thesis as fulfillment of the requirements for the Doctor of Philosophy Degree in Electrical Engineering

.....  
(Prof. Dr. Damrongsak Faroongsarng)

Dean of Graduate School



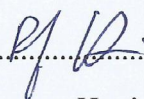
This is to certify that the work here submitted is the result of the candidate's own investigations. Due acknowledgement has been made of any assistance received.



.....Signature

(Assoc. Prof. Dr. Wiklom Teerapabkajorndet)

Major Advisor



.....Signature

(Mr. Pakpoom Hoyingcharoen)

Candidate



I hereby certify that this work has not been accepted in substance for any degree, and is not being currently submitted in candidature for any degree.

  
.....Signature

(Mr. Pakpoom Hoyingcharoen)

Candidate

<b>ชื่อวิทยานิพนธ์</b>	แบบการวิเคราะห์สำหรับพื้นที่ครอบคลุมทางความน่าจะเป็นของการตรวจจับและความสามารถในการเชื่อมต่อจุดรับข้อมูลในเครือข่ายเซนเซอร์ไร้สาย
<b>ผู้เขียน</b>	นายภาคภูมิ หอยิ่งเจริญ
<b>สาขาวิชา</b>	วิศวกรรมไฟฟ้า
<b>ปีการศึกษา</b>	2563

### บทคัดย่อ

เพื่อที่จะใช้งานเครือข่ายเซนเซอร์ไร้สายได้อย่างมีประสิทธิภาพ ไม่เพียงแต่การปฏิบัติงานรายวันของเครือข่ายเซนเซอร์ไร้สาย ที่ควรได้รับการศึกษาและออกแบบทางด้านวิศวะที่เหมาะสม การวางแผนและออกแบบก่อนการวางเครือข่ายก็ได้รับการศึกษาและควรได้รับการค้นคว้าวิจัยด้วย วิทยานิพนธ์ฉบับนี้ได้หาสมการคณิตศาสตร์ 2 สมการ สมการที่หนึ่งสำหรับการหาค่าการครอบคลุมทางความน่าจะเป็นของการตรวจจับโดยเฉลี่ย และอีกสมการหนึ่งสำหรับจำนวนเส้นทางโดยเฉลี่ยที่เซนเซอร์ไร้สายใดๆที่ไม่สามารถการเชื่อมต่อจุดรับข้อมูลได้โดยตรง จะสามารถการเชื่อมต่อจุดรับข้อมูลได้ วิทยานิพนธ์ฉบับนี้อยู่บนสมมติฐานว่ารูปแบบของการตรวจจับและรูปแบบของการสื่อสารต่างกัน โดยรูปแบบของการตรวจจับจะคล้ายเกาะเขียน เป็นสมการของระยะทางระหว่างเซนเซอร์กับวัตถุที่จะตรวจจับ ในขณะที่รูปแบบของการสื่อสารเป็นวงกลมที่ภายในวงกลมสื่อสารได้แน่นอน 100 เปอร์เซ็นต์ โดย 2 สมการที่หาออกมาในวิทยานิพนธ์ฉบับนี้พิจารณาสถานการณ์ที่มีจำนวนเซนเซอร์จำกัด เซนเซอร์ถูกวางแบบสุ่มด้วยความเป็นไปได้เท่ากันทุกจุด ในพื้นที่ 2 มิติขนาดจำกัด ที่เป็นสี่เหลี่ยมผืนผ้า โดยมีจุดรับข้อมูลตั้งอยู่ตรงกลางของพื้นที่ เนื่องด้วยการพิจารณาจากผลของเซนเซอร์ที่ตั้งอยู่ใกล้ขอบของพื้นที่การวางเครือข่ายเซนเซอร์ไร้สาย สมการทั้ง 2 แม่นยำมากเมื่อเทียบกับผลการจำลองการวางเซนเซอร์ในโปรแกรมแมทแล็บในสถานการณ์ต่างๆ โดยสมการสำหรับการหาค่าการครอบคลุมทางความน่าจะเป็นของการตรวจจับโดยเฉลี่ยมีผลต่างไม่เกินประมาณ 2.5 เปอร์เซ็นต์จากผลการจำลอง ในขณะที่สมการด้านการสื่อสารกับจุดรับข้อมูลแทบได้ผลตรงกับผลการจำลองในกรณีที่เหมาะสมในการใช้งานจริง

งานในวิทยานิพนธ์ฉบับนี้สามารถนำไปใช้ในการทำนายระดับการครอบคลุมและการสื่อสารกับจุดรับข้อมูลที่เกิดจากการวางเซนเซอร์แบบสุ่มด้วยความเป็นไปได้เท่ากันทุกจุด สำหรับจำนวนเซนเซอร์จำกัด ในพื้นที่ 2 มิติขนาดจำกัด สมการทั้ง 2 ยังสามารถหาค่าตัวแปรต่างๆที่ทำให้เกิดระดับการครอบคลุมและการสื่อสารที่ต้องการได้โดยใช้ค่าจากกราฟ สมการทั้ง 2 เหมาะกับการใช้

ในการขยายขนาดเครือข่ายไปเรื่อยๆจากการวางเซนเซอร์แบบเป็นกลุ่มในพื้นที่สี่เหลี่ยมจัตุรัส สมการสำหรับการหาค่าการครอบคลุมทางความน่าจะเป็นของการตรวจจับโดยเฉลี่ยใช้ได้กับรูปแบบของการตรวจจับอื่นๆที่เป็นสมการที่ขึ้นกับระยะทางระหว่างเซนเซอร์กับวัตถุที่จะตรวจจับ เมื่อพิจารณาการครอบคลุมและการสื่อสารพร้อมกัน วิทยานิพนธ์ฉบับนี้แสดงผลออกมาว่าความสัมพันธ์ของทั้ง 2 ไม่ตรงๆแบบ 1 ต่อ 1 สุดท้ายสมการทั้ง 2 สามารถนำไปใช้ในการวางแผนการนอนของเซนเซอร์แบบอิสระ นำไปใช้ในการวิเคราะห์ความสารถในการทนทานของเครือข่ายในกรณีที่เซนเซอร์ตายแบบอิสระปละสุ่ม ใช้ในการลดต้นทุนในการติดตั้งเครือข่ายให้มากที่สุดจากการพิจารณาการใช้เซนเซอร์ชนิดต่างๆ ที่จะถูกวางแบบสุ่มด้วยความเป็นไปได้เท่ากันทุกจุด

**คำสำคัญ** การครอบคลุมของการตรวจจับโดยเฉลี่ย ค่าการสื่อสารไปยังจุดรับข้อมูลโดยเฉลี่ย พื้นที่จำกัด รูปแบบการตรวจจับแบบความน่าจะเป็น สมการคณิตศาสตร์ เครือข่ายเซนเซอร์ไร้สาย

**Thesis Title** Analytical Models for Probabilistic Detection Coverage and Sink Connectivity in Wireless Sensor Networks  
**Author** Mr. Pakpoom Hoyingcharoen  
**Major Program** Electrical Engineering  
**Academic Year** 2020

## ABSTRACT

To efficiently employ WSNs, not only should the day-to-day operations of WSNs be studied and properly engineered, pre-deployment planning and design for sensor placement have been and should be investigated as well. This dissertation derives two mathematical formulae. One mathematical expression is for the expected probabilistic detection coverage, and the other is for the expected degree of sink connectivity for any sensor node (SN) that cannot directly transmit to the sink. This dissertation assumes that the sensing model and the connectivity models are different. The sensing model is Gaussian-like and a function of distance away from the sensor node, while the connectivity model is a binary disk. The two mathematical models derived in this dissertation consider a scenario where a finite number of object-detecting sensors are independently and uniformly distributed at random in a finite 2-D rectangular plane of which a sink is located at the center. With consideration of border effects, the striking accuracy of the formulae was demonstrated by comparing the numerical results from the proposed mathematical models with results from MATLAB simulations of random SN placement in uniform manner in various scenarios. To be exact, the proposed model for the expected probabilistic detection coverage is accurate within about 2.5 percent of the simulation results, while the sink connectivity model, in pragmatic scenarios, is practically exactly the same as the simulation.

The work in this dissertation can be used to predict the levels of coverage and sink connectivity of random SN placements in uniform manner for a given number of deployed SNs and a given dimension of the 2-D deployment area (DA). It can determine values of related parameters for specific degrees of coverage and sink connectivity using graphs. It is apt for scalability in clustered square WSNs. The model for the expected probabilistic detection coverage is applicable for other sensing models which are functions of the distance between an SN and the object to be detected. When examining both coverage and connectivity together, the dissertation shows that the relationship between coverage and connectivity is not straightforward. Finally, the formulae can be utilized in planning uncoordinated node scheduling schemes, analyzing the fault tolerance of networks in which the sensor nodes independently and randomly die, and optimizing the deployment cost from different sets of a finite number of homogeneous SNs that are uniformly and randomly deployed.

**Keywords** Expected detection coverage, Expected sink connectivity, Finite field, Probabilistic sensing model, Analytical model, Wireless sensor networks



## ACKNOWLEDGEMENTS

I would like to thank my mentor and advisor, Associate Professor Dr. Wiklom Teerapabkajorndet for his support, time, and guidance while I was doing my doctoral studies. His recommendations made me become more aware of my mistakes and helped me learn to improve myself. I also would like to thank him for giving me the opportunity to do my doctoral studies under his supervision.

I would like to thank Associate Professor Dr. Nattha Jindapetch for her patience, encouragement, and guidance while I was lost. I will always remember her generosity throughout the process of my doctoral studies.

I also would like to thank Dr. Kamol Kaemarungsi, the head of my dissertation committee and other dissertation committee members, Assistant Professor Dr. Kusumal Chalermyanont and Dr. Rakkrit Duangsoithong and for their time, valuable feedback, and guidance for my research work.

I would like to thank the Telecommunication Research and Industrial Development Institute (TRIDI), National Telecommunications Commission of Thailand for providing the grant for my doctoral studies and giving me the opportunity to begin my studies.

I would like to thank Graduate School of Prince of Songkla University for their support and help all through the process.

Special thanks to the faculty members and staff at the department of Electrical Engineering at Prince of Songkla University for their friendship, kindness, generosity, guidance, and help during the years of my doctoral studies.

Finally, I would like to thank my father, mother, and sisters for being constant supporters who have always given me love and encouragement for all those years.

Pakpoom Hoyingcharoen

## Table of Contents

List of Figures	xi
List of Abbreviations	xiv
บทคัดย่อ	v
Abstract	vii
Chapter 1 Introduction	1
1.1 Background Overview	1
1.2 Motivations	3
1.3 Problem Statement	4
1.4 Objectives of the Research	5
1.5 Scope of the Research	6
1.6 Contributions	6
Chapter 2 Background	8
2.1 Sensor Placement in WSNs and its Impacts	8
2.1.1 Coverage and Energy Consumption	9
2.1.2 Cost, Coverage, and Energy Consumption	10
2.1.3 Fault Tolerance ( $k$ -coverage and $k$ -connectivity)	10
2.1.4 Routing and Delay	11
2.1.5 Detection Probability	12
2.2 Research Overview on Wireless Sensor Placement	13
2.2.1 Related Work on Analytical Models on Sensing Coverage	14
2.2.2 Related Work on Analytical Models on Connectivity	17
2.2.3 Related Work on Analytical Models on Joint Sensing Coverage and Connectivity	17
2.3 Open Challenges	18
Chapter 3 Expected Degree of Sink Connectivity	20
3.1 Degree of Sink Connectivity in 2-D Rectangular Plane	20
3.2 Order Statistics	21
3.3 Expected Degree of Sink Connectivity by Order Statistics	22
Chapter 4 Expected Probabilistic Detection Coverage	28
4.1 Detection Probability and its Expectation	28
4.2 Probability Distribution of $k$	29
4.3 Probability Distribution of $r$	35
4.3.1 Finding $\varepsilon_{a,m,k}$	36
4.3.2 Finding $\varepsilon_{b,m,k}$	38
4.3.3 Finding $\varepsilon_{c,m,k}$	39

Chapter 5	Verifications, Applications, and Discussions	49
5.1	Simulation Design for the Verification of Expected Detection Probability	49
5.2	Simulation Implementation for the Verification of Expected Detection Probability	50
5.3	Verification of Expected Detection Probability	50
5.4	Simulation Design for the Verification of Expected Degree of Sink Connectivity	52
5.5	Simulation Implementation for the Verification of Expected Degree of Sink Connectivity	53
5.6	Verification of Expected Degree of Sink Connectivity	53
5.7	Discussions and Applications of the Models	57
Chapter 6	Conclusions, Limitations, and Future Work	62
6.1	Conclusions	62
6.2	Limitations	63
6.3	Future Work	63
	Bibliography	65
	Vitae	74

## List of Figures

Figure 2.1	A Typical Wireless Sensor Network	8
Figure 2.2	Two different SN placements with different coverage & energy consumption	9
Figure 2.3	Two different SN placements with different cost, coverage, energy consumption	10
Figure 2.4	Network with $k$ -Coverage of a target point where $k = 4$	11
Figure 2.5	Network with $k$ -Connectivity where $k = 4$	11
Figure 2.6	Impacts of SN placement on network connectivity and routing	12
Figure 2.7	Sensor nodes at different positions have different detection probabilities	12
Figure 3.1	Overlap of the two circles where closer-to-sink NNs lie	21
Figure 3.2	Areas for CDF computation when $r_t < s \leq a/2$	24
Figure 3.3	Areas for CDF computation when $a/2 < s \leq b/2$	24
Figure 3.4	Areas for CDF computation when $b/2 < s \leq (1/2)\sqrt{a^2 + b^2}$	25
Figure 4.1	Circular DR of radius $d_s$ when the AP is midway inside the DA	29
Figure 4.2	DR where the circle intersects the DA	30
Figure 4.3	3 SRs: $a$ , $b$ , and $c$ of an $p \times q$ rectangular DA	30
Figure 4.4	The area in which the deployed SNs could only be if $A = a$ . It is the entire area of the DA minus the areas of the four corners	32
Figure 4.5	The area in which the SNs could only be when $A = b$	33
Figure 4.6	The area in which the SNs could only be when $A = c$	33
Figure 4.7	The DR is not a complete circle when $A = b$ . The effective DR is the area of the DR that is within the boundary of the sensing field or the DA	34



- Figure 4.8 The DR when  $A = c$  and the distance from the AP to the corner is less than  $d_s$ . The effective DR is the area of the DR that is within the boundary of the sensing field or the DA. 34
- Figure 4.9 The DR when  $A = c$  and the distance from the AP to the corner is more than  $d_s$ . The effective DR is the area of the DR that is within the boundary of the sensing field or the DA 35
- Figure 4.10 The DR whose radius is  $d_s$  and the smaller DR whose radius is  $r$  for the CDF of  $r$  when  $A = a$  37
- Figure 4.11 Noncircular overlapped DR when  $A = b$  38
- Figure 4.12 The smaller DR within the DA and the effective DR used in the computation of the CDF of  $r$  when  $A = c$ , the AP is within the distance  $d_s$  from the corner of the DA, and  $\min(u, v) \leq r \leq \max(u, v)$  40
- Figure 4.13 The smaller DR within the DA and the effective DR used in the computation of the CDF of  $r$  when  $A = c$ , the AP is further than the distance  $d_s$  from the corner of the DA, and  $0 \leq r \leq \min(u, v)$  40
- Figure 4.14 The smaller DR within the DA and the effective DR used in the computation of the CDF of  $r$  when  $A = c$ , the AP is within the distance  $d_s$  from the corner of the DA, and  $0 \leq r \leq \min(u, v)$  41
- Figure 4.15 The smaller DR within the DA and the effective DR used in the computation of the CDF of  $r$  when  $A = c$ , the AP is within the distance  $d_s$  from the corner of the DA, and  $\max(u, v) \leq r \leq \sqrt{u^2 + v^2}$  42
- Figure 4.16 The smaller DR within the DA and the effective DR used in the computation of the CDF of  $r$  when  $A = c$ , the AP is within the distance  $d_s$  from the corner of the DA, and  $\sqrt{u^2 + v^2} \leq r \leq d_s$  42
- Figure 4.17 The smaller DR within the DA and the effective DR used in the computation of the CDF of  $r$  when  $A = c$ , the AP is further than the distance  $d_s$  from the corner of the DA, and  $\min(u, v) \leq r \leq \max(u, v)$  43

Figure 4.18	The smaller DR within the DA and the effective DR used in the computation of the CDF of $r$ when $A = c$ , the AP is further than the distance $d_s$ from the corner of the DA, and $\max(u, v) \leq r \leq d_s$	44
Figure 5.1	Discrepancies between analytical estimations and the simulation results for EDP at each level of ND	51
Figure 5.2	Discrepancies between analytical estimations and the simulation results at each level of ADP from simulations	52
Figure 5.3	Percentage differences between analytical values and simulation results for EDSC at each level ND for various $r_t$ and fixed DA 40x40	54
Figure 5.4	Percentage differences between analytical values and simulation results for EDSC at each level ND for square DA of various sizes and $r_t = 10$	55
Figure 5.5	Percentage differences between analytical values and simulation results for EDSC at each level ND for DA of various shapes and $r_t = 10$	56
Figure 5.6	Percentage differences between analytical values and simulation results for EDSC at different average degrees of SC for DA 40x40 and $r_t = 10$	56
Figure 5.7	EDP vs ND for various DA sizes with $d_s = 10$ and $\alpha_s = 4$	58
Figure 5.8	EDP vs number of deployed SNs for various DA sizes with $d_s = 10$ and $\alpha_s = 4$	59
Figure 5.9	EDSC vs number of deployed SNs for DA 40x40 with $r_t = 10, 12$	60
Figure 5.10	EDSC vs ND for various DA sizes with $r_t = 10$	60
Figure 5.11	EDP vs EDSC for DA 40x40 with $r_t = 10$ and various values of $d_s$ and $\alpha_s$	61

## List of Abbreviations

ADP	Average Detection Probability
AP	Arbitrary Point
DA	Deployment Area
DP	Detection Probability
DR	Detection Region
EDP	Expected Detection Probability
EDSC	Expected Degree of Sink Connectivity
EM	Electromagnetic
ND	Node Density
NN	Neighboring Node
NoCSNN	Number of Closer-to-Sink Neighboring Node
SC	Sink Connectivity
SN	Sensor Node
SR	Sub-Region
WSN	Wireless Sensor Network

## CHAPTER 1

### Introduction

For a random placement of a finite number of SNs in a finite rectangular 2-D deployment area (DA) in a WSN, this dissertation derives two mathematical expressions. One is for computing the expected detection probability (EDP) at any arbitrary point (AP) in the DA. The other is for calculating the expected degree of sink connectivity or the number of communication paths to the sink for sensor nodes (SNs) that cannot directly wirelessly transmit the information to it. This chapter introduces WSNs and the fundamental services they provide, namely sensing coverage and wireless connectivity, along with the corresponding benefits of having accurate estimates of these two qualities of service and the assessment problems of these two when a finite number of SNs are randomly placed. These lead to the overall motivations and the subsequent problem statement for this dissertation. Then the objectives and the scope of the research in this dissertation are presented. In closing of this chapter, the contributions of this thesis are then explained and followed by the outline of the dissertation.

### 1.1 Background Overview

Wireless Sensor Networks are networks of low-cost and low-power autonomous sensors that can wirelessly communicate with one another. Via other SNs in a multi-hop communication fashion, the SNs send the information they have sensed or detected back to a base station. Depending on the application of that particular WSN, the SNs in the network receive or detect the information of interest by transducing heat or humidity or chemical or biological compounds or electromagnetic (EM) or acoustic waves or any other physical quantity of interest. A number of applications of WSNs in military surveillance, security, industrial and environmental monitoring, underwater detections, and border monitoring employ the SNs that detect electromagnetic or acoustic signals radiated from the object of interest.

For those physical quantities, an inverse-square law states that the intensity of such physical quantities is inversely proportional to the square of the distance from the source of those physical quantities. There are also random electromagnetic or acoustic noises that can interfere with the sensing or the detection of the SNs. Combining these two physical phenomena, for those applications of WSNs, there should be increasing uncertainty for an SN to detect the object of interest as the distance between the SN and the object grows. Specifically, this uncertainty in detection or sensing can be mathematically modeled as a detection probability (DP) function. This DP function is a decreasing function of the distance between a SN and the object. In this function or mathematical model, the detection capability or probability of the SNs decreases as the object to be detected that radiates the signals is further away from the SNs. Another effect of the unavoidable interfering noises on the



sensing model is that, beyond a certain distance between an SN and the signal-emitting object of interest, on average these noises can overwhelm the signals of interest. As a result, the SN can no longer sense or detect the object or the DP in the sensing model is zero beyond a certain distance.

For this kind of SNs and their corresponding range-limited and decreasing DP of the sensing model, the amount of overall sensing coverage should not be the percentage of the area being covered by the SNs deployed. The reason is because it would not capture the essence of the uncertainty of sensing coverage in every spot in the DA. In the traditional binary sensing model where every spot within the sensing range of a SN is covered with 100% probability and zero everywhere else, adopting the percentage of the covered area as the benchmark of the total sensing coverage of the WSN coverage is perfectly reasonable. There is no uncertainty of sensing or detection within the sensing range of the SNs in the binary sensing model. On the other hand, when the DP within the sensing range of a SN is not 100%, the overall sensing coverage in the DA should also reflect this. It should not be the percentage of area that is covered with 100% certainty. In fact, the overall sensing coverage for the kind of sensing model with decreasing DP over the distance should also be a DP or expected DP of any AP in the DA.

This type of pre-deployment awareness for the overall picture of uncertainty in sensing coverage can assist WSN planners and implementers in accurately assessing risks associated with it and weigh its costs and benefits from increasing the level of DP coverage at the expense of higher deployment cost. Not only is this overall DP sensing information useful for conducting risk assessment and cost-benefit analysis, it also provides information needed for planning other measures in dealing with the resulting coverage liability.

Besides sensing or detection, another crucial and fundamental operation in a WSN is SNs sending the information they have sensed to the base station or the sink of the network. Since SNs in the WSNs are typically low-cost and low-power, in order for the WSNs to function as intended, majority of the SNs have to send this information to sink of the network in a multi-hop communication fashion. Each SN has a limited communication range. Only those with the sink within its communication range can send the data directly to the sink in a single hop. The rest of the SNs have to rely on others to relay or route the data back to the sink.

The further the SNs are from the sink, the higher number of communication hops they have to take. This could increase the issue of the communication unreliability. This reason is because each hop of communication can be broken either due to the receiving-end SN dies or the severe condition of the naturally time-varying wireless channel. The more hops it takes each SN to send the data back to the sink, the more likely that path of communication will be broken down. Having extra communication paths reserved in the routing table of each SN that is far from the sink could deal with this problem of increasing unreliability. In other words, the extra degrees of sink connectivity (SC) can provide fault tolerance or routing resilience to the communication aspect of the WSNs.

Knowing the degree of SC before the SN deployment not only can pre-ascertain and devise fault tolerance capability, it also can help design efficient routing

protocols and determine the possibility of communication traffic congestion. Efficient routing protocols need, along with other information, accurate knowledge about the number of available communication paths. Traffic congestion can increase as the number of available communication paths rises in case of flooding of information in the network. Knowing the credible pre-deployment overall degree of SC in the network can give the WSN operators both a better perception of the possibility of traffic congestion in a WSN and dependable information needed for the effective and efficient routing protocols.

Both sensing coverage and SC degree can be precisely determined beforehand when the SNs are deterministically placed, or after they have been deployed by having SNs exchanging their coverage and connectivity information. However, when the SN placement is random, both sensing coverage and connectivity may not be definitely determined before the deployment. They, nonetheless, can still be accurately estimated in advance with mathematical models. For overall sensing coverage that is the DP at any AP in the DA from random SN placement, precise prediction is impossible. Nevertheless, the expected or average DP at any AP in the DA resulted from a random placement can be accurately calculated. Likewise, it is mathematically viable to derive the expected or average degree of SC for the SNs that cannot directly transmit to the sink, even though a random SN placement makes it hard to determine the exact degree of SC in the pre-deployment phase for every SN.

## 1.2 Motivations

As alluded to earlier, sensing coverage and network connectivity are two of the fundamental concerns in designing and implementing WSNs [1]. The coverage provided by a WSN indicates its quality of monitoring or detecting service. As for connectivity, each of the WSNs typically has a sink or a base station to collect information observed by the SNs. As a result, connectivity to the sink from every SN must be required to ensure that the information obtained in all covered areas is delivered to the sink. This communication aspect is another vital and important quality of service of WSNs. In order to have an efficient WSN implementation and operation, these two quantities must be determined either in the post-deployment or the pre-deployment phase.

Previous pre-deployment analysis works, which will be discussed in Chapter 2, have analyzed and evaluated sensing coverage and connectivity in different scenarios and on a variety of assumptions. Despite all these works, challenges in modeling and determining coverage and connectivity in WSNs in the pre-deployment phase still remain. Specifically for this dissertation, the EDP at any AP in the DA and the expected degree of SC (EDSC) for SNs that cannot directly transmit to the sink are of the interest. As noted earlier, the EDP at any AP in the DA is a suitable metric for SNs that rely on electromagnetic or acoustic signals for their detection, while knowing EDSC is beneficial for routing, fault tolerance, and traffic congestion considerations.

In light of the above, this dissertation develops and proposes mathematical models for predicting both EDP at any AP in the DA and EDSC for SNs that cannot directly transmit to the sink. With consideration of border effects, the

striking accuracy of the formulae was demonstrated by the result comparisons with simulations in various scenarios. The models in this dissertation can determine values of related parameters for specific degrees of coverage and connectivity. This is useful for the pre-deployment planning stage of implementing WSNS. Because we can achieve cost efficiency for the desired expected levels of sensing coverage and sink connectivity by not over-employing SNs. Unlike previous works on joint coverage and connectivity analysis in WSNs, when examining both coverage and connectivity together, the models in this dissertation show that the relationship between coverage and connectivity is not straightforward. Furthermore, the formulae can be utilized in planning uncoordinated node scheduling schemes, analyzing the fault tolerance of networks in which the sensor nodes independently and randomly die, and optimizing the deployment cost from different sets of homogeneous SNs.

### 1.3 Problem Statement

This dissertation derives two mathematical expressions for a 2-D rectangular WSN with a finite size and a finite number of randomly placed SNs. The 2-D sensing areas are suitable for real terrestrial applications of WSNs [2, 3]. One is for the expected probabilistic detection coverage at any AP in the sensing field, and the other is for the EDSC for SNs that cannot direct transmit to the sink. These models could serve as a reference and a foundation for future test-bed experiments in real environments for any number of SNs. The dissertation assumes that a sink node is located at the center of the field, which is useful for balancing SN workload distribution. Moreover, not only do these assumptions make the work in the dissertation closer to real-life situations where the sensing field and the number of deployed SNs are finite than the asymptotic assumptions, they are also applicable for clustered WSNs of which the cluster head of each cluster is located in the middle. These clusters can be considered similar to the finite sensing field assumption in this dissertation with the centrally located sink node. All the SNs are assumed to be homogeneous with the same sensing and communication ranges. The sensing model is probabilistic, with the sensing or DP as a decreasing function of the distance away from the sensor node. The value of the DP tapers off like the Gaussian distribution. Each SN detects a target in the sensor field independently. Unlike the probabilistic sensing model, the communication model this dissertation assumes is the traditional binary disk. All the SNs are randomly and independently deployed according to the uniform distribution. The numerical results from the proposed mathematical models show that the discrepancies between the calculations from the two formulae and those from simulations are around one percent, and in some scenarios are practically zero. The high accuracy of both the mathematical models in this dissertation is aided by the consideration of border effects [4, 5, 6].

To be more specific, assumptions made in the dissertation are the following.

1. The sensing field is a finite rectangular plane of size  $p$  by  $q$  where  $p, q \geq 4$  times the sensing range of the SNs.
2. The sink node is located at the center of the DA.

3. A finite number of SNs are randomly placed according to the uniform distribution.

4. All the SNs are homogeneous. They all have the same sensing and communication models with the same sensing and communication ranges.

5. The sensing model is based on an idea that a SN detects an object from its signals [7]. These signals could be thermal energy, acoustic waves, radio waves, light waves, or magnetic field [7]. As these signals propagate over a distance before it reaches an SN, the strength of the signals weakens. As a result, the chances of detecting an object emitting these signals should decrease over the distance. To mimic this effect in the sensing model of the SNs in the coverage problem, this dissertation adopts a distance-dependent equation similar to Gaussian probability distribution. Let  $D_i(r_i)$  be the probability that SN  $i$  detects the object at distance  $r_i$  from the SN  $i$ . The equation for the probabilistic sensing model  $D_i(r_i)$  is as follows [8, 9, 10]:

$$D_i(r_i) = \begin{cases} \exp(-r_i^2/2\alpha_s^2), & 0 \leq r_i \leq d_s; \\ 0, & r_i > d_s. \end{cases} \quad (1.1)$$

A parameter,  $\alpha_s$ , similar to the standard deviation in the Gaussian distribution, determines how the DP is distributed over the distance  $r_i$ . The bigger the value of  $\alpha_s$ , the more flattened out or the more spread the value of the DP over the distance becomes. Another parameter,  $d_s$ , is the maximum sensing range beyond which the DP is zero. The rationale behind this sensing range  $d_s$ , is that, beyond a certain distance, the signal strength from the object falls below a detection threshold. Hence the SN can no longer detect the object farther than that distance.

6. Each SN detects the object independently.

7. The communication model is the traditional binary disk where connectivity exists within the communication range with probability of one. The dissertation notes that the work here with this simple assumption can serve as a basis for future works with more complicated communication models. This simple binary model also can be applied with an irregular communication model by multiplying the communication range with  $(1 - h)$  where  $h$  is the degree of irregularity as shown in [4].

## 1.4 Objectives of the Research

1.4.1 To be able to derive and propose an accurate mathematical expression of the expected detection probability at any arbitrary point in the finite 2-D rectangular deployment area of a wireless sensor network, assuming that a finite number of homogeneous SNs are placed and each SN independently detects an object with the detection probability based on a probabilistic sensing model that is a function of the distance between the SN and the object.



1.4.2 To be able to derive and propose an accurate mathematical expression of the expected degree of sink connectivity for SNs that cannot directly transmit to the sink which is located at the center of a finite 2-D rectangular deployment area of a wireless sensor work, assuming a binary communication model for the SNs and a finite number of homogeneous SNs are deployed.

1.4.3 To be able to verify the accuracy and validity of both mathematical models with simulation results.

1.4.4 To be able to analyze the causes of the discrepancies between the numerical results from the proposed mathematical models and those obtained from simulations.

1.4.5 To be able to analyze the ramifications of the numerical results produced by the proposed models.

1.4.6 To be able to show the applications of the proposed models in implementations of wireless sensor networks

## **1.5 Scope of the Research**

1.5.1 Both proposed mathematical models are based on assumptions that a finite number of homogeneous SNs are deployed in a finite 2-D rectangular sensing field or deployment area of a wireless sensor networks.

1.5.2 The sensing model of the SNs is probabilistic, a function of distance between the SN and the object to be detected, and has a finite detection or sensing range.

1.5.3 The communication model of the SNs is binary with a limited communication range, meaning a SN can communicate with other SNs within its communication range with probability of one and cannot communicate at all with other SNs outside the range.

1.5.4 The SNs are placed randomly with uniform distribution.

1.5.5 The sink of the wireless sensor network is located at the center of the deployment region.

1.5.6 The proposed models are for the calculations of the expected or average values of detection probability at an arbitrary point and degree of sink connectivity respectively. They are not for determining the detection probability value of any arbitrary point for the degree of sink connectivity of any SN.

## **1.6 Contributions**

To the best of the author's knowledge, the scientific contributions of this dissertation are summarized as follows:

- First, with consideration of border effects, to have derived an analytical expression for the EDP at any AP based on a probabilistic sensing model of a finite number of randomly and uniformly placed homogeneous SNs in a finite rectangular DA of a WSN.

- First to have obtained an analytical expression for EDSC based on a binary disk communication model for a finite number of randomly and uniformly placed homogeneous SNs that cannot directly transmit to the sink centrally located in a finite rectangular DA of a WSN.

- Contrary to the traditional relationship between coverage and connectivity [11], by numerical results from both the mathematical models, the dissertation has demonstrated that this relationship does not exist when the sensing model is probabilistic and the communication model is binary. An explanation for these results will be discussed in Chapter 5.

- Suggestion to modify the uncoordinated sleep scheduling schemes proposed by Yen, Wu, and Cheng [4] in an application of these mathematical models. The dissertation shows other potential utilities of the formulae in tracking or providing a snapshot of the degrees or fault tolerance capability of coverage and connectivity over time, and in choosing a set of homogeneous SNs that minimize the deployment cost.

The remainder of the dissertation is organized as follows. In Chapter 2, an overview of sensor placement in WSNs and its impacts, an overview of research in wireless sensor placement, and a survey of current sensing coverage and connectivity analyses in WSNs are presented. Subsequently, the analyses of the EDSC and EDP are demonstrated in Chapter 3 and 4 respectively. Chapter 5 presents the verifications of both analytical models with simulations, discussions of results, and examines the applications of the proposed models. Chapter 6 concludes this dissertation.

## CHAPTER 2

### Background

This chapter presents an overview of sensor placement in WSNs and its impacts. They are then followed by an overview of research in wireless sensor placement and a survey of current sensing coverage and connectivity analyses.

#### 2.1 Sensor Placement in WSNs and its Impacts

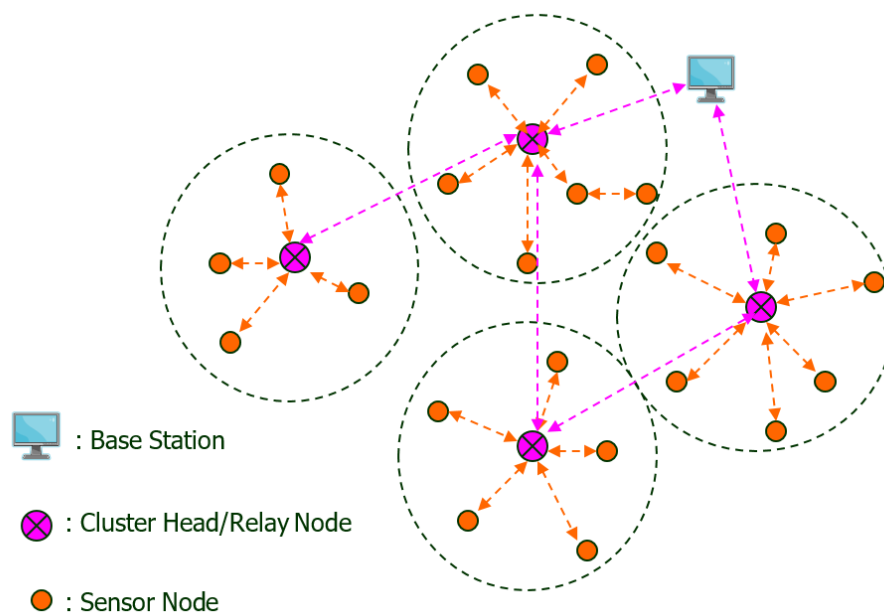


Figure 2.1. A Typical Wireless Sensor Network

A WSN is a network of sensors that communicate with one another wirelessly. A typical WSN is shown in Figure 2.1. It usually consists of three types of devices, namely sensor nodes, cluster heads or relay nodes and base stations [11, 12, 13, 14, 15, 16, 17, 18, 19, 20] [21, 22, 23, 24, 25, 26, 27, 28, 29, 30]. The duties of sensor nodes are to monitor an environment, collect data and then transmit the data back to the base station via a cluster head. Cluster heads are usually more complicated and have more computation, storage and transmission capabilities than the regular sensor nodes [14, 15, 16]. Besides the task of aggregating and then relaying data via other cluster heads back to the base station, cluster heads also could perform sensing duties if required [14, 15, 16]. The base station or the sink is then the transmission destination that collects all data packets within the network. Figure 2.1 shows four clusters within

which sensor nodes transmit their data to their cluster head. This type of network architecture is now prevalent in WSNs because of its scalability. A scalable network architecture is the one whose design can be implemented in all networks regardless of their sizes [14, 15, 16].

In terms of SN mobility, SN placement can be classified as either static or dynamic placement [30]. In dynamic placement, all three types of devices in WSNs which are sensor nodes, cluster heads or relay nodes and base stations, could reposition themselves. On the other hand, in static placement, they cannot. Static sensor placement in WSNs can either be deterministic or random [30]. Random sensor placement is carried out in the environments where deterministic sensor placement is not possible. Examples of these harsh environments are enemy territories, volcanic, and mining areas. Naturally, deterministic sensor placement is preferred to random placement whenever it is applicable [30]. The efficiency in energy consumption, network deployment cost, network coverage, fault tolerance, connectivity, routing, end-to-end delay, detection probability and even the ability by WSNs to classify objects of interest could all be enhanced or optimized via intelligent sensor placement strategies [11, 12, 13, 14, 15, 16, 17, 18, 19, 20] [21, 22, 23, 24, 25, 26, 27, 28, 29, 30]. The impacts of sensor placement on these qualities are overviewed in this section.

### 2.1.1 Coverage and Energy Consumption

In typical WSNs where data transmission occurs on a regular basis, energy of a SN is most depleted by transmission energy [31, 14, 32, 33]. As shown in Figure 2.2, both networks have the same number of SNs of six, but the one of the left has less energy consumption, and hence longer network lifetime than the one on the right, assuming all operations of both networks are the same. The reason is because all SNs are placed closer to the base station in the network on the left than the one on the right. So SNs on the left do not consume as much transmission energy as the ones in the right network. However, the left network covers a smaller area than the right one. As we can see here, sensor placement does impact coverage and energy consumption in WSNs, and they are two tradeoff qualities [11, 12, 18].

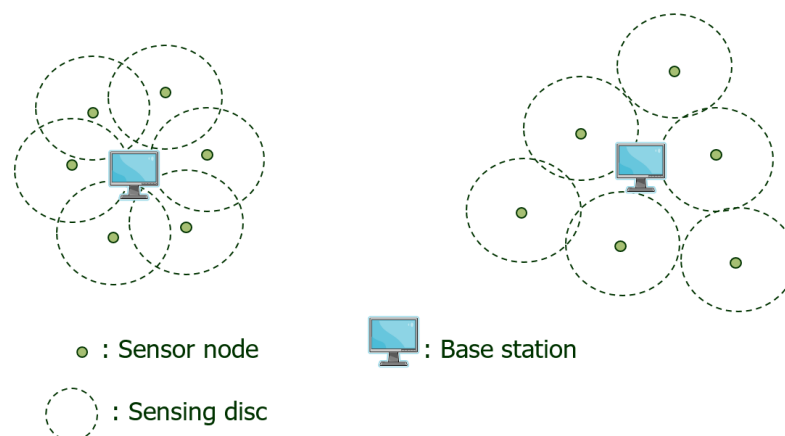


Figure 2.2. Two different SN placements with different coverage & energy consumption.

### 2.1.2 Cost, Coverage, and Energy Consumption

As shown in Figure 2.3, assuming that the sensing coverage and the transmission energy of each SN can be adjusted, for the same amount of sensing coverage, the left network when compared to the right network employs fewer SNs. Hence the left network has less SN deployment cost, but it also has shorter network lifetime because the SNs on the left have to transmit their data over longer distance and spend more energy [13, 14]. As we can see here, sensor placement does impact network cost, coverage and energy consumption.

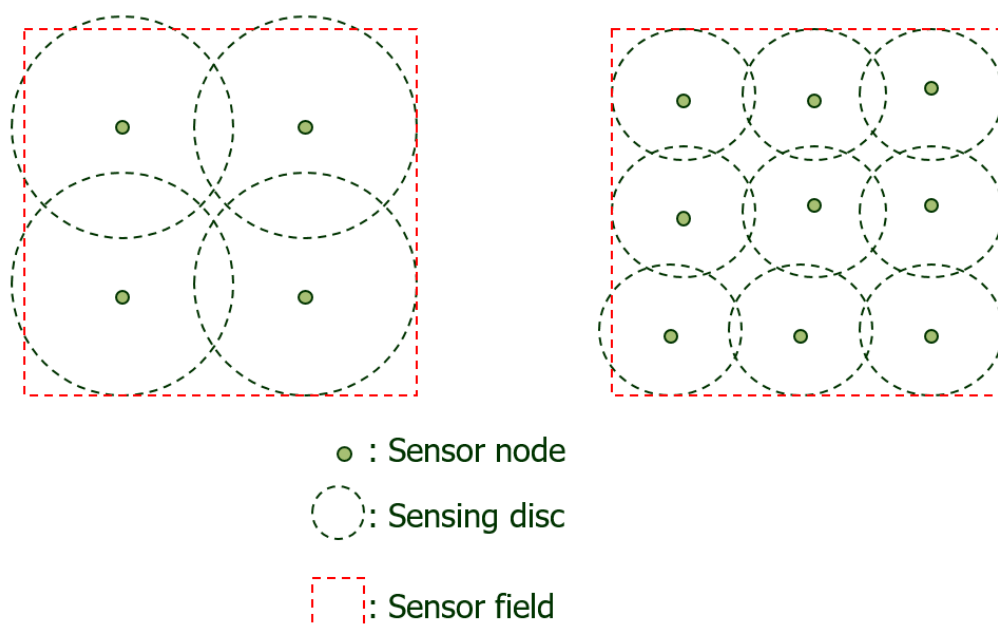


Figure 2.3. Two different SN placements with different cost, coverage, energy consumption

### 2.1.3 Fault Tolerance ( $k$ -coverage and $k$ -connectivity)

$k$ -coverage is the coverage whose existence is still guaranteed or the target point(s) of interest is still covered even after  $k - 1$  SNs have failed or been removed [11]. Figure 2.4 depicts the  $k$ -coverage of a target point where  $k = 4$ . As seen here, when any three of the four nodes that cover the target point or the target area fail, the target point or target area is still covered by one SN. Similarly,  $k$ -connectivity is the connectivity to the base station from any node that exists even after any set of  $k - 1$  SNs have failed or been removed from the network [11]. Figure 2.5 illustrates a network with  $k$ -connectivity where  $k = 3$ . When any set of two nodes fail in this network, the remaining SNs will still have at least a path to connect to the base station. As shown in Figure 2.4 and Figure 2.5, carefully planned sensor placements can establish these fault tolerant capacities in WSNs [11].



Figure 2.4. Network with  $k$ -Coverage of a target point where  $k = 4$ .

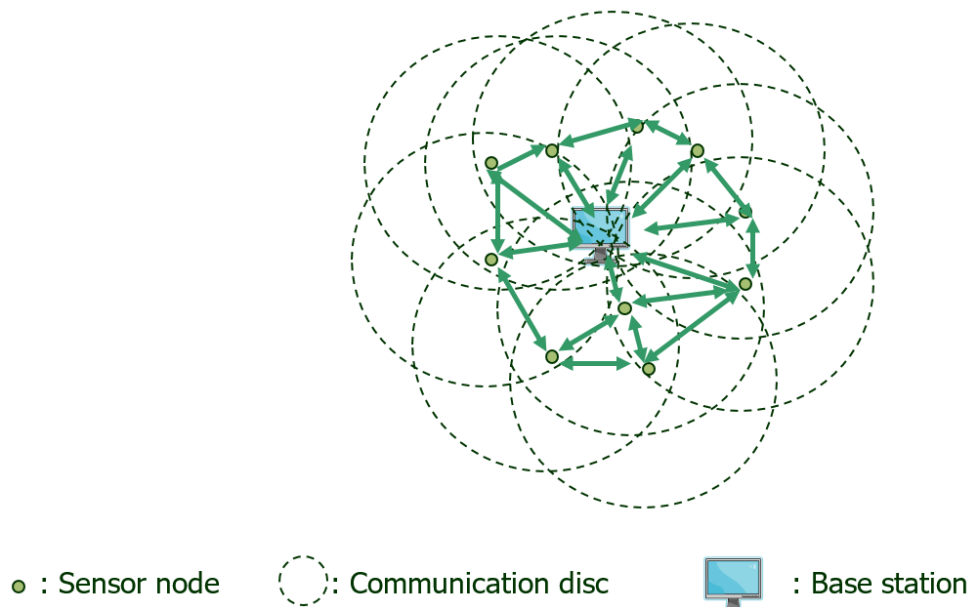


Figure 2.5. Network with  $k$ -Connectivity where  $k = 3$ .

### 2.1.4 Routing and Delay

As a result of sensor placement, SNs only have certain ways to relay their data back to the sink. Shown in Figure 2.6, one can see that each node in the network has its own specific communication route due to the limitation imposed by its position and those of its neighboring nodes. The amount of data traffic and the number of communication hops in each route are also affected by the positions of the SNs and

their transmission radii as illustrated in Figure 2.6. Since end-to-end delay of a route depends on the amount of traffic and the number of hops in it [34], one can expect the delay to be impacted by sensor placement as well.

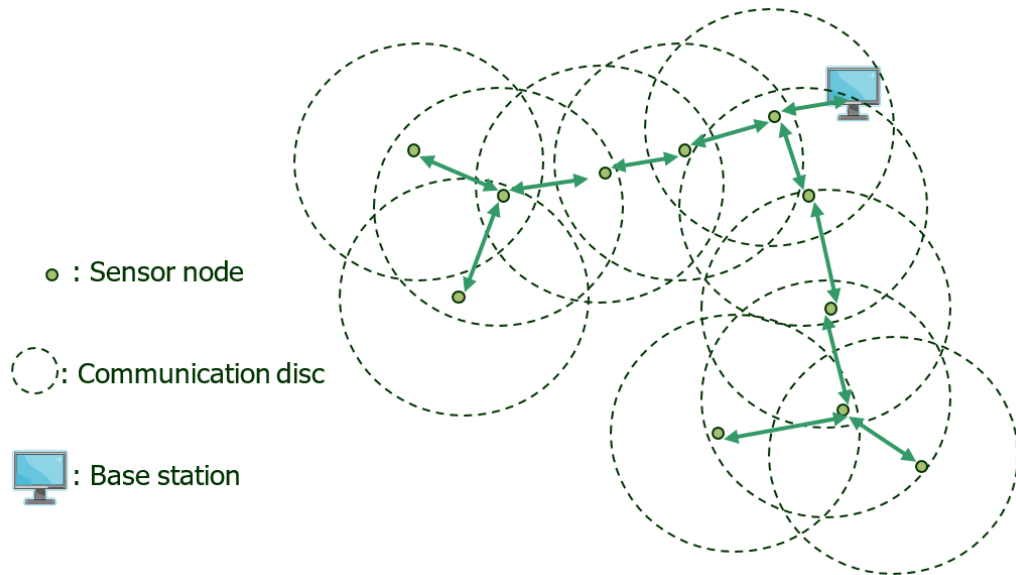


Figure 2.6. Impacts of SN placement on network connectivity and routing.

### 2.1.5 Detection Probability

Detection probability is the probability that an object of interest or an intruder is detected by a SN. This probability equals one minus the probability that none of the SNs capable of detecting the intruder detects it. The SNs that are capable of detecting the intruder are the SNs that have the intruder within its sensing or detecting range. Hence the number of these SNs and the corresponding detection probability of the intruder must depend on the SN placement. It is even more so when the detection probability of each SN depends on the distance between the SN and the target or the intruder, as noted and reasoned in Chapter 1, and as illustrated in Figure 2.7.

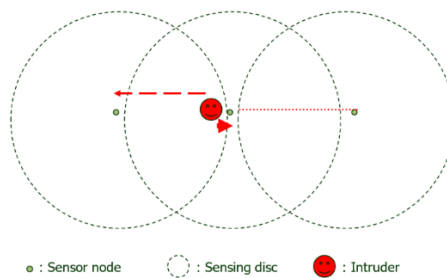


Figure 2.7. Sensor nodes at different positions have different detection probabilities

## 2.2 Research Overview on Wireless Sensor Placement

Since the inception of WSNs in 1989 [35], research in SN placement for WSNs has been focusing either on the optimization methodologies or strategies or the analytical models. As presented in the previous section, sensor placement can impact various aspects of the performance of WSNs. A deterministic placement can be optimized for a combination of these facets. Several placement optimization methodologies [11, 12, 13, 14, 15, 16, 17, 18, 19, 20] [21, 22, 23, 24, 25, 26, 27, 28, 29, 30] [36, 37, 38, 39, 40, 41, 42, 43] have been proposed to serve this purpose by taking a variety of these WSN performance aspects as optimization objectives and constraints in their sensor placement strategies. In deterministic deployment of SNs, the coverage and connectivity could be determined and guaranteed at the expense of offline SN placement design [36, 37, 38, 39, 40, 41, 42, 43]. However, in some scenarios where the deployment region is inaccessible or hazardous to human beings, SNs will have to be deployed randomly instead.

In this random deployment, both coverage and connectivity are not easily gauged. Nevertheless they both can be assessed by either a coverage or connectivity evaluation protocol [44] or an analytical model. An evaluation protocol would require the knowledge of actual SN locations and connectivity after they have been deployed and an elaborate information-exchanging scheme between the SNs to determine the coverage and connectivity resulted from random deployment [44]. It is carried out only after the deployment has taken place. It is more accurate and reflects the real network conditions. It can be used to guarantee desired levels of coverage and connectivity [44]. However, post-deployment procedures require overheads and SN energy [44]. Moreover, the protocols cannot forecast the levels of coverage and connectivity before the deployment, which is needed in employing efficient randomly-placed WSNs. These evaluation protocols can be categorized as post-deployment procedures for coverage and connectivity analyses.

Analytical models while based on random placement, on the other hand, can predict the coverage and connectivity before the actual deployment. Studies on the analytical models for SN placement also have largely been on sensing coverage and connectivity. The models mostly aim to assess the levels of coverage and connectivity for a given number of SNs deployed, the size and type of the DA, and the sensing and communication models of the SNs. Analytical models are mathematical equations that can easily and readily evaluate or predict coverage or connectivity, and can be used if only such basic information is available. They are pre-deployment calculations. The analytical models used in determining the sensing coverage and the network connectivity also could serve as a tool in designing and efficiently arranging uncoordinated SN sleep scheduling schemes in order to extend the network lifetime [4, 45, 46, 47]. The models could possibly be employed as performance benchmarks for optimized deterministic SN placement schemes. Proper optimized SN placements should at least outperform any random placement in terms of cost and quality of service proficiency. Accurate analytical models could be tools to systematically demonstrate this.

This dissertation is interested in analytical models for sensing coverage and sink connectivity in WSNs based on a uniform random static placement of a finite



number of uniform SNs in a finite 2-D area. As such, in this section, related work in sensing coverage and connectivity analytical models is presented.

### 2.2.1 Related Work on Analytical Models on Sensing Coverage

A number of different analytical models for sensing coverage in WSNs have been proposed [48, 49, 45, 50, 51, 52, 47, 53, 54] [55, 56, 46, 57, 58, 7, 59, 60, 61, 4] [62, 63, 64]. They were all different from one another due to their different assumptions and scenarios. The models can be categorized according to: A. the type of the terrain on which the WSN is deployed, whether it is 2-D or 3-D, B. the kind of the sensing model, binary or probabilistic, C. the coverage metric used, area or detection probability, and D. the way the SNs are distributed, Poisson or uniform or clustered.

The models [49, 45, 50, 51, 52, 47, 53, 54, 55, 56] [46, 57, 58, 7, 59, 60, 61, 4, 62, 63] all assumed the 2-D sensing field. Only the models proposed in [48, 64] looked at the analytical models for sensing coverage from the 3-D perspective. In [48], the model computed the minimum sensor spatial density needed for  $k$ -coverage in a 3-D deployment field, utilizing the concept of Reuleaux tetrahedron. In this work [48] the degree of coverage,  $k$ , also had to be at least four. It cannot compute the expected detection probability at an arbitrary point, when a probabilistic sensing model is assumed. Work in [64] derived the coverage degree and target detection probability for autonomous underwater vehicles in the 3-D underwater environment. The target of detection in [64] can be either static or mobile. In the scenario where the target is mobile, the analytical detection model proposed in [64] also takes into account the exposure time and the moving speed of the mobile target. The sensing or detection model for each autonomous underwater vehicle in [64] is binary.

In terms of the type of the sensing model, [49, 45, 50, 52, 47, 53, 54, 56, 46, 57] [58, 59, 61, 4, 64] based their analytical studies on the binary sensing model. Work by [49] sought the critical SN density required to guarantee what they called, barrier coverage, on thin 2-D strips. The existence of barrier coverage meant that an intruder, the object to be sensed, could not cross the sensing field from one side to the other without being in the area covered by the SNs. In [45], the authors derived the expected probability that the target or the intruder would be detected while traveling across the 2-D sensing field, assuming that each SN was turned on and off according to two different probability values that add up to one. Once, the SN was on or off, it stayed in that state for a certain amount of time before selecting the on-off state again based on the same probabilities. The authors in [50, 53] were also interested in deriving the probability of detecting the traversing intruder. Work in [50] investigated a scenario where jammers were present in the sensing field. These jammers were assumed to be capable of rendering all the SNs within their jamming range useless, causing coverage holes in the field. The locations of the jammers were random, just like those of the SNs. Based on a novel non-existence information-based target detection model, the authors in [52] proposed a closed-form solution for visual  $k$ -coverage probability estimation in a crowded environment with occlusions. Work by [53] focused their derivation for the detection probability in the case where the sensing area of each SN was in an arbitrary shape, not the typical circle or the disk. The authors in [54] derived

the expected coverage ratio of randomly deployed homogeneous camera sensors by first finding the expected coverage of single camera sensor. The authors in [47] studied the relation between the number of deployed SNs, the probability that each SN is active, the sensing range of the SN, and the degree of coverage,  $k$ , for 2-D sensing fields. Work by [47] proposed a function for computing the critical value of the active probability of the SNs that would guarantee that the probability of  $k$ -coverage at all interested points in 2-D fields approaches one as the number of SNs go to infinity. The authors in [56] developed analytical models for redundant coverage based on a model of natural clustering of SNs. Specifically, the authors derived the mean number of coverage disks per unit area assuming a Poisson Cluster Point Process for the SN distribution. Work in [56] also obtained an analytical model for vacancy in coverage resulted from natural clustering. The authors in [46] found the expected detection probability for the traversing target similar to what the authors in [45] did. The difference was that in this work by [46], the SNs switched on and off according to a duty cycle. In each duty cycle, the SNs stayed on and off for certain amount of time. After each duty cycle ended, another one started with the same amount of time for the on-off states. Work by [57] introduced a new performance metric for multi-perspective coverage in visual sensor networks, and also analytically computed the multi-perspective coverage for a given number of uniformly deployed camera sensors. The authors in [58] were interested in finding the probability that a target was covered by  $k$  visual SNs. The visual SNs had the sensing coverage of a circular sector instead of the normal disk. Work by [58] also considered the scenario where there were occlusions that blocked the fields of view of the SNs. The authors in [59] examined the relation between the probability of every point of interest being covered by  $k$  SNs, the sensing range, and the number of deployed SNs. Work in [61] found the sensing coverage in terms of covered area to the total area of the sensing field by taking border effects into account. However, the consideration of the border effects did not differentiate the case where the SNs were close to the corners of the sensing field, and the case where the SNs were close to the four sides of the field. Work in [4] attained an analytical model for the expected area that were covered by  $k$  SNs, given that the size of the 2-D field, the sensing range of the SNs, and the number of deployed SNs were provided. The authors in [4] also examined all the possible cases of border effects in their derivation. All these works reviewed here assumed the binary sensing models for their analytical models. Hence, their models could not be applied to find the expected detection probability at an arbitrary point, when the probabilistic sensing model is assumed.

Overall, existing work for sensing coverage analysis, in terms of the type of the sensing model, majority of prior analytical work [4, 47, 56, 59, 61, 49, 5, 65, 66] assumed the traditional binary disk model, and hence used the covered area ratio as the coverage metric. Other work [58, 46, 45, 53, 50, 67, 64, 68] derived a detection probability (DP), yet still by assuming the binary disk for the sensing model. The authors in [67] also found the probability that an event is detected before it goes out. Work in [68] derived the DP for barrier coverage assuming that an intruder has a preferred or favorite path which was based on real life observations.

A probabilistic sensing model was adopted in work on sensing coverage analyses in [51, 55, 7, 60], but their performance measure for sensing coverage was all the ratio of the covered area to the total area, not the expected detection probability at

an arbitrary point. Work in [63] was based on a combination of two probabilistic sensing models, Elfes and log normal shadow fading, and the overall sensing performance metric was still the coverage area fraction. In [62] using a probabilistic sensing model, the minimum energy connected target  $\varepsilon$ -probability coverage problem was proven to be nondeterministic polynomial-hard. The authors in [62] also proposed an algorithm for the solution to the problem adopting a minimum weight maximum flow technique. The authors in [51] derived the coverage ratio using Elfes sensing model, and also investigated the impact of one node failure on the coverage ratio for the coverage degree of one and two. Work in [55] modeled their sensing model after the model for signal reception power in shadowing environment. The coverage area that the authors in [55] analyzed was equated to the probability that a point in the circular 2-D sensing field would be covered by at least an SN. In their derivation, work in [55] also considered the border effects. The authors in [7] did the same thing as the authors in [55], except they did not factor in the border effects. Work in [60] explored an analytical model for the sensing coverage from an angle of how data fusion and noisy measurements impacted the coverage. The area coverage that the authors in [60] were interested in was defined according to the false alarm probability and detection probability. Data fusion in this work meant that the signal measurement in their sensing model was the sum of signal measurements from all the SNs that covered an arbitrary point in the sensing field. The coverage work in [60] investigated was still the area not the expected detection probability at an arbitrary point. The authors in [69] also investigated a data fusion model assuming the traditional binary disc sensing model in their sensing coverage analysis. Work in [70] proposed a new localization-oriented sensing model and found the localization-oriented coverage probability for randomly deployed wireless camera sensor networks. There still has not been work that derives the EDP at any arbitrary point AP in a finite sensing field based on a probabilistic Gaussian-like disk model.

Work in [45, 50, 52, 53, 54, 46, 58] considered the detection probability for the performance metric of sensing coverage in their analytical works. Yet, all their sensing models were the binary sensing model which would not represent the sensing capability of signal detection SNs as well as a probabilistic sensing model. Other work [48, 49, 51, 47, 55, 56, 57, 7, 59, 60] [61, 4] employed the ratio of the covered area to the total area of the sensing field as the sensing coverage metric.

Another interesting aspect of analytical works for sensing coverage in WSNs is how the SNs are randomly distributed. Work in [48, 45, 50, 54, 46, 57, 61, 4] assumed in their works that the SNs were randomly distributed with uniform distribution. On the other hand, work in [49, 51, 52, 47, 53, 55, 58, 7, 59, 60] presumed the Poisson distribution. The difference between uniform distribution and Poisson distribution is that Poisson distribution is the asymptotic estimate of binomial distribution, which is what used in the derivations for uniform SN distribution, when the number of deployed SNs approaches infinity [53, 58, 7]. Work in [56] considered cluster distribution of SNs.

### 2.2.2 Related Work on Analytical Models on Connectivity

As for connectivity, earlier work without consideration of a sink was interested in the number of neighboring nodes (NNs) or a node degree needed for overall peer-to-peer connectivity [71] and the minimum node density (ND) for an almost surely connected subarea on an infinite plane [72] or a single large connected component [61, 73, 74, 75], or end-to-end connectivity in thin strips [49]. The authors in [76] however argued that, due to the existence of “critical nodes”, the minimum node degree alone is not enough to indicate peer-to-peer connectivity in sparse and medium-density networks. Analytical models involving the node degree were also found for shadow fading environments [77]. Work in [78] derived node isolation probability considering both interference and fading. The authors in [79, 80] analyzed both 2-D and 3-D connectivity under fading and shadowing effects. Other analytical work also investigated the probability of peer-to-peer connectivity [81, 82, 6]. The probability of connecting a source to a sink on a one-dimensional (1-D) network through SNs of random communication ranges was derived by the authors in [83]. Also considering sink connectivity (SC), the authors in [84] proposed an arithmetic average of expected probability that each SN can transmit to a sink in a three-dimensional (3-D) grid field, assuming the SNs were placed at grid vertices. The authors in [85] derived the lower and upper bounds of SC for Poissonly distributed underground SNs considering soil water content, sensor burial depth, sink antenna height, the SN density, the operating frequency, a Rayleigh fading channel for the above ground path, and the tolerable latency of the networks. In [86], the probability of sink connectivity for underwater optical WSNs with the consideration of the sensors’ divergence angle was derived. This work was based on a random sector directed graph and the assumption that the number of SNs deployed approached infinity. In [87], the connectivity of the WSNs was investigated in the framework of network security.

Another important question of expected number of paths to a sink that each randomly and uniformly placed SN has in a two-dimensional (2-D) field, given that a finite number of SNs have been deployed, still hasn’t been explored so far. WSNs, as noted earlier, gather information from SNs by having the SNs transmit the information in a single- or multi-hop fashion to a base station or a sink node. Thus, it is imperative to know that each SN has connectivity to the sink when a WSN is deployed. Assuming a finite number of deployed SNs makes the model more applicable and accurate in practice than asymptotic assumption of infinite number of SNs. Furthermore, SNs or communication links in WSNs do fail from time to time [6]. Multiple distinct paths can provide redundancy needed to ensure that there is no observed data missing at the receiving end. The analytical work on connectivity in this dissertation aims to find the answer to this number-of-path-to-sink connectivity question for WSNs with a finite number of randomly placed SNs.

### 2.2.3 Related Work on Analytical Models on Joint Sensing Coverage and Connectivity

Typically, analytical work on joint coverage and connectivity was largely based on a theorem [11] about a relationship between coverage and peer-to-peer

connectivity which states that the degree of peer-to-peer network connectivity is the same as the degree of sensing coverage when the communication range of the SNs is at least twice as big as the sensing range. Consequently, earlier work on joint coverage and connectivity analysis assumed that both sensing and communication models were binary disks or spheres. Thanks to this assumption and the theorem, deriving coverage could lead to the derivation of connectivity [49, 67, 73, 74, 48, 88]. The relationships between coverage and peer-to-peer connectivity in 3-D were found in [48]. The authors in [48] proved that, in a 3-D sensing field, probabilistically  $k$ -covered SNs are connected when a stochastic communication range is at least equal to a stochastic sensing range. They also found a bound of connectivity degree to the sink when the coverage degree is at least four in the 3-D field. Work in [88] found a tighter relationship between the sensing range and the communication range for 1-coverage to imply peer-to-peer connectivity in a rectangular DA by introducing a constraint of the minimum allowed distance between SNs. If this minimum allowed distance between SNs is zero, for the 1-coverage to imply peer-to-peer connectivity, the communication range still has to be at least twice the sensing range. In [89, 90], using continuum percolation, critical densities for coverage and connectivity for directional and fixed directional sensor networks were found respectively. The authors in [2] developed probabilistic models for  $k$ -coverage and connectivity in randomly deployed sensor networks near the boundary. In [91], they derived expressions for  $k$ -coverage and  $m$ -connectivity in 3-D heterogeneous directional WSNs. In [92], a method to calculate the network density for the specified DP while maintaining connectivity of linear WSNs was proposed. Coverage and connectivity for 3-D WSNs were also analyzed in [93], while link probability, node degree, and coverage were studied in [94]. Unlike prior work, the study in this dissertation assumes that only the communication model is the binary disk. The sensing model employed in this dissertation is probabilistic, not binary. As a result, the mathematical approaches in deriving the probabilistic coverage and the degree of SC of each SN in the dissertation are different.

In summary, since the sensing model of the SNs assigns the DP at any point within the sensing range  $d_s$ , we measure the level of sensing coverage resulted from randomly deploying a finite number of such SNs by the EDP at any point within the DA. The first derivation finds this expectation. The second derivation of this dissertation analyzes the expected number of paths to the sink for the SNs that cannot directly transmit to it, to determine the level of connectivity and the fault tolerance in SC of the WSNs.

### 2.3 Open Challenges

Thanks to a variety of applications, scenarios, types of SNs employed in WSNs, deriving analytical models for sensing coverage and connectivity in WSNs remains an important challenge. Despite numerous models having been proposed over the years, there are still challenges ahead. One important scenario of a random uniform deployment of a finite number of homogeneous SNs that detect objects from their EM waves or acoustic signals or other similar physical quantity is one of the challenges. Being able to accurately predict the expected probabilistic detection coverage and expected sink connectivity in this scenario could prove fruitful in practice for several

real-world applications. Not only can the models be used for a cost-efficient deployment of WSNs, but they can also be employed in planning uncoordinated sleep scheduling, determining fault tolerance capability of coverage and connectivity over time, and gauging the performance of deterministic sensor placement strategies. These are what motivates the research in this dissertation.

## CHAPTER 3

### Expected Degree of Sink Connectivity

This chapter shows the derivation of the expected degree of sink connectivity (EDSC) of SNs that cannot directly transmit to the sink which is located in the center of deployment area (DA). It begins with how the degree of sink connectivity can be found based on work in [38], and what this means in the geometry of 2-D rectangular DA. Then order statistics which is a mathematical tool used to derive the EDSC is presented. Then the derivation of the EDSC based on the order statistics is shown. The chapter ends with the final form of the mathematical model for the EDSC and some discussions observed during the derivation.

#### 3.1 Degree of Sink Connectivity in 2-D Rectangular Plane

A WSN has  $k$  degrees of connectivity when any  $k-1$  SNs fail, and each remaining SN still has a connectivity left. This connectivity can be either to any other SN in the case of peer-to-peer connectivity, or to a sink for SC. This dissertation is interested in knowing the EDSC of the SNs that are uniformly deployed at random in a finite rectangular plane with a sink located in the middle. In [38], Bari, Jaekel, and Bandyopadhyay has theoretically proved that a network of nodes has  $k$  degrees of SC if all the nodes that cannot directly transmit to the sink have at least  $k$  neighboring nodes (NNs) that are closer to the sink than themselves. This means that for a network of randomly deployed SNs, the minimum number of closer-to-sink neighboring SNs of the SNs without direct transmissions to the sink is the network degree of SC. Therefore, the EDSC of which this dissertation is deriving an analytical expression, is the expectation of this minimum number.

Before the expectation of the minimum number of closer-to-sink NNs (NoCSNNs) of the SNs without direct transmissions to the sink is obtained, where these CSNNs are located must be identified. The NNs are the ones that are within the transmission range of a SN. Being closer to the sink than the SN itself means that if one draws a circle whose center is the sink and radius equals the distance between the sink and the SN, these nodes will be located in this circle. Thus the CSNNs lie at the overlap of the two circles; one whose center is the SN and radius equals the SN transmission range  $r_t$ , and another whose center is the sink and radius equals the distance  $s$  between the sink and the SN. Figure 3.1 illustrates this overlapped area.

Since the minimum NoCSNNs for each iteration of sensor deployment is a discrete random variable (r.v.) depending on the number of SNs deployed, the size of the rectangular sensing field, and the communication range of the SNs, to determine its expected value, its probability mass function (PMF) as a function of these factors must be found. The PMF for the SC degree problem here is the probability distribution of a minimum number. Thus it can be found by utilizing order statistics [95].

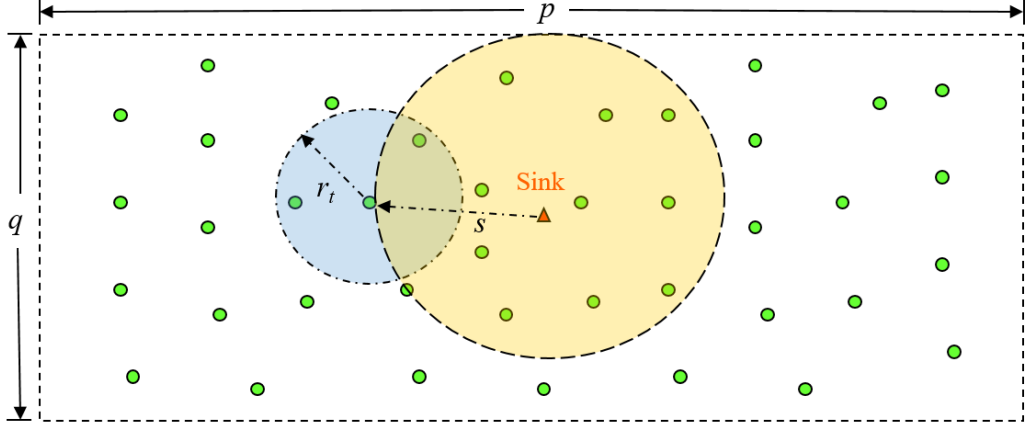


Figure 3.1. Overlap of the two circles where closer-to-sink NNs lie

To compute the EDSC, let  $X_{(1)}$  denote the minimum NoCSNNs of the SNs without direct transmission to the sink, and  $DSC$  be the network degree of SC. It yields that,

$$E[DSC] = E[X_{(1)}] = \sum_{k=0}^{n-1} k \Pr(X_{(1)} = k) \quad (3.1)$$

where  $\Pr(X_{(1)} = k)$  is the probability that the minimum NoCSNNs is  $k$  or the PMF of the minimum NoCSNNs for each iteration of sensor deployment. As alluded to earlier,  $\Pr(X_{(1)} = k)$  is found by applying the 1<sup>st</sup> order statistic in order statistics [95].

### 3.2 Order Statistics

Given that  $X$  is a discrete r.v., and  $M$  is the number of independent observations or samples of  $X$ , it follows that  $X_{(1)}$  is the 1<sup>st</sup> order stat or the minimum of the samples,  $X_{(M)}$  is the  $M^{\text{th}}$  order stat or the maximum of the samples, and so on. By order stats [95], the probability distribution of  $X_{(1)}$  is the following:

$$\Pr(X_{(i)} = k) = \sum_{u=0}^{i-1} \sum_{w=0}^{M-i} \binom{M}{u, M-u-w, w} \pi_1^u \pi_2^{M-u-w} \pi_3^w \quad (3.2)$$

where  $\pi_1 = B(k-1)$ ,  $\pi_2 = \beta(k)$ ,  $\pi_3 = 1 - B(k)$ ,  $B(c) = \sum_{\alpha=0}^c \beta(\alpha)$ , and  $\beta(k) = \Pr(X = k)$ . When  $k = 0$ ,  $B(k-1) = 0$ .



From (3.2),  $\Pr(X_{(i)} = k)$  is a multinomial distribution that accounts for all the different and mutually exclusive cases for when  $X_{(i)} = k$  or the  $i^{\text{th}}$  order stat is  $k$  [95]. When  $X_{(i)} = k$  and the number of observations is  $M$ , there are  $u$  observations below  $X_{(i)} = k$ ,  $(M - u - w)$  observations of  $X_{(i)} = k$ , and  $w$  observations above  $X_{(i)} = k$ , with the respective probabilities as shown in (3.2) [95]. Of the interest of the particular research problem in this dissertation, the first order stat,  $\Pr(X_{(1)} = k)$  is what applies here. From (3.2), it immediately follows that,

$$\Pr(X_{(1)} = k) = \sum_{w=0}^{M-1} \binom{M}{M-w, w} \pi_2^{M-w} \pi_3^w \quad (3.3)$$

### 3.3 Expected Degree of Sink Connectivity by Order Statistics

In the EDSC problem, the random variable  $X$  in the order stats represents the number of SNs in the overlap of the two circles, and  $M$ , the number of observations in the order stats, equals the number of SNs that cannot directly transmit to the sink. On average, in the EDSC problem, this  $M$  number should be equal to  $n \left( \frac{pq - \pi r_t^2}{pq} \right)$ , assuming that the deployment area is rectangular and of the size  $q$  by  $p$  and  $p > q$  as shown in Figure 3.1. However, depending on the number of deployed SNs,  $n$ , the dimension of the deployment area which are  $q$  and  $p$ , and  $r_t$ , this  $M$  number more often than not is not an integer. Since in the order stats the number observations must be an integer all the time, to be able to apply the order stats to the EDSC problem, this  $n \left( \frac{pq - \pi r_t^2}{pq} \right)$  is rounded for  $M$ .

In order stats, each observation of  $X$  is assumed to be i.i.d. However, in the EDSC problem of this dissertation, each observation in order stats which is the NoCSNNs of each SN that cannot directly transmit to the sink is not identically distributed. The reason for this is because the probability that the NoCSNNs equals a certain number depends on where the SN is. As shown in Figure 3.1, the further a SN is away from the sink, the slightly bigger its overlap area is because of the marginally bigger the circle whose center is the sink. Hence, it is slightly more likely for the SNs that are further away from the sink to have a higher NoCSNNs. Similarly, on the other hand, SNs closer to the sink are more likely to have fewer NoCSNNs. As a result, each observation of the NoCSNNs is not identically distributed. It depends on how far this observed SN is from the sink. To be able to accurately apply the concept of order stats in the derivation of the EDSC, each observation of the number of the neighbors must be approximated to be identically distributed. This is carried out by first finding the probability mass function (PMF) of the NoCSNNs at a particular distance of the observed SN to the sink, then averaging this PMF over all the distances starting from the observed SN's transmission range away from the sink, in order to account for only the SNs that cannot directly transmit to the sink, to the edge of the DP.

Let  $\Pr(X = k|s)$  denote the probability that the NoCSNNs is  $k$  for a SN

that is at distance  $s$  away from the sink. One can write,

$$\Pr(X = k|s) = \binom{n-1}{k} \{p|s\}^k \{1-p|s\}^{n-1-k} \quad (3.4)$$

where  $n$  is total number of SNs deployed in the sensing field as mentioned before, and  $p|s$  is the probability that there is one SN in the overlap area of the SN that is at distance  $s$  away from the sink, as shown Figure 3.1. This  $p|s$  clearly depends on the size of the overlap area as shown in the equation above. Since the size of the overlap area depends on the distance  $s$ , so does  $p|s$  and hence  $\Pr(X = k|s)$ . The probability  $\Pr(X = k|s)$  is not the same for all observations of  $X$ . It depends on the distance  $s$ , which is a continuous random variable. In order to approximate each observation of the NoCSNNs of an SN as identically distributed,  $\Pr(X = k|s)$  is averaged over  $s$ , and this average will be used for all the observations of the SNs that cannot directly transmit to the sink as the i.i.d. PMF or  $\beta(k) = \Pr(X = k)$  in (3.3).

Without loss of generality, again assuming that the DA is a rectangular plane of size  $q$  by  $p$  and  $p > q$  as shown in Figure 3.1. **Overlap of the two circles where closer-to-sink NNs lie**

, and  $r_t$  is the transmission range of the SNs, by geometry one has,

$$p|s = \frac{r_t^2 \cos^{-1}\left(\frac{r_t}{2s}\right) + s^2 \cos^{-1}\left(\frac{2s^2 - r_t^2}{2s^2}\right) - \left(\frac{r_t}{2}\right) \sqrt{4s^2 - r_t^2}}{pq}. \quad (3.5)$$

The numerator in equation (3.5) is the size of the overlap area as a function of  $r_t$  and  $s$ . Since  $r_t$  is a given constant, the size of the overlapped area depends only on  $s$ , the distance between the observed SN and the sink. Now one can write that  $\beta(k|s) = \Pr(X = k|s)$ . Since  $s$  is a continuous r.v. Thus  $\beta(k)$  in equations (3.2) and (3.3) which is the approximated i.i.d. PMF of the NoCSNNs can be calculated as follows:

$$\beta(k) = \int \beta(k|s) f(s) ds \quad (3.6)$$

where  $f(s)$  is the p.d.f. of  $s$ . A p.d.f. is the derivative of a cumulative distribution function (CDF). To find a p.d.f., its CDF first has to be found.

The lower bound of the integral in equation (3.6) is  $r_t$  because only the neighbors of the SNs that do not have a direct transmission to the sink are considered. These SNs are located at the distance of at least  $s = r_t$  away from the sink. To attain

the p.d.f.  $f(s)$  for equation (3.6), one can first observe that it is not just one function. Due to the three different shapes of the areas in considering the CDF of  $s$  as shown in Figure 3.2, Figure 3.3, and Figure 3.4, there are three of its p.d.f.'s. They are named  $f_1(s)$ ,  $f_2(s)$ , and  $f_3(s)$ . The first p.d.f.  $f_1(s)$  is for  $r_t < s \leq \frac{q}{2}$ , the second p.d.f.  $f_2(s)$  is for  $\frac{q}{2} < s \leq \frac{p}{2}$ , and the last p.d.f.  $f_3(s)$  is for  $\frac{p}{2} < s \leq \left(\frac{1}{2}\right)\sqrt{q^2 + p^2}$ . Also, based on these, it yields the following:

$$\beta(k) = \int_{s=r_t}^{\frac{q}{2}} \beta(k|s)f_1(s)ds + \int_{s=\frac{q}{2}}^{\frac{p}{2}} \beta(k|s)f_2(s)ds + \int_{s=\frac{p}{2}}^{\left(\frac{1}{2}\right)\sqrt{q^2+p^2}} \beta(k|s)f_3(s)ds \quad (3.7)$$

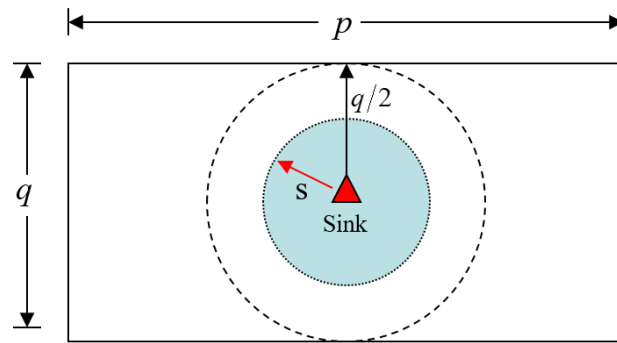


Figure 3.2. Areas for CDF computation when  $r_t < s \leq \frac{q}{2}$

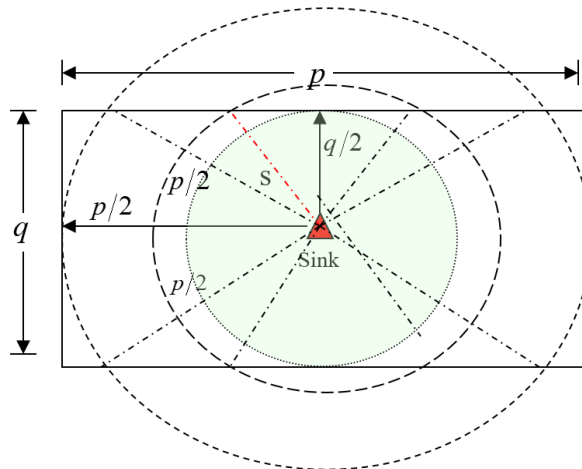


Figure 3.3. Areas for CDF computation when  $\frac{q}{2} < s \leq \frac{p}{2}$

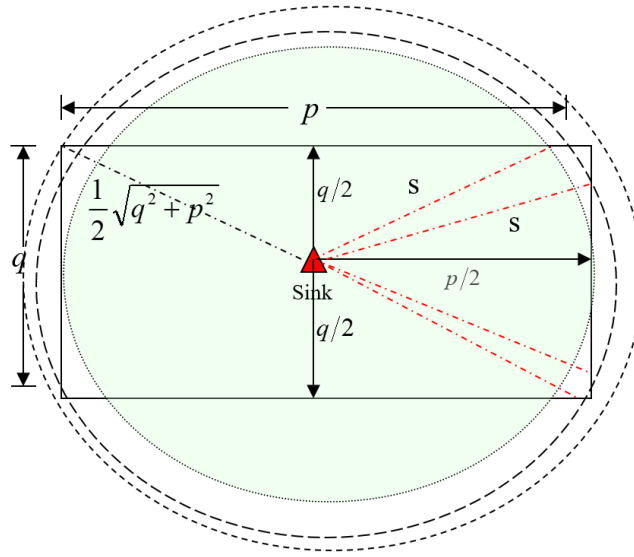


Figure 3.4. Areas for CDF computation when  $\frac{p}{2} < s \leq \left(\frac{1}{2}\right)\sqrt{q^2 + p^2}$

The three sections of the p.d.f.'s of  $s$  are all calculated by first finding their CDF's. In the first section,  $r_t < s \leq \frac{q}{2}$ , the probability that a point selected at random lies within  $s$  units of the center of the circle whose radius is  $\frac{q}{2}$ , is the area of the circle whose radius is  $s$ , divided by the area of the circle whose radius is  $\frac{q}{2}$ , as shown in Figure 3.2. This probability,  $\Pr(S \leq s)$ , represents the CDF of  $s$ ,  $F_1(s)$ , in the first section. From Figure 3.2, one can write  $F_1(s)$  as shown in equation (3.8).

$$F_1(s) = \frac{\pi s^2}{\pi (q/2)^2} = \frac{4s^2}{q^2} \quad (3.8)$$

Subsequently, the first p.d.f.  $f_1(s)$ , which is the derivative of  $F_1(s)$  with respect to  $s$ , can be found as illustrated in equation (3.9) below.

$$f_1(s) = \frac{d}{ds} F_1(s) = \frac{d}{ds} \left( \frac{4s^2}{q^2} \right) = \frac{8s}{q^2} \quad (3.9)$$

Similarly, for the second section,  $\frac{q}{2} < s \leq \frac{p}{2}$ , since the shapes of the areas for calculating the second CDF of  $s$ ,  $F_2(s)$ , are the overlaps of the circles with the rectangular DA as shown in Figure 3.3. It follows that  $F_2(s)$ ,  $\Pr(S \leq s)$ , is the area of the overlap between the circle with the radius  $s$  with the DA, divided by the area of the overlap between the circle with radius  $\frac{p}{2}$  with the DA. By geometry, the area of the overlap between the circle with radius  $\frac{p}{2}$  with the DA can be found by summing the

areas of the four triangles with catheti of  $\frac{q}{2}$  and  $\frac{p}{2}$  with the areas of the remaining circular sectors. Let  $A_2$  represent this area. It can be found as shown below in equation (3.10).

$$A_2 = \frac{q}{2}\sqrt{p^2 - q^2} + \pi \frac{p^2}{4} \left(1 - \frac{2}{\pi} \cos^{-1} \left(\frac{q}{p}\right)\right) \quad (3.10)$$

From equation (3.10),  $F_2(s)$  is found as follows.

$$F_2(s) = \frac{\frac{q}{2}\sqrt{4s^2 - q^2} + \pi s^2 \left(1 - \frac{2}{\pi} \cos^{-1} \left(\frac{q}{2s}\right)\right)}{A_2} \quad (3.11)$$

Hence, the second p.d.f.  $f_2(s)$ , which is the derivative of  $F_2(s)$  with respect to  $s$ , is as follows.

$$f_2(s) = \frac{d}{ds} F_2(s) = \frac{2\pi s - 4s \cos^{-1} \left(\frac{q}{2s}\right)}{A_2} \quad (3.12)$$

Finally, for the third section,  $\frac{p}{2} < s \leq \left(\frac{1}{2}\right)\sqrt{q^2 + p^2}$ , from Figure 3.4,  $F_3(s)$  or  $\Pr(S \leq s)$ , is the area of the overlap between the circle with the radius  $s$  with the DA, divided by the area of the DA. Using the same geometric analysis employed in finding  $A_2$  for  $F_2(s)$  in equation (3.11), we can get  $F_3(s)$  as follows.

$$F_3(s) = \frac{\frac{q}{2}\sqrt{4s^2 - q^2} + \frac{p}{2}\sqrt{4s^2 - p^2} + \pi s^2 - 2s^2 \cos^{-1} \left(\frac{q}{2s}\right) - 2s^2 \cos^{-1} \left(\frac{p}{2s}\right)}{pq} \quad (3.13)$$

Therefore, by taking the derivative of  $F_3(s)$  respect to  $s$ , the final p.d.f.  $f_3(s)$  is as follows.

$$f_3(s) = \frac{d}{ds} F_3(s) = \frac{2\pi s - 4s \cos^{-1} \left(\frac{q}{2s}\right) - 4s \cos^{-1} \left(\frac{p}{2s}\right)}{pq} \quad (3.14)$$

With the three p.d.f.'s of  $s$  as found in equations (3.9), (3.12), and (3.14),  $\beta(k)$  in equation (3.3) can be computed as shown in equation (3.7). However, there is no closed form expression for  $\beta(k)$ . As a result, there is no closed form expression for

$\Pr(X_{(1)} = k)$  in equation (3.3), and neither is there for  $E[DSC]$  in equation (3.1). Only the analytical expression of EDSC is achieved, and it can be computed through numerical methods. It is worth noting that besides approximating each observation of the NoCSNNs as identically distributed and using the rounded number of SNs that cannot directly transmit to the sink for the number of observations in equation (3.3), another round of approximation in (3.5) for  $p|s$  is also performed. In equation (3.5), the shape of the overlap in which CSNNs reside changes when it crosses a border. However, for  $p|s$ , these border effects are not taken into account. These three adjustments have impacts on the accuracy of the connectivity analytical model in this dissertation, and they govern the scenarios in which the mathematical expression proposed in the dissertation is the most accurate. This will be investigated further in the Chapter 5 on the verification by simulation results and discussions of the EDSC analytical expressions.

## CHAPTER 4

### Expected Probabilistic Detection Coverage

This chapter presents the derivation of the expected detection probability (EDP) at arbitrary point (AP) in the deployment area (DA). First the detection probability of the object at the arbitrary point is discussed along with its expectation. Then the subsequent probability distributions needed for the formulation of the EDP are presented. The chapter ends with the mathematical model for the EDP and a discussion of the ramifications of the derived model.

#### 4.1 Detection Probability and its Expectation

To calculate the EDP at an arbitrary point (AP) in the sensing field, first the detection probability (DP) at a point must be found. The DP at a point in the deployment area (DA) is the probability that an object at the point is detected by at least one SN. Since each SN has the sensing range of  $d_s$ , it means that only the SNs that are within the distance  $d_s$  from that point can detect the object there. Assuming that there are  $k$  SNs that are located within the distance  $d_s$  from the point or the object, the probability that at least one out of  $k$  SNs detects it equals one minus the probability that none of the  $k$  SNs detect it. By assuming that each SN independently detects the object, one can write DP as follows.

$$DP = 1 - \prod_{i=1}^k (1 - D_i(r_i)) \quad (4.1)$$

$D_i(r_i)$  is the probability that SN  $i$  detects the object and assumed to be as shown in equation (**Error! Reference source not found.**), and  $r_i$  is the distance between the SN  $i$  and the object at the AP.

Since the SNs are uniformly deployed at random,  $k$  and  $r_i$  are r.v.'s when analyzing the EDP. More specifically,  $k$  is a discrete r.v., and  $r_i$  is a continuous one. In addition,  $r_i$  can simply be replaced by just  $r$ . The reason for this is because, when one analyzes the EDP, all the SNs are the same in a sense that they are all randomly deployed with uniform distribution. Thus, the EDP becomes,

$$E[DP] = E\left[1 - \prod_{i=1}^k (1 - D(r))\right] \quad (4.2)$$

where  $D(r)$  is the DP of any SN that is within the distance  $d_s$  from the AP and the same as what is shown in equation (**Error! Reference source not found.**). The EDP at an AP is the DP averaged over all the APs in the entire sensing field.

In order to derive  $E[DP]$ , the probability distributions of  $k$  and  $r$  must be determined. These distributions are dictated by where in the deployment area the AP is. Recall that only the SNs that are within the distance  $d_s$  from the AP can detect the object there. In this dissertation, the region in which the SNs that can detect the object are located, is called a detection region (DR). The shape and size of this region affects the probability distributions of  $k$  and  $r$ . When the AP is in middle area, the DR is a circle as shown in Figure 4.1. When the AP is close to a border of the deployment area, the DR becomes an overlap of the circle with the deployment area as seen in Figure 4.2. This overlap area which happens when the AP is close to the borders or in sub-region (SR)  $b$  and  $c$  will be referred to as the effective DR. Its shape and size vary depending on the location of the AP. This effective DR clearly affects the probability distributions of  $k$  and  $r$ . Therefore, to accurately account for all the effects of these in the mathematical model of the expectation for the DP, the deployment area is partitioned into three SRs [4] as demonstrated in Figure 4.3 to correctly find the corresponding probability distributions of  $k$  and  $r$ .

## 4.2 Probability Distribution of $k$

The number of SNs,  $k$ , that have the object to be detected within their sensing range is a discrete random variable. Its value depends on where the AP at which the object is located is. As mentioned earlier, because of the border effects and the assumption of uniform distribution for SN placement, it is likely to have fewer SNs located due to a smaller DR when the AP is around the borders. Hence, the number of SNs,  $k$ , is expectedly smaller for the APs close to the border. The reason for this is again because some part of the DR whose center is a point near the border is cut off as shown in Figure 4.2. When the area containing potential SNs that could detect the object or the DR becomes smaller, so is the number of SNs potentially inside the DR. This would possibly result in smaller DP's for APs near the border. To derive the analytical model for the EDP, the 2-D rectangular sensing field is divided into three types of SRs:  $a$ ,  $b$ , and  $c$ , the same way that the authors in [4] did in their work. The SRs  $c$  are square areas located at the four corners of the sensing field. The dimension of each square area  $c$  is  $d_s$  by  $d_s$ . The SRs  $b$  are strips whose width is  $d_s$ , and they are located along each side of the border of the rectangular sensing field. Finally, the SR  $a$  is the rest of the area in the sensing field after excluding the SRs  $b$  and  $c$ . Figure 4.3 illustrates how the 2-D rectangular sensing field whose dimension is  $p$  by  $q$  is segmented into three different kinds of SRs.



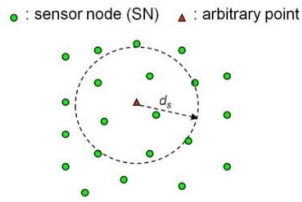


Figure 4.1. Circular DR of radius  $d_s$  when the AP is midway inside the DA

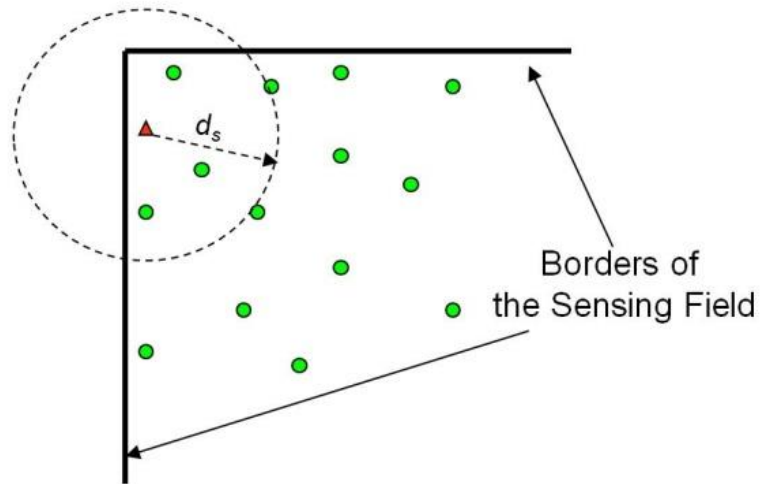


Figure 4.2. DR where the circle intersects the DA

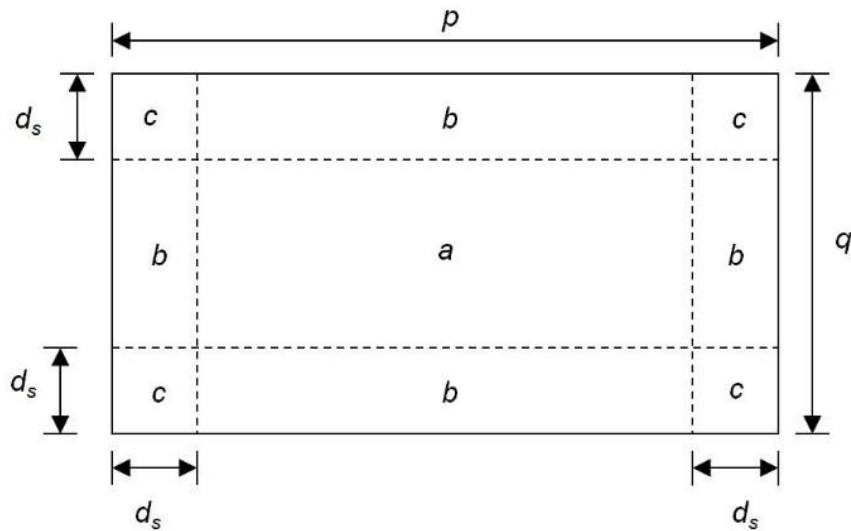


Figure 4.3. 3 SRs:  $a$ ,  $b$ , and  $c$  of an  $p \times q$  rectangular DA.

After dividing the sensing field into three types of SRs, one can now take the expectation of the DP in equation (4.2) as shown below. Let  $\gamma_i$  denote the EDP when the AP is in SR  $i$ , or the conditional EDP. Due to three different types of SRs, it follows that,

$$E[DP] = \gamma_a P_A(a) + \gamma_b P_A(b) + \gamma_c P_A(c) \quad (4.3)$$

where  $P_A(i)$  is the probability that the AP is in SR  $i$ .  $A$  denotes a r.v. representing the type of SR in which the AP or the object is located.  $P_A(a)$  is the probability that  $A = a$ , i.e. the AP is in SR  $a$ .  $P_A(b)$  is the probability that  $A = b$ , i.e. the AP is in SR  $b$  and so forth. This means that the expected detection probability  $E[DP]$  is the sum of conditional EDPs when  $A = a$ ,  $A = b$ , and  $A = c$ . Since the point at which the object is located is arbitrary and with uniformly distributed SNs at random,  $P_A(a)$ ,  $P_A(b)$ , and  $P_A(c)$  are the ratios of the area of the corresponding SR,  $a$ ,  $b$ , and  $c$  to the total DA. In other words,  $P_A(i)$  equals the total area of the SR  $i$  divided by  $pq$ . With the dimensions of the sensing field and the SRs assumed as shown in Figure 4.3, the values of  $P_A(a)$ ,  $P_A(b)$ , and  $P_A(c)$  are as the following.

$$\begin{aligned} P_A(a) &= \frac{(p - 2d_s)(q - 2d_s)}{pq} \\ P_A(b) &= \frac{2d_s(p + q - 4d_s)}{pq} \\ P_A(c) &= \frac{4d_s^2}{pq} \end{aligned} \quad (4.4)$$

Now, each conditional EDP in equation (4.3),  $\gamma_i$ , must be calculated. As mentioned earlier, the number of SNs,  $k$ , that could potentially sense the object at the AP is a discrete random number. Let  $K$  be the discrete r.v. for  $k$ . In addition, this number  $k$  is drawn out of the all possible number of SNs that could possibly be in the DR when the AP at which the object is located is in a particular SR  $a$ ,  $b$ , or  $c$ . Let the number of all SNs that could possibly be in the DR be  $m$ , and let  $M$  be its discrete random variable. This means that the probability that  $M = m$  and  $K = k$  when  $A = a$  or  $A = b$  or  $A = c$  can be found accordingly. Notice that this  $m$  number cannot be equal to  $n$ , the total number of SNs deployed, because, for example when the AP is in SR  $a$ , there are areas at the four corners of the deployment area where the SNs that could possibly be in DR will never be, as shown in Figure 4.4. This means, in other words, that out of  $n$  SNs that have been deployed, there are some SNs get left out of the possibility of being in the DR when the AP is in SR  $a$  because they are in those four corners. Similarly, the areas where the SNs that could possibly be in the DR when the AP is in SR  $b$  and  $c$  are shown in Figure 4.5 and Figure 4.6 respectively. Since both  $M$  and  $K$  are discrete r.v.'s, the conditional EDP in each SR  $i$  equation (4.3),  $\gamma_i$ , when  $A = a$ ,  $A = b$ , and  $A = c$  can be expanded as the sums as follows:

$$\gamma_i = \sum_{m=0}^n \sum_{k=0}^m \beta_{i,m,k} P(m, k|i) \quad (4.5)$$

where  $\beta_{i,m,k}$  is the EDP when the AP is in SR  $i$ , the number of SNs that could possibly be inside the DR is  $m$ , and there are  $k$  SNs that in that DR.  $P(m, k|i)$  is the probability that, when the AP is in SR  $i$ , there are exactly  $k$  SNs in the DR while there are  $m$  SNs that could possibly be in it. Again let it be emphasized that that the number  $m$  is not the same as the total number of SNs deployed  $n$ . This is because when the AP is in a certain SR, it is not necessary that all  $n$  SNs could be in the DR. Thus, this number  $m$  is less than or equal to  $n$ , as shown in Figure 4.4, Figure 4.5, and Figure 4.6.

It then also follows that  $P(m, k|i) = P(k|m, i)P(m|i)$ .  $P(m|i)$  is a binomial distribution of having  $m$  SNs that could be in the DR from the total  $n$  deployed SNs when the point is in SR  $i$ . This is because of the assumption that the total number of SNs,  $n$ , are independently and uniformly distributed over the entire DA, and the fact that when the AP is in a particular SR. Then the probability of each event or success in this binomial distribution  $P(m|i)$  is the proportion of the total area in which a SN could be, given SR  $i$ , to the whole DA. For the SR  $a$ , one has,

$$P(m|a) = \binom{n}{m} \rho^m (1 - \rho)^{n-m}, \quad \rho = \frac{pq - (4 - \pi)d_s^2}{pq} \quad (4.6)$$

The reason for  $\rho$  in  $P(m|a)$  to be as shown is again because, not all the  $n$  SNs that have been deployed could possibly be the candidates to be inside the DR. Given the AP is in a particular SR, there will be some areas in which the SNs that could plausibly be inside the DR will never be. Figure 4.4 illustrates this for when the AP is in SR  $a$ .

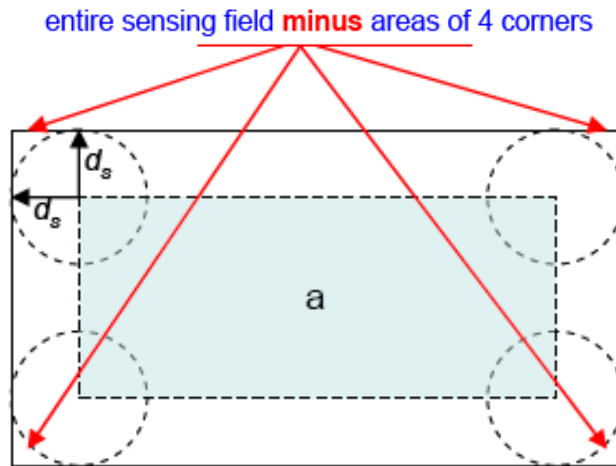


Figure 4.4. The area in which the deployed SNs could only be if  $A = a$ . It is the entire area of the DA minus the areas of the four corners.

Figure 4.4 demonstrates that when  $A = a$ , the area in which the SNs that could possibly in the DR are located is the entire DA minus the areas in which the SNs will never be. By the same fashion when  $A = b$  and  $A = c$ , the sizes of the respective areas in which the SNs could only be are  $4d_s(q + p - 4d_s)$  and  $(12 + \pi)d_s^2$ . These areas which are shown in Figure 4.5 and Figure 4.6 are then used in the computation of the probability of success in the binomial distribution of choosing  $m$  SNs from  $n$  SNs,  $P(m|i)$ , when  $A = b$  and  $A = c$ . To be precise,  $\rho$ 's for  $P(m|b)$  and  $P(m|c)$  are  $(4d_s(q + p - 4d_s))/pq$  and  $((12 + \pi)d_s^2)/pq$  respectively.

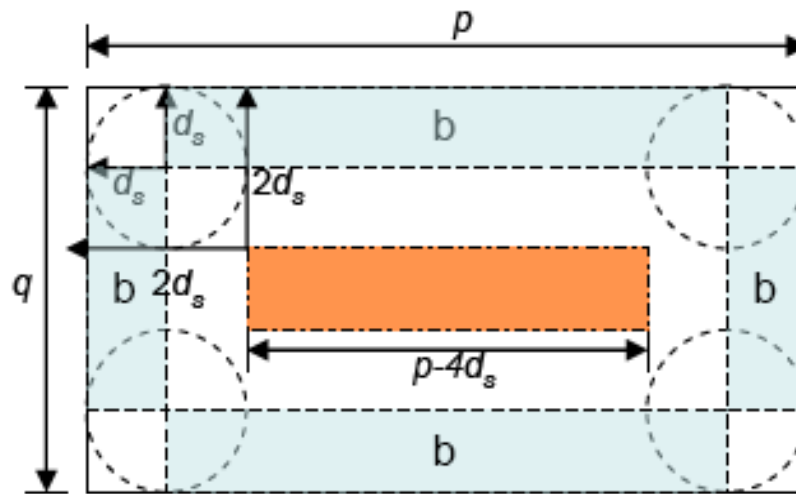


Figure 4.5. The area in which the SNs could only be when  $A = b$ .

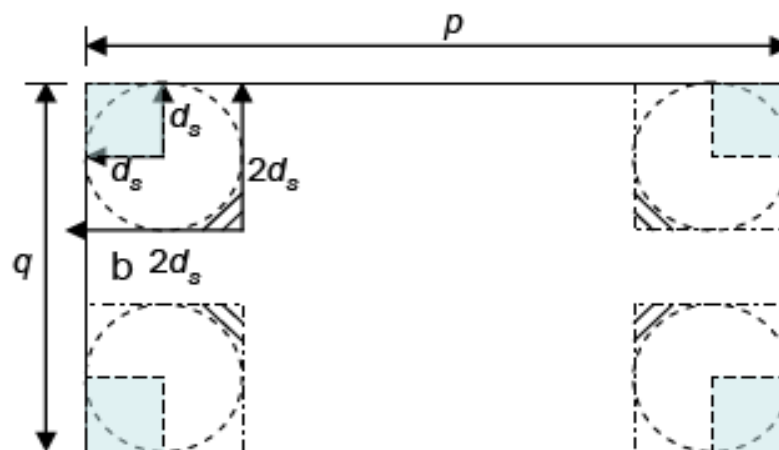


Figure 4.6. The area in which the SNs could only be when  $A = c$ .

Similarly,  $P(k|m, i)$  is another binomial distribution with probability in accordance with the SR  $i$  in which the AP is. This probability that  $K = k$  given that  $M = m$  and  $A = a$  or  $A = b$  or  $A = c$  is the probability that there will be exactly  $k$  SNs inside the DR when there are  $m$  available SNs that could be inside it. This probability is essentially the probability of the binomial distribution of choosing  $k$  SNs out of possible  $m$  SNs with the probability of each success equaling the area of the average effective DR divided by the area that the SNs could only be for a given SR. As noted earlier, this is due to the border effects, which cut off some parts of the DR. Figure 4.7, Figure 4.8, and Figure 4.9 demonstrate how some parts of the DR are cut off or are outside the boundary of the sensing field or the DA, when  $A = b$  and  $A = c$ . The area of the effective DR is the area of the DR circle that is inside the DA. This area varies in size depending on the location of the AP. Therefore, to compute the probability that  $K = k$  given that  $M = m$  and  $A = a$  or  $A = b$  or  $A = c$ , one has to use the average size of the effective DR for each given SR. When  $A = a$ , the size of the effective DR is a complete circle, which is  $\pi d_s^2$ . When  $A = b$ , the average size of the effective DR is  $(\pi - 2/3)d_s^2$  [4], while when  $A = c$ , the average size of the effective DR is  $(\pi - 29/24)d_s^2$  [4].

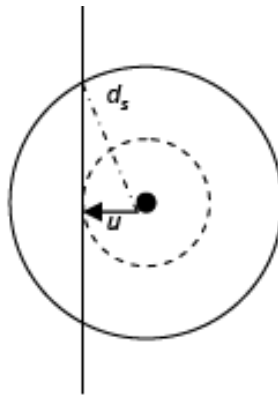


Figure 4.7. The DR is not a complete circle when  $A = b$ . The effective DR is the area of the DR that is within the boundary of the sensing field or the DA.

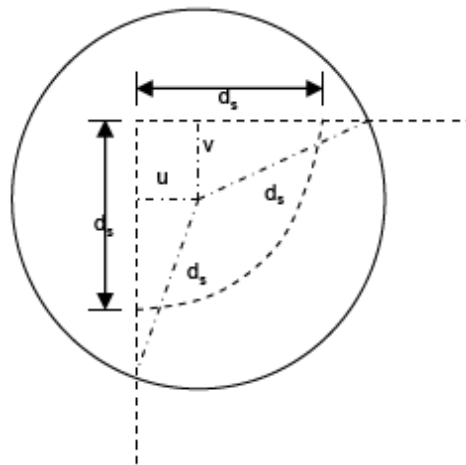


Figure 4.8. The DR when  $A = c$  and the distance from the AP to the corner is less than  $d_s$ . The effective DR is the area of the DR that is within the boundary of the sensing field or the DA.

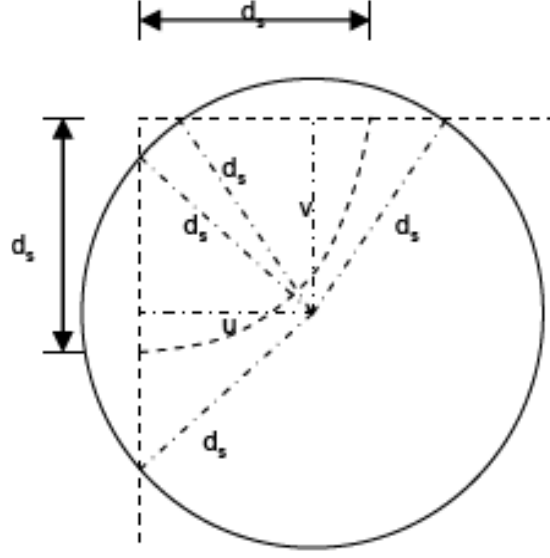


Figure 4.9. The DR when  $A = c$  and the distance from the AP to the corner is more than  $d_s$ . The effective DR is the area of the DR that is within the boundary of the sensing field or the DA.

$P(k|m, i)$  for three SRs can be written as follows:

$$P(k|m, a) = \binom{m}{k} \rho^k (1 - \rho)^{m-k}, \quad \rho = \frac{\pi d_s^2}{pq - (4 - \pi)d_s^2} \quad (4.7)$$

$$P(k|m, b) = \binom{m}{k} \rho^k (1 - \rho)^{m-k}, \quad \rho = \frac{(\pi - 2/3)d_s^2}{4d_s(q + p - 4d_s)} \quad (4.8)$$

$$P(k|m, c) = \binom{m}{k} \rho^k (1 - \rho)^{m-k}, \quad \rho = \frac{\pi - 29/24}{12 + \pi}. \quad (4.9)$$

Each of those probabilities  $\rho$ 's is the average size of the effective DR in each SR  $i$  over the size of the SR. After having  $P(m|i)$  and  $P(k|m, i)$  for all three SRs,  $P(m, k|i)$  in equation (4.5) can be readily computed as the product of these two probabilities.

### 4.3 Probability Distribution of $r$

In equation (4.5),  $\beta_{i,m,k}$  is the EDP when the AP is in SR  $i$  and there are  $k$  out of the possible  $m$  SNs in the DR. It can be written as follows:

$$\beta_{i,m,k} = E[(1 - \prod_{i=1}^k (1 - D(r)))] | i, m, k]. \quad (4.10)$$

Since the SNs are randomly placed with uniform distribution, the expectations of the products become the products of the expectations. One can rewrite  $\beta_{i,m,k}$  as follows,

$$\beta_{i,m,k} = 1 - (E[(1 - D(r))|i, m, k])^k. \quad (4.11)$$

Since  $r$  is continuous r.v. representing the random distance between the AP and any SN inside the DR, one can write,

$$E[(1 - D(r))|i, m, k] = \int (1 - D(r))f_i(r)dr \quad (4.12)$$

where  $f_i(r)$  is the p.d.f. of  $r$  when the AP is in SR  $i$ . This expectation is the conditional EDP for any SN inside the DR. As noted earlier, the probability distribution of this continuous r.v.,  $r$ , which is the random distance between a SN within the DR to the AP, depends on where the AP is inside the deployment area. The reason is because, the CDF of  $r$ , from which its corresponding p.d.f. is derived, is the ratio of the area with radius  $r$  from the AP to the area of the effective DR. When the AP is close to the borders, or in other words in SR  $b$  and  $c$ , the shapes and the sizes of both the area with radius  $r$  from the AP and the effective DR change. As a result, in order to accurately derive the CDF of  $r$ , the careful and accurate considerations of all the cases for all the different shapes and sizes of those areas must be carried out. In the subsequent subsections, all these cases will be explicitly shown along with the calculation of the CDF's and the p.d.f.'s. Letting  $\varepsilon_{i,m,k} = E[(1 - D(r))|i, m, k]$ ,  $f_i(r)$  which is the p.d.f. of  $r$  has to be found for each SR  $i$ , and then the corresponding  $\varepsilon_{i,m,k}$  can be calculated.

#### 4.3.1 Finding $\varepsilon_{a,m,k}$

Let  $R$  be the continuous r.v. for the distance from the center of the DR, which represents an AP, to any SN inside the DR. Similar to when EDSC is derived in Chapter 3, the CDF of  $r$  is the probability that a point selected randomly lies within  $r$  distance units of the center of the DR. It is written as shown below.

$$F(r) = P(R \leq r) = P(0 \leq R \leq r) \quad (4.13)$$

Thus, the CDF of  $r$  is the area with radius  $r$  from the AP, divided by the area of the effective DR whose radius is  $d_s$ .

When  $A = a$ , both the area with radius  $r$  from the AP and the effective DR are complete circles as illustrated in Figure 4.10. Their areas are then readily computed. As a result, the CDF of  $r$  when  $A = a$ , is written as the following.

$$F_a(r) = \frac{\pi r^2}{\pi d_s^2} \quad (4.14)$$

Thus, its corresponding  $f_a(r) = dF_a(r)/dr = 2r/d_s^2$ . From equation (4.12), one can write,

$$\varepsilon_{a,m,k} = \int_{r=0}^{d_s} (1 - D(r)) \left(\frac{2r}{d_s^2}\right) dr \quad (4.15)$$

Applying  $D(r)$  as assumed in equation (**Error! Reference source not found.**), one can simplify equation (4.15) further to:

$$\varepsilon_{a,m,k} = 1 - \left(\frac{2\alpha_s^2}{d_s^2}\right) \left(1 - \exp\left(-\frac{d_s^2}{2\alpha_s^2}\right)\right) \quad (4.16)$$

One can now compute  $\beta_{i,m,k}$  in equation (4.11) when the AP is in SR  $a$ .

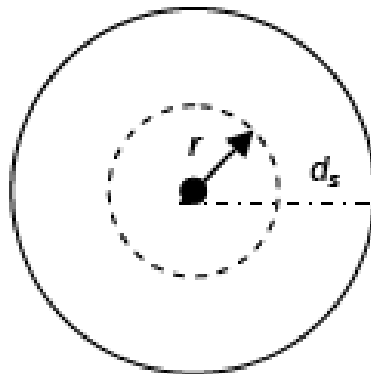


Figure 4.10. The DR whose radius is  $d_s$  and the smaller DR whose radius is  $r$  for the CDF of  $r$  when  $A = a$



### 4.3.2 Finding $\varepsilon_{b,m,k}$

Deriving  $\varepsilon_{b,m,k}$ , again, starts by calculating the CDF of  $r$  in SR  $b$ ,  $F_b(r)$ . This computation is more involving due to the border effects and hence most of the time a noncircular effective DR as illustrated in Figure 4.11. The effective DR in Figure 4.11 is the overlap between the circle whose center is the AP and radius equals  $d_s$  and the deployment area. The shape of the DR in SR  $b$  remains the same, but its size varies depending on how far the AP is from the border.

On the other hand, the area with radius  $r$  from the AP inside the effective DR in Figure 4.11 is sometimes a complete circle, and some other times it is not. As seen in Figure 4.11, when  $r$  is less than or equal to  $u$ , the area with radius  $r$  from the AP is a complete circle. However, when it is more than  $u$ , the area with radius  $r$  from the AP has the same shape as the effective DR, and it is not a circle. Recalling Figure 4.3, the width of the subarea  $b$  is  $d_s$ . Thus  $u$ , which is a r.v., has the value of 0 to  $d_s$ . Moreover, it is a uniform continuous random variable. The reasons for this are because it is the distance from the center of the effective DR which represents the AP to the border of the deployment area, and the fact that the AP is picked arbitrarily. As for the effective DR, whether or not it is a complete circle depends on  $u$ . When  $u = d_s$ , the effective DR circle is complete. When  $u$  is less than  $d_s$ , the effective DR is not a circle.

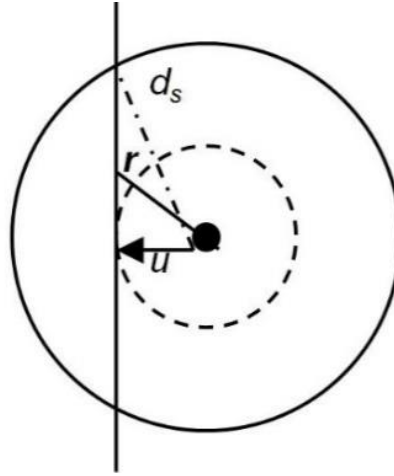


Figure 4.11. Noncircular overlapped DR  $A = b$ .

The shapes and the sizes of the area with radius  $r$  from the AP and the effective DR and when they are in such shapes are now used in the computation of the CDF of  $r$ . Let  $AD_b$  be the area of the effective DR when the AP is in SR  $b$  for a given  $u$ . By geometry, one can obtain the following:

$$AD_b(u) = u\sqrt{d_s^2 - u^2} + (\pi - \cos^{-1}\left(\frac{u}{d_s}\right))d_s^2, \quad (4.17)$$

where  $u$  is a continuous r.v. for the distance from the AP to the border. Since the SNs are uniformly distributed at random, the p.d.f. of  $u$ ,  $f(u)$ , is  $1/d_s$ . Since the shape and the size of the area with radius  $r$  from the AP depend on the value of  $r$  relative to the given  $u$  as explained before, one has to derive the CDF of  $r$  for two cases. Then using the same technique that derives  $F_a(r)$ , one can get  $F_b(r|u)$  for two cases where  $r \leq u$  and  $u < r \leq d_s$ . They are  $F_{b1}(r|u) = \pi r^2 / AD_b$  and  $F_{b2}(r|u) = (u\sqrt{r^2 - u^2} + (\pi - \cos^{-1}(u/r))r^2) / AD_b$ . The subscripts  $b1$  and  $b2$  represent the cases where  $r \leq u$  and  $u < r \leq d_s$  respectively. It then follows that  $f_{b1}(r|u) = dF_{b1}(r)/dr = 2\pi r / AD_b$  and  $f_{b2}(r|u) = dF_{b2}(r)/dr = (2\pi r - 2r\cos^{-1}(u/r)) / AD_b$ .

From equations (**Error! Reference source not found.**) and (4.12), one can rewrite  $\varepsilon_{i,m,k}$  for SR  $b$  as follows,

$$\varepsilon_{b,m,k} = \int_u^{d_s} \int_{r=0}^{d_s} \left(1 - e^{\frac{-r^2}{2\alpha_s^2}}\right) f_b(r|u) f(u) dr du \quad (4.18)$$

Expanding equation (4.18) further, one can write,

$$\begin{aligned} \varepsilon_{b,m,k} = & \int_{u=0}^{d_s} \int_{r=0}^u \left(1 - e^{\frac{-r^2}{2\alpha_s^2}}\right) f_{b1}(r|u) \left(\frac{1}{d_s}\right) dr du \\ & + \int_{u=0}^{d_s} \int_{r=u}^{d_s} \left(1 - e^{\frac{-r^2}{2\alpha_s^2}}\right) f_{b1}(r|u) \left(\frac{1}{d_s}\right) dr du. \end{aligned} \quad (4.19)$$

### 4.3.3 Finding $\varepsilon_{c,m,k}$

The same technique is used to obtain  $\varepsilon_{c,m,k}$ . To compute  $f_c(r)$ , one first considers the corresponding CDF. As in the case of SR  $b$ , in SR  $c$  the effective DR is also not a circle. Unlike in SR  $b$ , here both the shape and the size of the effective DR change depending on how far the AP is from the corner. When the distance between the AP and the corner is less than  $d_s$ , the effective DR is the overlapped area as shown in Figure 4.12. When the distance is more than  $d_s$ , the effective DR becomes what is illustrated in Figure 4.13.

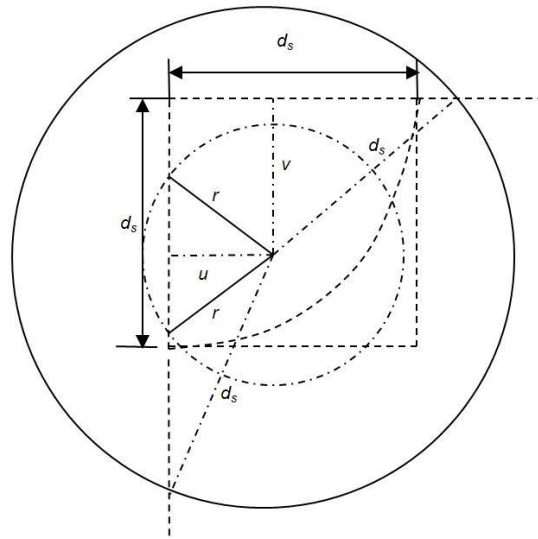


Figure 4.12. The smaller DR within the DA and the effective DR used in the computation of the CDF of  $r$  when  $A = c$ , the AP is within the distance  $d_s$  from the corner of the DA, and  $\min(u, v) \leq r \leq \max(u, v)$ .

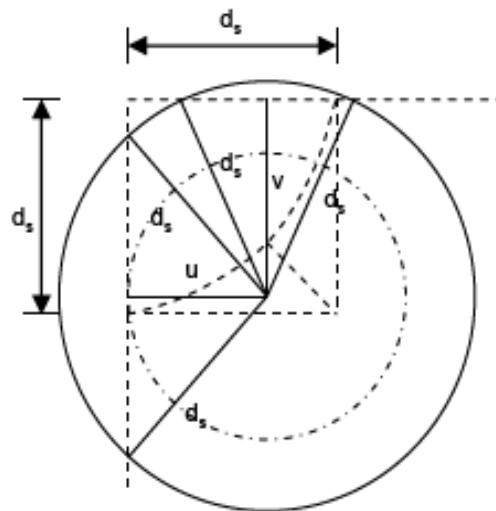


Figure 4.13. The smaller DR within the DA and the effective DR used in the computation of the CDF of  $r$  when  $A = c$ , the AP is further than the distance  $d_s$  from the corner of the DA, and  $0 \leq r \leq \min(u, v)$ .

Figure 4.12, Figure 4.14, Figure 4.15, and Figure 4.16 show the shapes of the area with radius  $r$  from the AP inside the effective DR and the effective DR when the AP is within the distance  $d_s$  from the corner of the deployment area. In Figure 4.14, the area with radius  $r$  from the AP inside the effective DR is a full circle when  $r$  is less than the minimum of  $u$  and  $v$ , which in this case is  $u$ . The effective DR for when the AP is within the distance  $d_s$  from the corner of the deployment area, is only partially

inside the deployment area as shown in all four figures. Note that the r.v.'s  $u$  and  $v$  represent the random distances from the AP to the side and the top borders of the deployment area respectively. When  $r$  is more than  $u$  or  $\min(u, v)$  but less than the maximum of  $u$  and  $v$  which is  $v$  in this case, the area with radius  $r$  from the AP inside the effective DR is not a complete circle and it becomes a different shape as illustrated in Figure 4.12. Once  $r$  is more than  $v$  or  $\max(u, v)$  but smaller than the square root of  $u^2+v^2$  or the distance from the center of the DR to the corner, the area with radius  $r$  from the AP inside the effective DR also changes to another shape as shown in Figure 4.15. Finally when  $r$  is more than the square root of  $u^2+v^2$  but less than or equal to  $d_s$ , one has the area with radius  $r$  from the AP inside the effective DR in the same shape as the effective DR as displayed in Figure 4.16. Notice that in Figure 4.12, Figure 4.14, Figure 4.15, and Figure 4.16, the AP or the center of the DR is in the lower half of the subarea  $c$  if the subarea  $c$  is divided by the diagonal line in the subarea  $c$ . This is why  $\min(u, v)$  is  $u$  and  $\max(u, v)$  is  $v$ . However if the AP is in the upper half of the subarea  $c$ ,  $\min(u, v)$  then becomes  $v$  and  $\max(u, v)$  becomes  $u$ . When one derives the CDF of  $r$  for the case  $A = c$ , it is mathematically necessary to differentiate these two variables  $u$  and  $v$ . Hence when computing the area with radius  $r$  from the AP inside the effective DR and the area of the effective DR for the condition  $A = c$ , one has to consider the scenarios in which the AP is in the lower and the upper parts of the subarea  $c$ . This is in addition to the scenarios for all the values of  $r$  relative to  $\min(u, v)$ ,  $\max(u, v)$ , and  $d_s$ , and also the scenarios where the distance from the AP to the corner of the deployment area is less or more than  $d_s$ .

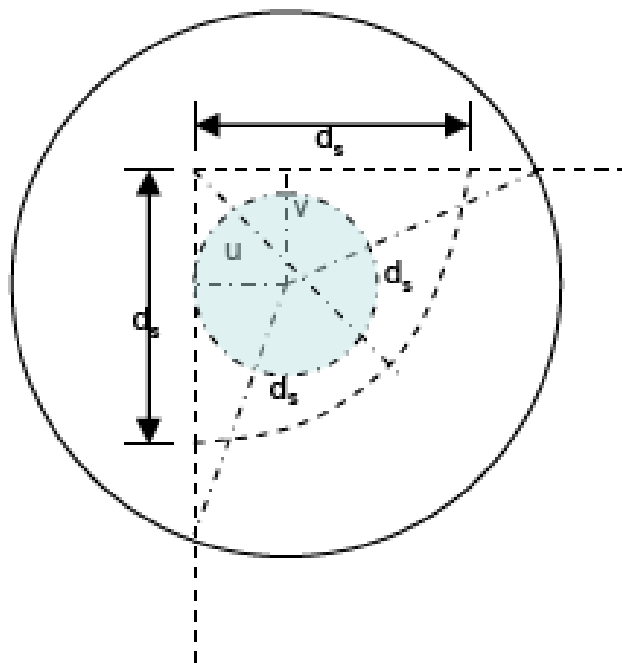


Figure 4.14. The smaller DR within the DA and the effective DR used in the computation of the CDF of  $r$  when  $A = c$ , the AP is within the distance  $d_s$  from the corner of the DA, and  $0 \leq r \leq \min(u, v)$ .

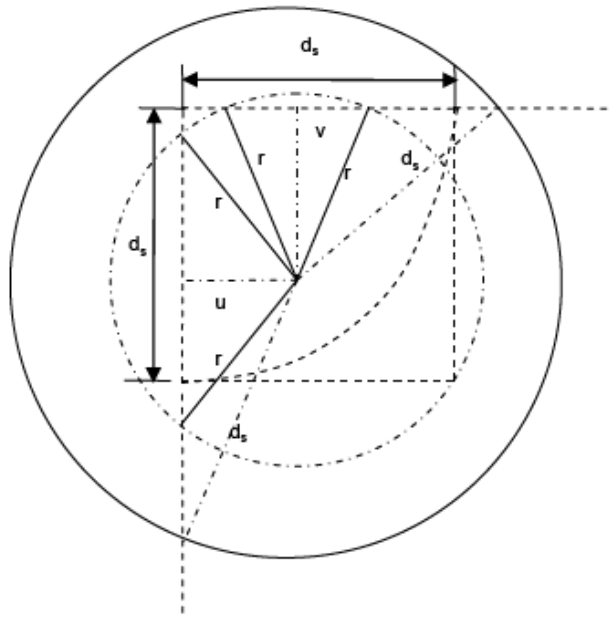


Figure 4.15. The smaller DR within the DA and the effective DR used in the computation of the CDF of  $r$  when  $A = c$ , the AP is within the distance  $d_s$  from the corner of the DA, and  $\max(u, v) \leq r \leq \sqrt{u^2 + v^2}$ .

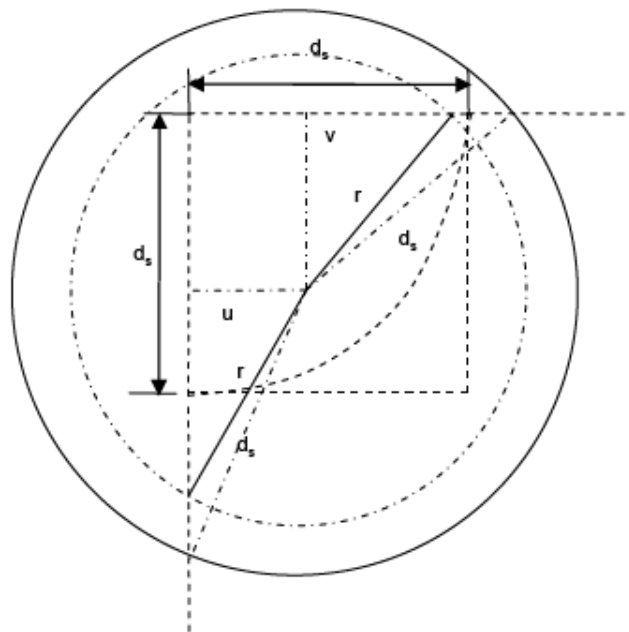


Figure 4.16. The smaller DR within the DA and the effective DR used in the computation of the CDF of  $r$  when  $A = c$ , the AP is within the distance  $d_s$  from the corner of the DA, and  $\sqrt{u^2 + v^2} \leq r \leq d_s$ .

Let  $C$  be the continuous r.v. for the distance from the AP to the corner of the deployment area. Now consider the shapes of the area with radius  $r$  from the AP inside the effective DR and the effective DR for all scenarios of  $r$  when  $C \geq d_s$ . In this case, the effective DR is of a different shape than what one has found when  $C < d_s$ . Figure 4.13, Figure 4.17, and Figure 4.18 illustrate the effective DR when  $C \geq d_s$ . the area with radius  $r$  from the AP inside the effective DR is a complete circle when  $r \leq \min(u, v)$  which again is  $u$ , because the AP is in the lower half of the subarea  $c$ . This is shown in Figure 4.13. Note again that, just like when  $C < d_s$ , one also has to separately consider the two scenarios where the AP is in the lower and the upper parts of the subarea  $c$  when  $C \geq d_s$ . When  $\min(u, v) < r \leq \max(u, v)$ , the area with radius  $r$  from the AP inside the effective DR becomes a different shape as illustrated in Figure 4.17. In the last scenario of  $r$ , which is  $\max(u, v) < r \leq d_s$ , it can be seen in Figure 4.18 that the shape the area with radius  $r$  from the AP is the same as the one of the effective DR.

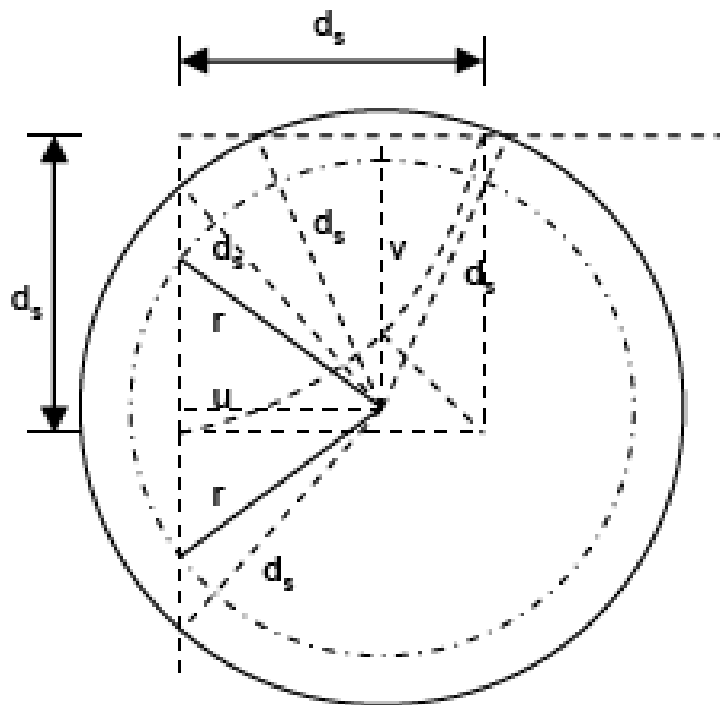


Figure 4.17. The smaller DR within the DA and the effective DR used in the computation of the CDF of  $r$  when  $A = c$ , the AP is further than the distance  $d_s$  from the corner of the DA, and  $\min(u, v) \leq r \leq \max(u, v)$ .

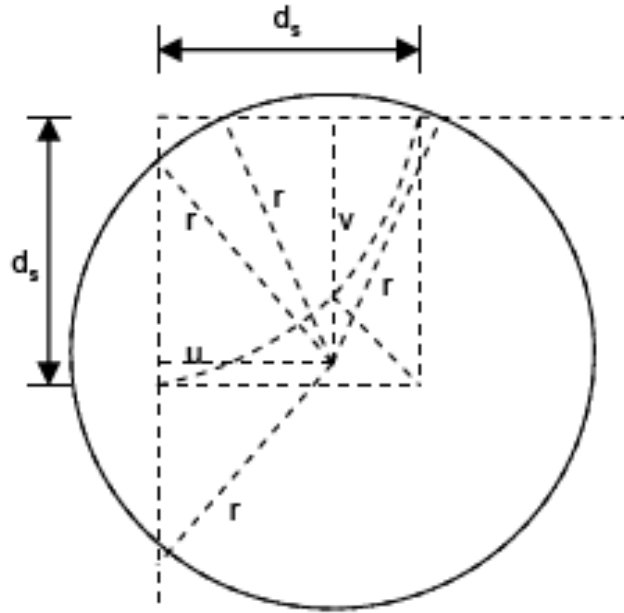


Figure 4.18. The smaller DR within the DA and the effective DR used in the computation of the CDF of  $r$  when  $A = c$ , the AP is further than the distance  $d_s$  from the corner of the DA, and  $\max(u, v) \leq r \leq d_s$ .

After considering the geometry of all possible scenarios and given  $u$  and  $v$ , let  $AD_{cLess}$  and  $AD_{cMore}$  be the areas of the effective DR in SR  $c$  when the distance to the corner is less than  $d_s$  and more than  $d_s$  respectively. By geometry, one can write,

$$AD_{cLess} = uv + \frac{u\sqrt{d_s^2 - u^2}}{2} + \frac{v\sqrt{d_s^2 - v^2}}{2} + \left(1 - \frac{\cos^{-1}\left(\frac{u}{d_s}\right) + \cos^{-1}\left(\frac{v}{d_s}\right) + \frac{\pi}{2}}{2\pi}\right)\pi d_s^2 \quad (4.20)$$

$$AD_{cMore} = u\sqrt{d_s^2 - u^2} + v\sqrt{d_s^2 - v^2} + \left(1 - \frac{\cos^{-1}\left(\frac{u}{d_s}\right) + \cos^{-1}\left(\frac{v}{d_s}\right)}{\pi}\right)\pi d_s^2 \quad (4.21)$$

where  $u$  and  $v$  are continuous r.v.'s for the distances from the AP to the two borders of the deployment area. One can then apply the equations of these areas in (4.20) and (4.21) in the derivations of the CDF's of  $r$ , and hence the pdf's of  $r$ .

Let  $F_c(r)$  denote the CDF of  $r$  in SR  $c$  for a given pair of  $u$  and  $v$ . One has,

$$F_c(r) = F_c(r|less)P(less) + F_c(r|more)P(more) \quad (4.22)$$

where  $P(less)$  and  $P(more)$  are the probabilities that the distance  $C$  is less and more than  $d_s$  respectively. By geometry,  $P(less) = (1/4)\pi d_s^2/d_s^2 = \pi/4$  and thus  $P(more)$  equals  $(1 - \pi/4)$ . From equation (4.22), correspondingly, one can write,

$$f_c(r) = f_c(r|less)P(less) + f_c(r|more)P(more) \quad (4.23)$$

Both  $F_c(r|less)$  and  $F_c(r|more)$  can be expanded further as follows:

$$\begin{aligned} F_c(r|less) &= F_c(r|less, u < v)P(u < v|less) \\ &\quad + F_c(r|less, u \geq v)P(u \geq v|less) \end{aligned} \quad (4.24)$$

$$\begin{aligned} F_c(r|more) &= F_c(r|more, u < v)P(u < v|more) \\ &\quad + F_c(r|more, u \geq v)P(u \geq v|more) \end{aligned} \quad (4.25)$$

By geometry,  $P(u < v|less) = (1/8)\pi d_s^2/(1/4)\pi d_s^2 = 1/2$ .

Hence,  $P(u \geq v|less) = 1/2$ . Similarly,  $P(u < v|more) = ((d_s^2 - (1/4)\pi d_s^2)/2)/(d_s^2 - (1/4)\pi d_s^2) = 1/2 = P(u \geq v|more)$  as well.

From equations (4.24) and (4.25), it follows that,

$$\begin{aligned} f_c(r|less) &= f_c(r|less, u < v)P(u < v|less) \\ &\quad + f_c(r|less, u \geq v)P(u \geq v|less) \end{aligned} \quad (4.26)$$

$$\begin{aligned} f_c(r|more) &= f_c(r|more, u < v)P(u < v|more) \\ &\quad + f_c(r|more, u \geq v)P(u \geq v|more) \end{aligned} \quad (4.27)$$

As explained earlier, when the distance  $C$  is less than  $d_s$  as shown in Figure 4.12, Figure 4.14, Figure 4.15, and Figure 4.16,  $F_c(r|less, u < v)$  and  $F_c(r|less, u \geq v)$  are



determined for four cases of  $r$ . They are when  $0 \leq r \leq \min(u, v)$ ,  $\min(u, v) < r \leq \max(u, v)$ ,  $\max(u, v) < r \leq \sqrt{u^2 + v^2}$ , and  $\sqrt{u^2 + v^2} < r \leq d_s$ . Thus one writes,

$$F_c(r|less) = \frac{1}{2} \sum_{i=1}^4 F_{c1i}(r|less, u < v) + \frac{1}{2} \sum_{i=1}^4 F_{c1i}(r|less, u \geq v) \quad (4.28)$$

where each subscript  $c1i$  for  $1 \leq i \leq 4$  represents each of the four cases of  $r$  in the order as previously described. It turns out that,

$$F_{c11}(r|less, u < v) = F_{c11}(r|less, u \geq v) = \pi r^2 / AD_{cLess}. \quad (4.29)$$

Thus, one has,

$$f_{c11}(r|less, u < v) = f_{c11}(r|less, u \geq v) = (2\pi r) / AD_{cLess}. \quad (4.30)$$

Similarly, one can derive that,

$$f_{c12}(r|less, u < v) = (2\pi r - 2r \cos^{-1}(u/r)) / AD_{cLess} \quad (4.31)$$

$$f_{c12}(r|less, u \geq v) = (2\pi r - 2r \cos^{-1}(v/r)) / AD_{cLess} \quad (4.32)$$

$$f_{c13}(r|less, u < v) = f_{c13}(r|less, u \geq v) = (2\pi r - 2r \cos^{-1}(u/r) - 2r \cos^{-1}(v/r)) / AD_{cLess} \quad (4.33)$$

$$\begin{aligned}
f_{c14}(r|less, u < v) &= f_{c14}(r|less, u \geq v) \\
&= (3\pi r - 2rcos^{-1}(u/r) \\
&\quad - 2rcos^{-1}(v/r))/2AD_{cLess}. \tag{4.34}
\end{aligned}$$

As a result, one now have computed  $f_c(r|less)$  needed for  $f_c(r)$  in equation (4.23).

Similarly for the case when the distance  $C$  is more than  $d_s$ ,  $F_c(r|more, u < v)$  and  $F_c(r|more, u \geq v)$  are computed for three cases of  $r$ . From Figure 4.13, Figure 4.17, and Figure 4.18, they are when  $0 \leq r \leq \min(u, v)$ ,  $\min(u, v) < r \leq \max(u, v)$ , and  $\max(u, v) < r \leq d_s$ . As a result, one has,

$$\begin{aligned}
F_c(r|more) &= \frac{1}{2} \sum_{i=1}^3 F_{c2i}(r|more, u < v) \\
&\quad + \frac{1}{2} \sum_{i=1}^3 F_{c2i}(r|more, u \geq v) \tag{4.35}
\end{aligned}$$

where here, each subscript  $c2i$  for  $1 \leq i \leq 3$  represents each of the three cases of  $r$ . One then obtains,

$$\begin{aligned}
f_{c21}(r|more, u < v) &= f_{c21}(r|more, u \geq v) \\
&= (2\pi r)/AD_{cMore} \tag{4.36}
\end{aligned}$$

$$\begin{aligned}
f_{c22}(r|more, u < v) &= (2\pi r - 2rcos^{-1}(u/r))/ \\
&\quad AD_{cMore} \tag{4.37}
\end{aligned}$$

$$\begin{aligned}
f_{c22}(r|more, u \geq v) &= (2\pi r - 2rcos^{-1}(v/r))/ \\
&\quad AD_{cMore} \tag{4.38}
\end{aligned}$$

$$\begin{aligned}
f_{c23}(r|more, u < v) &= f_{c23}(r|more, u \geq v) \\
&= (2\pi r - 2rcos^{-1}(u/r) \\
&\quad - 2rcos^{-1}(v/r))/AD_{cMore}. \tag{4.39}
\end{aligned}$$

These are used to find  $f_c(r|more)$  in equation (4.23). One now has derived  $f_c(r)$  for a pair of  $u$  and  $v$ . Subsequently because the joint p.d.f.'s of  $u$  and  $v$  are  $1/(\pi d_s^2/4)$  and  $1/(d_s^2(1 - \pi/4))$  when the distance  $C$  is less than  $d_s$  and more than  $d_s$  respectively, it

yields that,

$$\begin{aligned}
\varepsilon_{c,m,k} = & C_1 \iiint (1 - D(r))f_c(r|less, u < v)drdvdu \\
& + C_1 \iiint (1 - D(r))f_c(r|less, u \geq v)drdvdu \\
& + C_2 \iiint (1 - D(r))f_c(r|more, u < v)drdvdu \\
& + C_2 \iiint (1 - D(r))f_c(r|more, u \geq v)drdvdu
\end{aligned} \tag{4.40}$$

where  $C_1 = (\pi/4)(1/2)(8/\pi d_s^2)$ , and  $C_2 = (1 - \pi/4)(1/2) \times \{1/[(1-\pi/4)(d_s^2/2)]\}$ . One then obtains,

$$\begin{aligned}
\varepsilon_{c,m,k} = & \left(\frac{1}{d_s^2}\right) \iiint (1 - D(r))f_c(r|less, u < v)drdvdu \\
& + \left(\frac{1}{d_s^2}\right) \iiint (1 - D(r))f_c(r|less, u \geq v)drdvdu \\
& + \left(\frac{1}{d_s^2}\right) \iiint (1 - D(r))f_c(r|more, u < v)drdvdu \\
& + \left(\frac{1}{d_s^2}\right) \iiint (1 - D(r))f_c(r|more, u \geq v)drdvdu
\end{aligned} \tag{4.41}$$

where the bounds on the integrals correspond to all the cases of  $r$ 's for  $f_c(r|less, u < v)$ ,  $f_c(r|less, u \geq v)$ ,  $f_c(r|more, u < v)$ , and  $f_c(r|more, u \geq v)$ .

The closed-form expressions for both  $\varepsilon_{b,m,k}$  and  $\varepsilon_{c,m,k}$  cannot be found. Hence numerical integration is needed to evaluate both of them. However having analytical expressions for  $\varepsilon_{i,m,k}$ 's for all the three SRs, one can find each corresponding  $\beta_{i,m,k}$  and thus  $\gamma_i$  in equation (4.5). Then, finally, the analytical expression for the EDP at AP in a finite 2-D rectangular DA as expressed in equation (4.3) has been obtained. It is also worth noting that this analytical model can be applied to any other probabilistic sensing models as long as they are also a function of the distance  $r$  between the SN and the object to be detected. The derivation here can still be applied for those sensing models, because the probability distributions of  $r$  have already been derived here, and are ready to be used for the computation of the EDP that are based on those other models that are functions of the distance  $r$ .

## CHAPTER 5

### Verifications, Applications, and Discussions

This chapter presents the verifications of both analytical models with simulations, discussions of results, and examines the applications of these models. The verifications of both proposed mathematical models are carried out by comparing the numerical results from the models with those obtained from MATLAB simulations. Since the final forms of both mathematical models derived in this dissertation contain integrands whose antiderivatives are very hard or impossible to reduce, the numerical results from equation (**Error! Reference source not found.**) are obtained by Mathcad, which can compute numerical integrations. After the accuracy of both models have been verified, the numerical results are investigated more closely to gain more insight into the EDP and the EDSC. Then, the practical applications of the models are proposed and discussed in this chapter.

#### 5.1 Simulation Design for the Verification of Expected Detection Probability

On the computer used for simulations for this dissertation, Mathcad can only calculate up to the factorial of 170. Since the analytical expression for the EDP has factorial computations in it, and one of the input values for these factorial computations is the number of SNs deployed, it means that the numerical values for the proposed EDP mathematical models can only be obtained up to 170 SNs deployed. This puts a restriction on the kinds of scenarios in MATLAB that can be simulated to have meaningful comparisons.

The first goal for the simulations is to verify the accuracy of the proposed EDP mathematical model. Thus the MATLAB simulation is designed to test the accuracy at various number of SNs deployed, hence the different levels of node density for a fixed sensing range,  $d_s$ , and the fixed sensing parameter,  $\alpha_s$ , in a fixed size of the deployment area. The objective is to be able to observe the accuracy of the EDP model at various levels of EDP. Thus, first, the appropriate levels of  $d_s$  and  $\alpha_s$  for a deployment area that can offer various values of the average detection probability from the MATLAB simulations must be found.

After successfully be able to investigate the accuracy of the EDP for this particular set of values of  $d_s$ ,  $\alpha_s$ , and the deployment area size, the next batch of simulations are carried out by varying the levels of node density and both  $d_s$  and  $\alpha_s$  for various sizes and dimensions of the deployment area until the accuracy of the EDP model is satisfactorily confirmed.

All in all, depending on the size of the deployment field, the number of deployed SNs is varied from 4 to 170. The maximum number of SNs deployed is capped at 170, because in equation (**Error! Reference source not found.**) there are factorial computations based on this maximum number as stated earlier. This also

results in lines in some figures presented in this dissertation to appear as if they are missing some data. Nevertheless, an enough variety of simulation scenarios can be carried out to validate the mathematical expression for the EDP. The random placements of SNs with uniform distribution are simulated on three different sizes of the DA, 50x50, 70x70, and 100x100. The sensing range of all the SNs,  $d_s$ , is set at 10, while the parameter  $\alpha_s$  in equation (**Error! Reference source not found.**) is assumed to be 4.

## 5.2 Simulation Implementation for the Verification of Expected Detection Probability

The values of the average detection probability (ADP) at an arbitrary point (AP) from MATLAB simulations are calculated in two ways. One is by picking an AP from each of the 100,000 random simulations and averaging it. The other is by picking 100,000 APs from one simulation and then taking the average. From these results, it has been found that both methods yield practically the same ADP numerical results and are interchangeable. This shows ergodicity of these MATLAB simulations. These average numbers of the detection probability at an AP are then used to demonstrate the correctness of the analytical expression found in equation (**Error! Reference source not found.**) by comparing them with the expected values computed in Mathcad based on the analytical expression.

Thanks to ergodicity of these simulations, the final version of the MATLAB simulation program used to find ADP picks 100,000 APs from one simulation and averages them. In MATLAB, the simulation starts by using the uniform random distribution for the values of x- and y- coordinates for the placement location of each SN, then uniformly randomly picks 100,000 APs using the same MATLAB uniform distribution function. Note that the MATLAB uniform distribution function does not use initial seed, thus each iteration of the simulation is all different from the others. This MATLAB simulation takes the number of deployed SNs, the number of APs, the dimension of the deployment area, and values of  $d_s$  and  $\alpha_s$  as its inputs.

After uniformly picking 100,000 APs at random, the simulation program computes its detection probability from the SNs that are within the distance  $d_s$  based on the sensing model in (**Error! Reference source not found.**). Finally, the ADP can be calculated for this particular set of input values of the simulation program.

## 5.3 Verification of Expected Detection Probability

The correctness of the analytical expression is calculated by computing the discrepancy. This discrepancy is defined as the values of the EDP from our analytical expression minus those of the average from the MATLAB simulations. Figure 5.1 shows these discrepancies versus the number of deployed SNs per the unit area of the DA or the Node Density (ND). Figure 5.2 illustrates the discrepancies versus the average values from the simulations. The reason the ADPs from the simulations are used on the x-axis in Figure 5.2 is because the ADPs represent the real practical values that the proposed analytical model is measured up against.

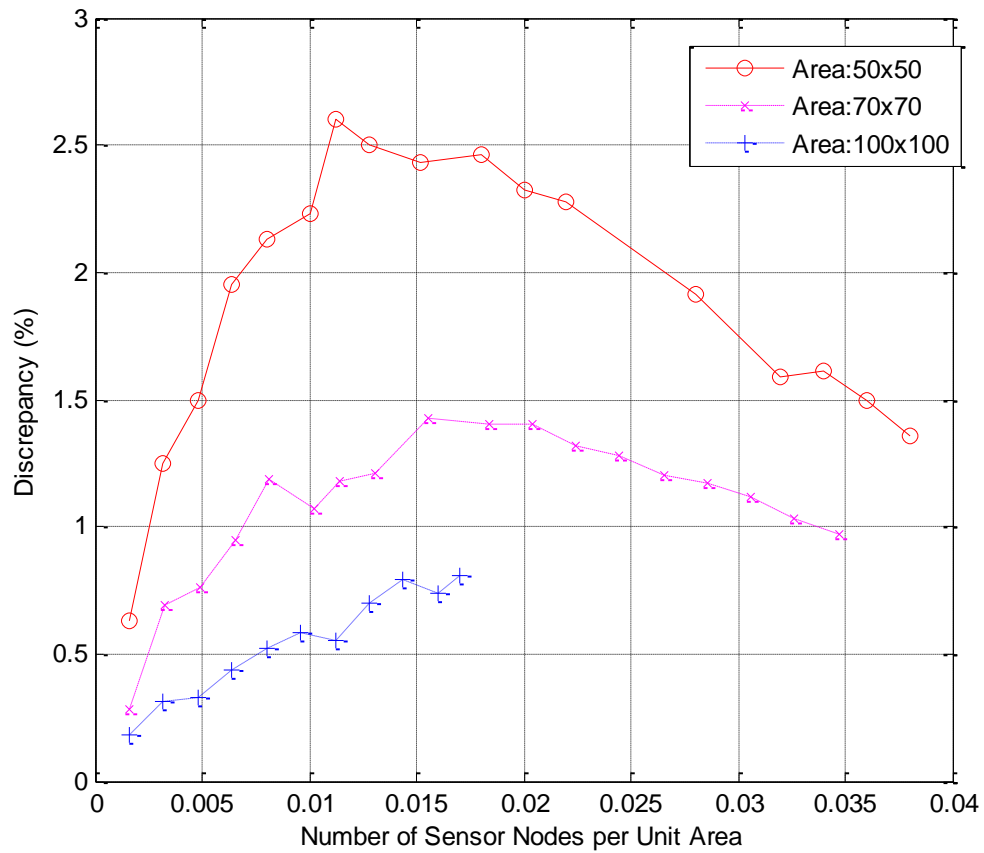


Figure 5.1. Discrepancies between analytical estimations and the simulation results for EDP at each level of ND

From Figure 5.1 and Figure 5.2, it can be said that the proposed mathematical expression for the EDP is strikingly accurate. As shown in both Figure 5.1 and Figure 5.2, the proposed formula never overestimates the ADP more than three percent in all scenarios. Moreover, as the ND or the ADP increases, the overestimation plateaus at no more than 1.5 percent for the node density above 0.035. In some cases, the discrepancies are practically zero or very close to zero. The analytical expression also becomes more accurate when the DA gets bigger. The reason for this is because for bigger areas, the impacts from the border effects in our model are lessened as the SR  $a$  in our calculation gets bigger. From these numerical results, it can be concluded that the proposed analytical expression is an accurate prediction for the EDP at any AP in a rectangular deployment plane.

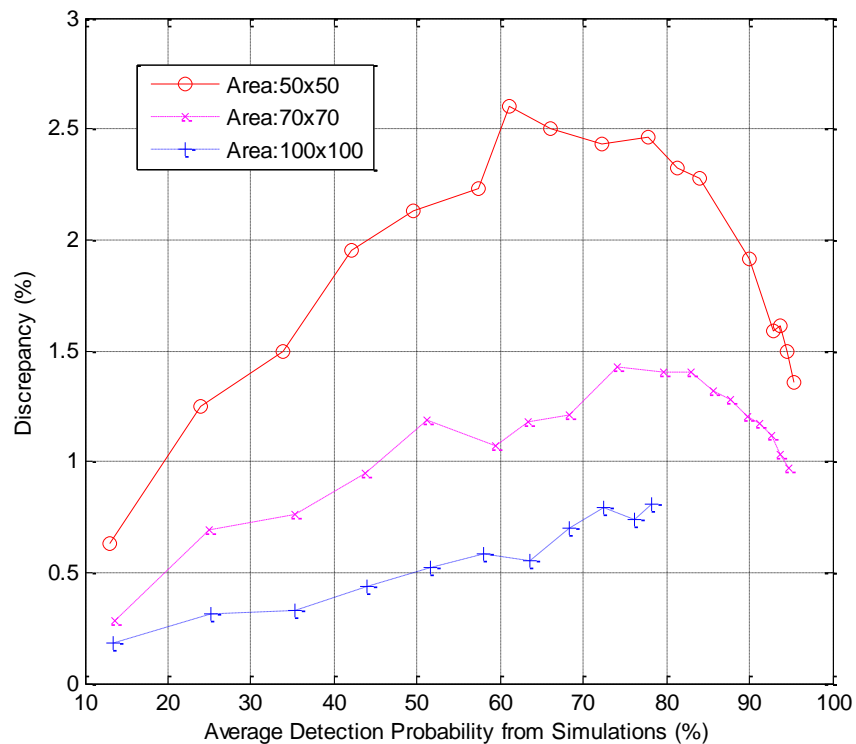


Figure 5.2. Discrepancies between analytical estimations and the simulation results at each level of ADP from simulations.

#### 5.4 Simulation Design for the Verification of Expected Degree of Sink Connectivity

The mathematical model for the EDSC also has factorial computations in it, and one of its input values for these factorial computations is also the number of SNs deployed. Thus, the Mathcad restriction of the maximum 170 factorials still applies here. Hence some figures appear to be missing partial data. However, more scenarios for the EDSC model verification can be simulated in meaningful ways than those for EDP verification.

As in the case of the simulation design for the verification of EDP, the first goal for the simulations here is to establish the accuracy of the proposed EDSC mathematical model. Again, the objective is to be able to inspect the accuracy of the EDSC model at various levels of EDSC. Therefore, first, the appropriate levels of  $r_t$  for a deployment area that can offer various values of the average degree of sink connectivity from the MATLAB simulations must be identified.

Again after successfully be able to study the accuracy of the EDSC for this particular set of values of  $r_t$ , and the deployment area size, more simulations are carried out by varying the levels of node density and  $r_t$  for various sizes and dimensions of the deployment area until the accuracy of the EDSC model is substantiated.

In the MATLAB simulations for the verification of the EDSC model, the number of deployed SNs is varied from 17 to 170. The transmission range of the SNs,  $r_t$ , is varied from 7 to 15 for a DA of 40x40. When  $r_t$  is fixed at 10, the size of a square deployment area ranges from 35x35 to 70x70. Also for  $r_t$  equals 10, the shape of the deployment area is varied from a square of 40x40 to a rectangle of 40x50 and 40x60.

## 5.5 Simulation Implementation for the Verification of Expected Degree of Sink Connectivity

The MATLAB simulation program for the verification of EDSC takes the number of deployed SNs, the dimension of the deployment area, the transmission range  $r_t$ , and the number of simulations as the inputs of the function. The degree of SC for each MATLAB simulation is the minimum NoCSNNs found among all the SNs that cannot directly transmit to the sink. Each value of the average degree of SC from MATLAB is calculated from 5,000 experiments or simulations. The discrepancy between the analytical calculation values and these experimental results is defined as the percentage difference. It is the analytical estimate from the EDSC model minus the average value of the sink connectivity from the MATLAB experiments times 100 and divided by the average MATLAB number.

The simulation program first starts by placing the sink at the center of the deployment area according to its dimension. It then runs each experiment or simulation by initially placing SNs with uniform distribution function as described for the simulation program for computing the ADP in section 5.2. The program then computes the distance from all the SNs to the sink to identify the SNs that cannot directly transmit to the sink. For all the SNs that cannot directly transmit to the sink, the program finds the SNs that are within the transmission range of each of them. These are neighboring SNs. Then from these neighboring SNs of each SN, the program determines the neighboring SNs that are closer to the sink than itself. The final part of the program finds the smallest number of these NoCSNNs for all these SNs that cannot directly transmit to the sink. Next, as mentioned earlier, the average degree of sink connectivity is then found by averaging over 5,000 MATLAB experiments.

## 5.6 Verification of Expected Degree of Sink Connectivity

It is found that in the majority of scenarios simulated, the analytical predictions overestimate the average degree of SC. In others, they slightly underestimate. As the transmission range  $r_t$  gets bigger relative to the size of the deployment field, the overestimate becomes bigger. Likewise, as  $r_t$  becomes smaller, the overestimate gets smaller and smaller to the point where the discrepancies become an underestimate. The degree of this underestimate also increases as  $r_t$  decreases for a fixed size of the DA. Figure 5.3 illustrates this point for a fixed DA of 40x40 and  $r_t$  varying from 7 to 15. Figure 5.3 also shows that the discrepancies vary from about +4.7% to -2.4% when the ND is higher than 0.06 for  $r_t = 7$  to  $r_t = 12$ . For  $r_t = 10$ , the theoretical predictions are most accurate as the ND increases. The discrepancies



for  $r_t = 10$  are close to zero for ND higher than 0.8 as shown in Figure 5.4. This means that the proposed analytical model for the EDSC is accurate enough in general and can be strikingly accurate for an appropriate set of  $r_t$  and the deployment area size. Specifically, the appropriate ratio of the dimension of the square deployment area to the transmission range,  $r_t$ , is around 4 as shown in Figure 5.6.

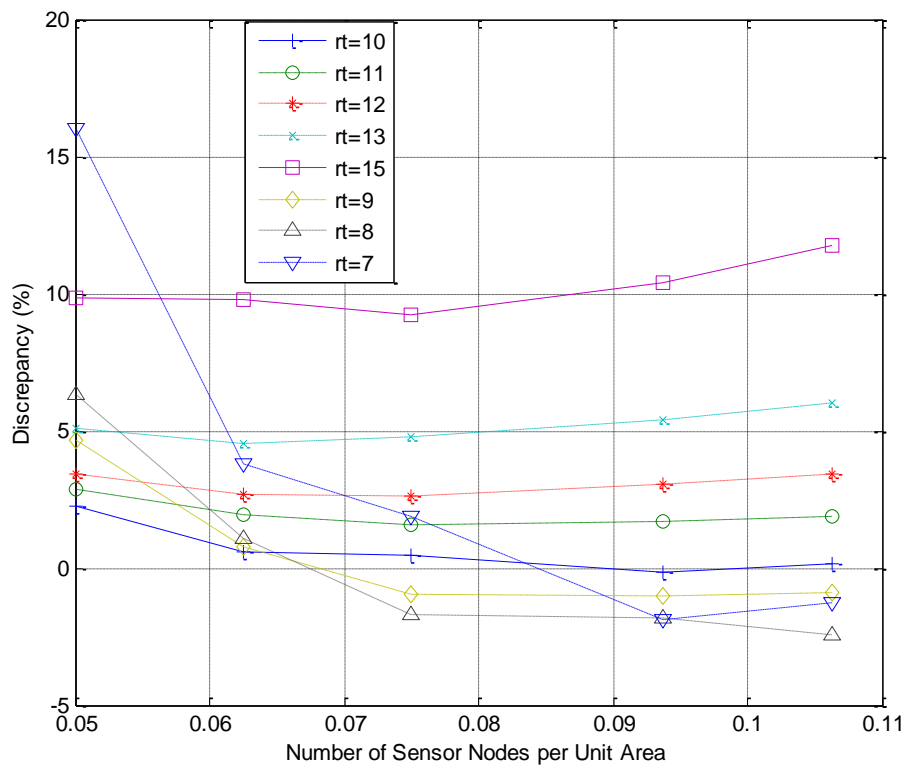


Figure 5.3. Percentage differences between analytical values and simulation results for EDSC at each level ND for various  $r_t$  and fixed DA 40x40.

Figure 5.4 shows the discrepancies for  $r_t = 10$  and a number of different square DAs. It shows that for the ND higher than 0.6, the discrepancies are close to zero, and as the more SNs are deployed, the more accurate the analytical estimations for the proposed EDSC become. It can also be observed that as the DA becomes smaller relative to  $r_t$ , the overestimate becomes bigger. When the DA gets bigger, the discrepancies change to underestimate. This is in accordance with what has been observed in Figure 5.3.

The reason for the overestimate is suspected to be due to the border effects on the overlap area in the calculation in equation (3.5). The probability in equation (3.5) does not take into account the change of the overlap area for SNs close to the border. This results in overestimating of our analytical model. When  $r_t$  is big relative to the DA, the overlap area used in equation (3.5) becomes bigger for SNs close to the borders than it actually is. This results in overestimation for relatively big  $r_t$ . As for the underestimate, it can be speculated that it is resulted from the compromise on

the i.i.d. assumption of observations in order stats used to derive the EDSC model. When  $r_t$  is relatively small compared to the DA, the SNs which are equivalent to the observations in order stats become more and more non-identically distributed. It is reasonable to assume that this is the reason why underestimate is observed for relatively small  $r_t$ . To test this hypothesis about the underestimation, observations are made for the discrepancies for  $r_t = 10$  while the shape of the DA is varied. Figure 5.5 shows that as the DA becomes more rectangular hence resulting in SNs to become more non-identically distributed, the discrepancies change from overestimate for DA 40x40 to underestimate in area 40x50 and 40x60. Figure 5.5 though still shows that the proposed formula for EDSC becomes more accurate with the discrepancies close to zero when the ND is high enough which is around at 0.04.

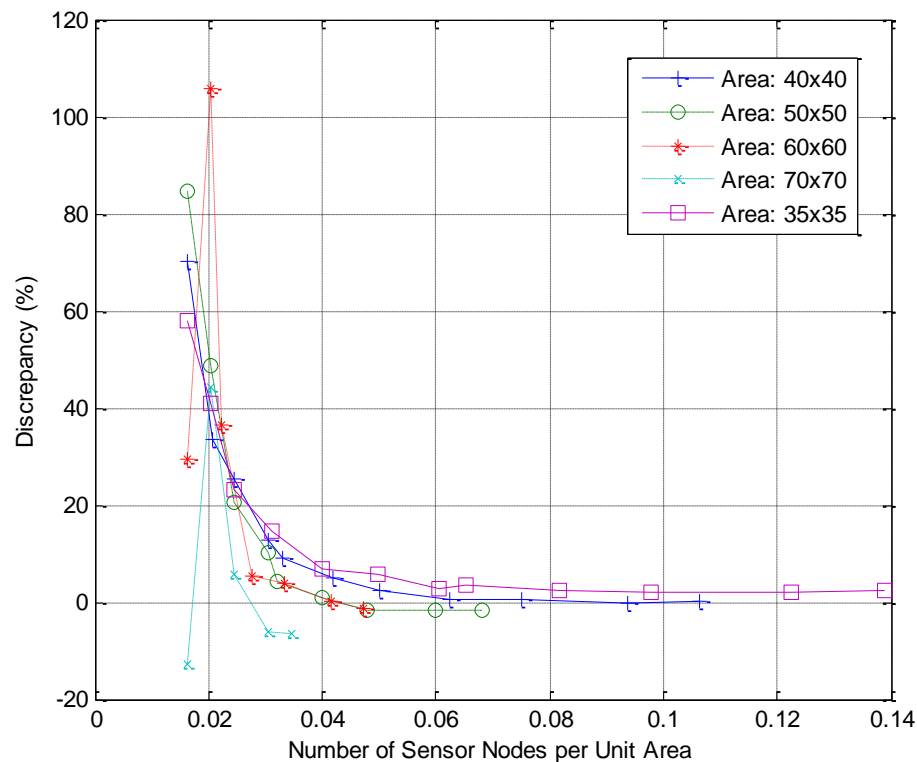


Figure 5.4. Percentage differences between analytical values and simulation results for EDSC at each level ND for square DA of various sizes and  $r_t = 10$ .

From Figure 5.4 and Figure 5.5, the discrepancies between analytical estimates and those from MATLAB experiments are high for ND that is lower than 0.04. However, these high levels of discrepancies are not worrying, because they occur when the average degree of SC is much lower than one. Figure 5.6 demonstrates this. It can be seen from Figure 5.6 that for average degree of SC that equals or is higher than one, the discrepancies are less than 5% and become smaller and smaller for the higher average degrees. Since in practice, when the analytical model is used for pre-deployment network planning, one is only interested to know how many SNs are

needed for each degree of SC. The big discrepancies that happen when the average degree of connectivity is less than one are not concerning. In conclusion, the proposed analytical model of EDSC is accurate when it matters.

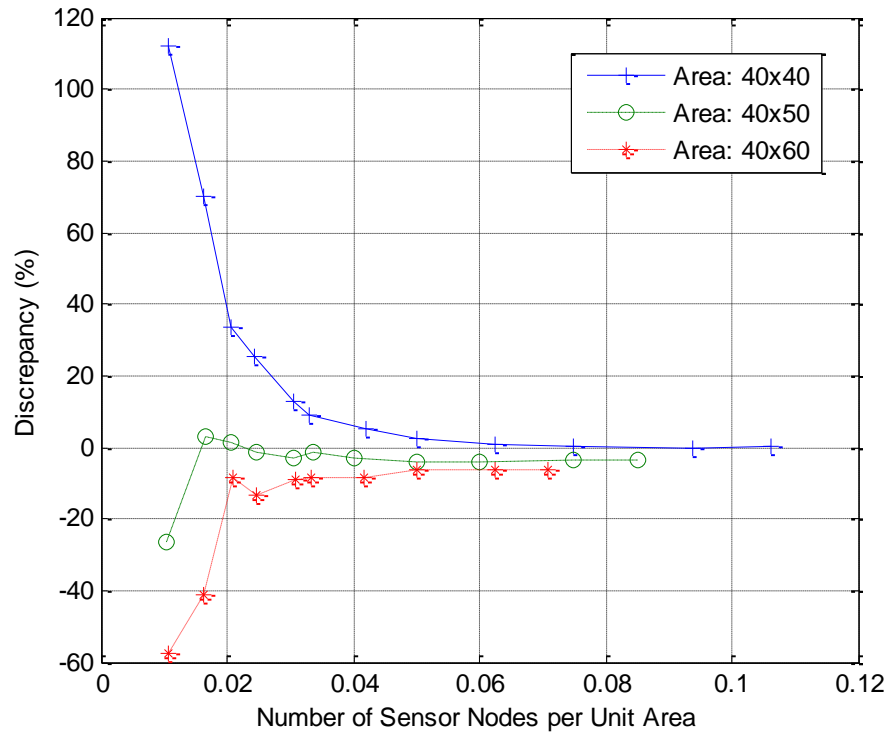


Figure 5.5. Percentage differences between analytical values and simulation results for EDSC at each level ND for DA of various shapes and  $r_t = 10$ .

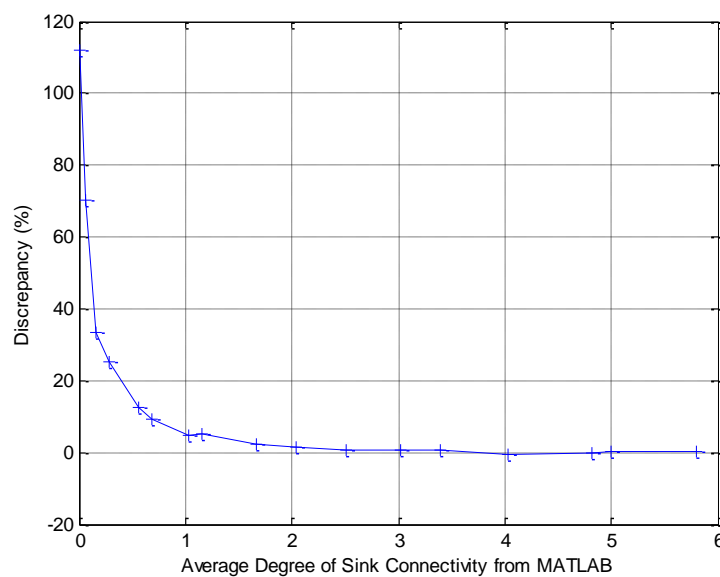


Figure 5.6. Percentage differences between analytical values and simulation results for EDSC at different average degrees of SC for DA 40x40 and  $r_t = 10$ .

## 5.7 Discussions and Applications of the Models

The model for the EDP is accurate for all the three simulation scenarios that are run, while the EDSC is accurate when the ND is high enough and the transmission range  $r_t$  is not too big or too small for a DA. This means that when one would like to determine the levels of coverage and connectivity from a random deployment of object-detecting SNs, the environments for which both the proposed analytical expressions are suitable at the same time are clustered networks. Clustered networks are networks in which nodes are grouped in clusters with cluster heads which usually act as relay nodes situated in the middle of the clusters. The sizes of the clusters are also typically not big relative to  $r_t$ . This scenario would fit perfectly with where the proposed models in this dissertation can give the most accurate predictions. Moreover, although the analytical expressions in this dissertation do not render their inverse counterparts, one can still estimate the values of these parameters needed for certain degrees of probabilistic coverage and sink connectivity from the graphs of EDP and EDSC with each of these parameters.

Based on work in [4], the models proposed in the dissertation can also help determine the required active-to-sleep ratio in uncoordinated sleep scheduling for the desired degrees of coverage and connectivity. Using the graphs from the proposed analytical expressions, one can find the number of SNs required for certain degrees of coverage and connectivity. This number is then used as the expected number of active nodes in an uncoordinated sleep scheduling scheme to calculate the required active-to-sleep ratio [4]. Similarly, both the mathematical expressions found in this dissertation can predict coverage and connectivity for any other applications or scenarios that know the number of active SNs at any time. This also means if one can model the probability that a SN dies over time, the proposed formulae can be used to determine the degrees of both coverage and connectivity over any period of active operation of the networks one is interested in. This could help in the studies of the fault tolerance capability of WSNs over a period of time. Since the proposed formulae are based on uniform and random deployment of SNs, they can also be used to provide a snapshot of EDP and EDSC for networks of SNs with random mobility.

It also has been observed that, for connectivity, the higher EDSC, the more likely the traffic congestion can happen. Thus, this dissertation proposes to modify the uncoordinated sleep scheduling scheme by limiting EDSC as  $C_{min} \leq EDSC \leq C_{max}$  and EDP as  $S_{min} \leq EDP$  where  $C_{min}$  and  $S_{min}$  are the minimum degree of sink connectivity and minimum level of coverage required respectively, while  $C_{max}$  is the maximum degree of sink connectivity for the acceptable level of traffic congestion. From these two constraints one can get the number of active nodes used to find the active-to-sleep ratio where the mean time for sleeping is not greater than the maximum delay allowed for the network.

The EDP and EDSC formulae can also be utilized to find the type of homogeneous SNs that minimizes the deployment cost by constraining  $EDP \geq S_{min}$  and  $EDSC \geq C_{min}$ . For SN type  $i$ , the deployment cost optimization equation is  $\min_i cost_i = \min_i N_i c_i$  where  $N_i$  is the number of SNs of type  $i$  calculated from  $\max_{N_i} [\min_{N_i} EDP \geq S_{min}, \min_{N_i} EDSC \geq C_{min}]$  and  $c_i$  is the cost of one SN of type  $i$

depending on  $d_s$ ,  $\alpha_s$ , and  $r_t$ .

From numerical results of both of the proposed mathematical models, it can also be observed that at the same level of ND, the EDP is largely the same for all sizes of the square DA. This is shown in Figure 5.7. Furthermore, one can see a diminishing return from the number of SNs deployed for the EDP. Figure 5.8 shows that rate of increase of EDP is slower for higher number of SNs deployed. For larger DAs, this diminishing return in expected level of coverage is however less noticeable.

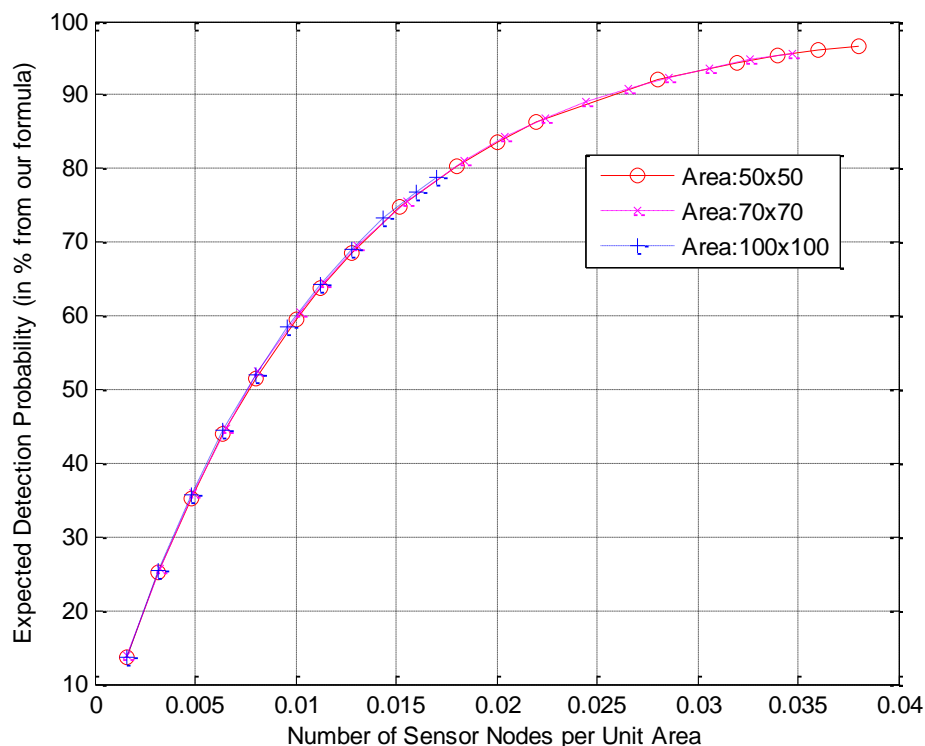


Figure 5.7. EDP vs ND for various DA sizes with  $d_s = 10$  and  $\alpha_s = 4$ .

For the EDSC, the numerical results from the proposed model show that the first degree of connectivity requires the biggest number of SNs. The subsequent degrees require fewer SNs. However, after a certain degree of SC, the number of SNs needed for the next degree plateaus to a constant. This is illustrated in Figure 5.9. Figure 5.9 also shows that on average several SNs have to fail to reduce the degree of SC by one. This is different from the strict definition of  $k$ -connectivity where  $k - 1$  SNs die, all the remaining SNs still have a connectivity left. In Figure 5.9, it shows that for an expected  $k$  degrees of SC, a greater number of SNs than  $k - 1$  must fail in order for the remaining SNs to have just a connectivity left on average. In terms of the relationship between the EDSC and the ND, taking into account of the accuracy observations of our EDSC formula shown in Figure 5.4, Figure 5.10 shows that, with the same ND, the EDSC is approximately the same for all DA sizes. There is also a linearity between the EDSC and the ND. It can also be postulated that the bigger  $r_t$ , the higher the slope of this

linearity.

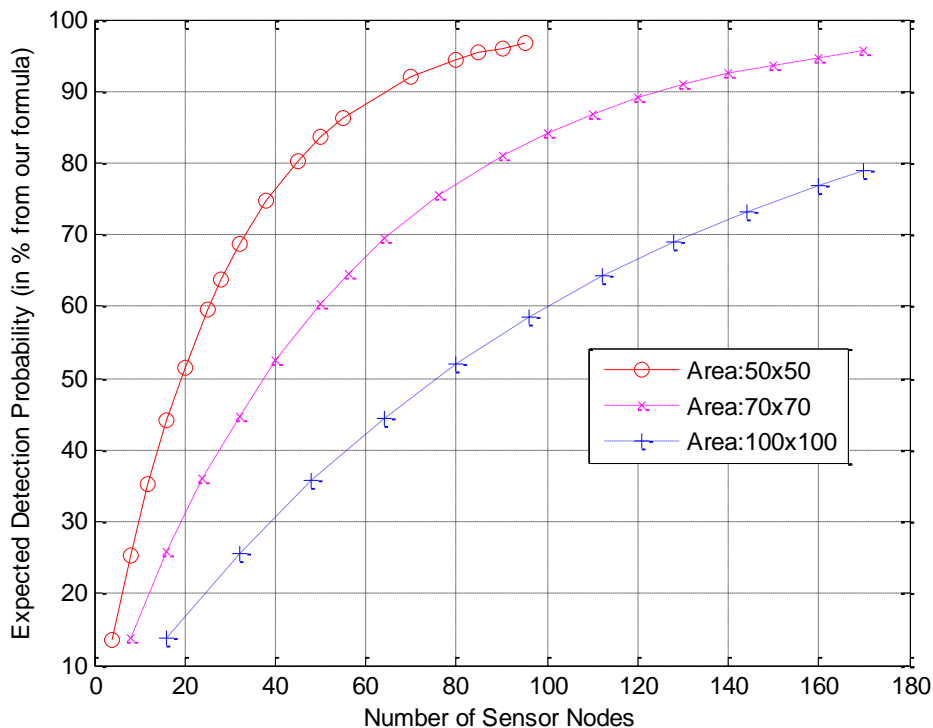


Figure 5.8. EDP vs number of deployed SNs for various DA sizes with  $d_s = 10$  and  $\alpha_s = 4$ .

This dissertation finds both the EDP and the EDSC models. However, unlike majority of previous analytical work on joint coverage and connectivity, the studies in this dissertation do not derive these based on the relationship between the sensing and communication ranges. The reason for this, as mentioned earlier in this dissertation, is because the sensing model in this research is not the traditional binary disk, while the communication model is. So both the proposed models are derived and thus can be computed independently. This helps in scenarios where the sensing and communication models are not alike.

When one tries to investigate the numerical results of both of the proposed analytical expressions jointly, one finds that knowing the degree of one does not tell one about the other. Figure 5.11 shows the EDSC for the transmission range  $r_t = 10$  with the EDP at various values of sensing range  $d_s$  and the parameter for DP distribution  $\alpha_s$  in a DA of  $40 \times 40$ . One can see that there are no relationships between the degrees of coverage and SC regardless of the ratio of sensing and communication ranges. At a certain EDSC, there are varying levels of EDP that can be achieved depending on  $\alpha_s$  and  $d_s$ . When both sensing and communication models are binary and  $r_t \geq 2d_s$ , the relationship between sensing coverage and network connectivity is 1-to-1 [11]. However, when the sensing model is not binary but continuous-valued like the one in this dissertation while the connectivity model still is, the 1-to-1 relationship

between coverage and connectivity does not exist. It becomes 1-to-many. One level of EDSC can result in infinite levels of EDP as suggested by results in Figure 5.11. Hence, it can be postulated that when the sensing and communication models are not both binary as in the case for this dissertation, the coverage and SC have to be analyzed separately. One cannot automatically use the relationship or the ratio of the sensing and communication ranges to determine the level of SC by the level of coverage. There are no clear relationships between the sensing coverage level and the SC level when the sensing and communication models are different.

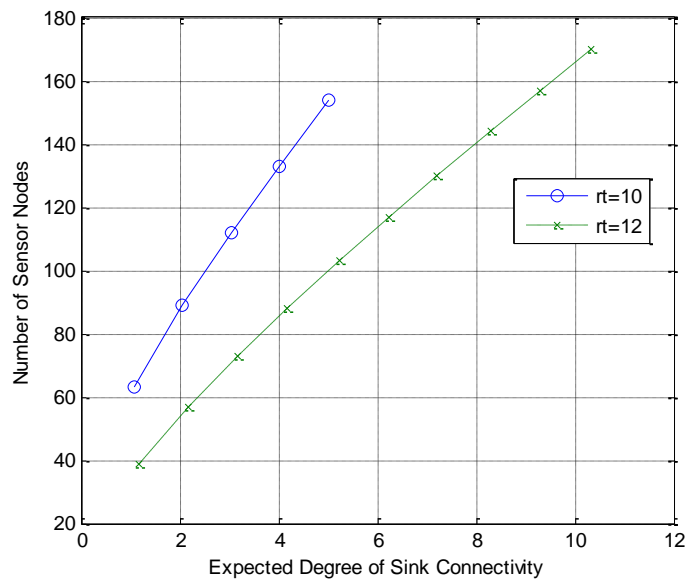


Figure 5.9. EDSC vs number of deployed SNs for DA 40x40 with  $r_t = 10, 12$ .

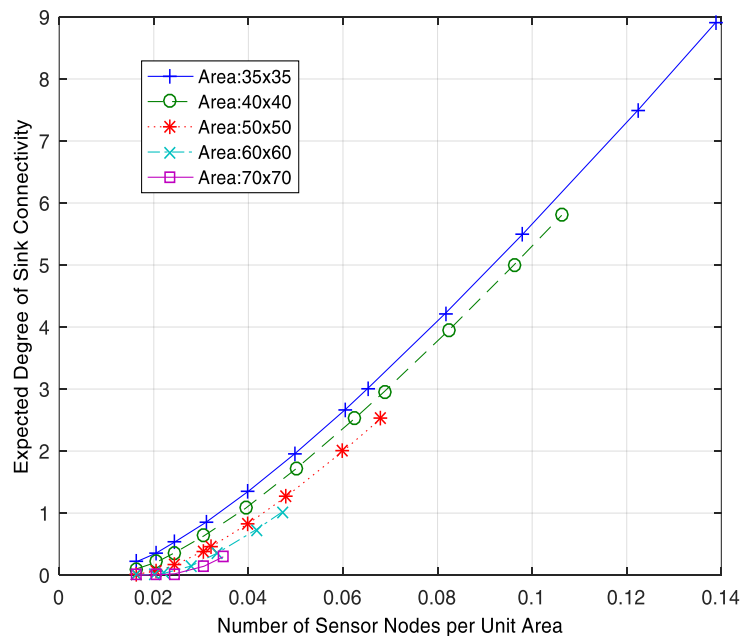


Figure 5.10. EDSC vs ND for various DA sizes with  $r_t = 10$ .

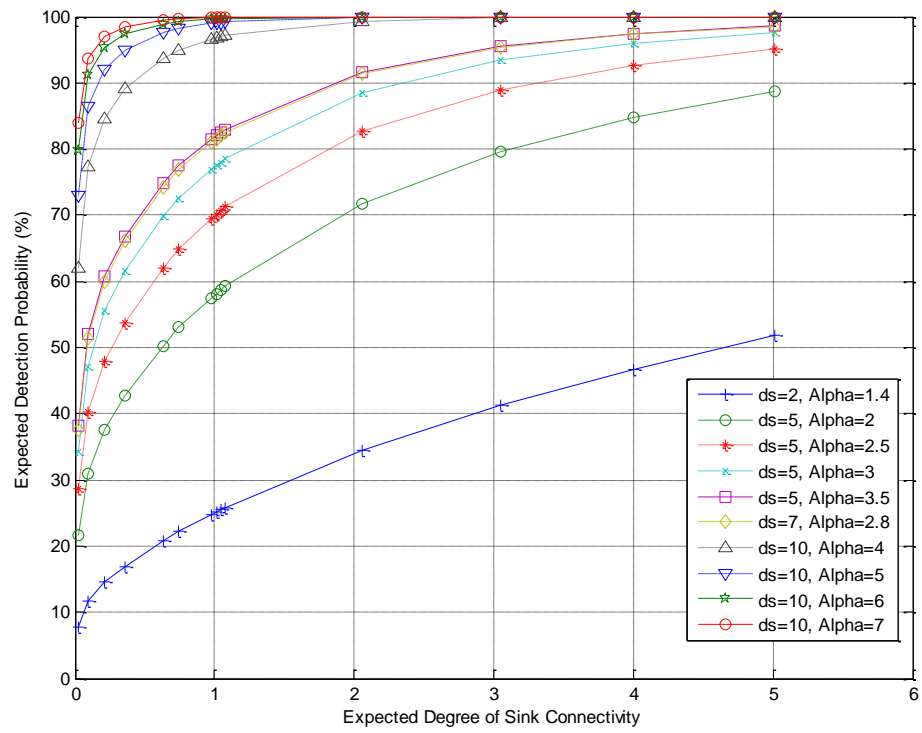


Figure 5.11. EDP vs EDSC for DA 40x40 with  $r_t = 10$  and various values of  $d_s$  and  $\alpha_s$ .



## CHAPTER 6

### Conclusions, Limitations, and Future Work

This dissertation derives two analytical or mathematical models, one for the expected probabilistic detection coverage and the other one is for the expected sink connectivity degree in WSNs for SNs that cannot directly transmit to the sink. Unlike prior joint coverage and connectivity analysis for WSNs, the research work in this dissertation is based on a probabilistic sensing model, while the connectivity model is binary. This dissertation also focuses on a finite number of homogeneous SNs that are uniformly distributed at random in a finite DA. It is more practical than the asymptotic assumption previously normally used in previous WSN coverage and connectivity studies. The models are derived by taking the border effects into account as comprehensive as possible and based on order stats, expectation and probability calculations. Chapter 2 presents an overview of sensor placement in WSNs and its impacts on various aspects of WSN performance. Then an overview of related research in wireless sensor placement and a survey of current sensing coverage and connectivity analyses are presented. Chapter 3 derives the EDSC, while Chapter 4 presents the derivation of the EDP at any AP in the DA. Chapter 5 shows the verification of both derived models with numerical results from simulations, then discusses findings from the results from the models including the applications in which the proposed models can be utilized. The rest of this chapter will summarize the overall major findings from this research, and discuss the limitations of the proposed models, and some possible future work based on this dissertation.

#### 6.1 Conclusions

Overall contributions and findings of this dissertation are as follows.

1. In derivations of both models, a careful consideration of geometry and its implications in finding the CDF of each related parameters in the model is necessary in achieving accurate models.
2. To achieve precise models, all border effects must be taken into account in order for the models to be exact for all scenarios.
3. Every little approximation made in the derivation of the models does have impact on their accuracy. The magnitude of the impacts depends on the scenarios in which the models are applied.
4. The models derived in the dissertation can still achieve high accuracy thanks to careful consideration of border effects and judicious approximations. Its accuracy is within around 2.5 percent of the simulation results, and in pragmatic scenarios the discrepancies can be close to zero.
5. The proposed models are best suited for clustered networks in

DA with appropriate sizes relative to the transmission range of the SNs. From the results, the appropriate ratio of the dimension of the square deployment area to the transmission range,  $r_t$ , is about 4.

6. The EDP model can be applicable for any other probabilistic sensing models that are functions of  $r$ .

7. The related parameters for desired degrees of coverage and connectivity can be estimated from graphs.

8. Unlike most other works on joint coverage and connectivity analysis, ours can be used to compute the coverage and connectivity separately thanks to the models that are based on different sensing and communication models.

9. This work also shows that when the sensing and communication models are not both the binary disk model, the relationship between the sensing and communication ranges cannot indicate the connectivity from the coverage.

10. The models in this dissertation can be utilized in uncoordinated node scheduling schemes to find the active-to-sleep ratio for each SN, fault tolerance and traffic congestion analysis of networks, and optimizing the deployment cost.

11. Node density is what determines the level of the probabilistic sensing coverage, and as the number of deployed SNs increases, the smaller the increase of the level of coverage.

12. Node density also controls EDSC regardless of the size of the DA.

13. For the EDSC, the first degree of sink connectivity requires the highest number of SNs. The subsequent degree will require fewer and later be almost a constant, suggesting that previously placed SNs help make the connectivity for the later deployed SNs easier.

## 6.2 Limitations

Both the proposed models contain integrands that so far cannot be reduced to closed form expressions. As a result, the reverse functions of both models are yet to exist. Accordingly, in order to find specific values of input parameters such as the number of deployed SNs needed for a specific level of expected detection coverage and expected degree of sink connectivity, one has to use graphs such as those in **Error! Reference source not found.** and **Error! Reference source not found.**. Also if the computer used to compute the numerical values from both models are not powerful enough, it can then only compute the values up to a certain number of deployed SNs. The reason is because of the factorial computation of the number of deployed SNs. As in the case of this dissertation, it is limited to 170.

## 6.3 Future Work

The work in this dissertation could serve as another piece in the foundation of other future related works in trying to analyze coverage and connectivity from random SN deployments in other scenarios. In the future, if it becomes financially feasible and sensors based on the probabilistic sensing model assumed in this dissertation are available, the investigations into various test-bed experiments in a number of interesting real-life scenarios could be conducted. Also, the proposed concept of deployment cost optimization based on this function,  $\max_{N_i} [\min_{N_i} EPD \geq S_{min}, \min_{N_i} EDSC \geq C_{min}]$ , as mentioned in section 5.7 could be investigated in more detail.

## Bibliography

- [1] A. Ghosh and S. Das, "Coverage and Connectivity Issues in Wireless Sensor Networks: A Survey," *Pervasive and Mobile Computing*, vol. 4, no. 3, pp. 303-334, 2008.
- [2] H. P. Gupta, S. V. Rao and V. Tamarapalli, "Analysis of Stochastic k-Coverage and Connectivity in Sensor Networks With Boundary Deployment," *IEEE Trans Intelligent Transportation Systems*, vol. 16, no. 4, pp. 1861-1871, 2015.
- [3] M. H. e. al, "A Wireless Sensor Network Border Monitoring System: Deployment Issues and Routing Protocols," *IEEE Sensors Journal*, vol. 17, no. 8, pp. 2572-2582, 2017.
- [4] L. Yen, C. Yu and Y. Cheng, "Expected k-Coverage in Wireless Sensor Networks," *Ad Hoc Networks*, vol. 4, no. 5, pp. 636-650, 2006.
- [5] H. Gupta, S. Rao and T. Venkatesh, "Critical Sensor Density for Partial Coverage under Border Effects in Wireless Sensor Networks," *IEEE Trans. Wireless Communications*, vol. 13, no. 5, pp. 2374-2382, 2014.
- [6] L. Laranjeira and G. N. Rodrigues, "Border Effect Analysis for Reliability Assurance and Continuous Connectivity of Wireless Sensor Networks in the Presence of Sensor Failures," *IEEE Trans Wireless Communications*, vol. 13, no. 8, pp. 4232-4246, 2014.
- [7] Y. Tsai, "Sensing Coverage for Randomly Distributed Wireless Sensor Networks in Shadowed Environments," *IEEE Trans. Vehicular Technology*, vol. 57, no. 1, pp. 556-564, 2008.
- [8] Q. Wu, N. Rao, X. Du, S. Iyengar and V. Vaishnavi, "On Efficient Deployment of Sensors on Planar Grid," *Computer Communications*, vol. 30, no. 14-15, pp. 2721-2734, 2007.
- [9] A. Tripathi, H. P. Gupta, T. Dutta, R. Mishra, K. K. Shukla and S. Jit, "Coverage and Connectivity in WSNs: A Survey, Research Issues and Challenges," *IEEE Access*, vol. 6, pp. 26971-26992, 2018.
- [10] A. Shan, X. Xu, Z. Cheng and W. Wang, "A Max-Flow Based Algorithm for Connected Target Coverage with Probabilistic Sensors," *Sensors*, vol. 17, no. 6, 2017.
- [11] M. Thai, F. Wang, D. Du and X. Jia, "Coverage Problems in Wireless Sensor Networks: Designs and Analysis," *Int'l Journal Sensor Networks*, vol. 3, no. 3, pp. 191-200, 2008.

- [12] S. Habib and M. Safar, "Sensitivity Study of Sensors Coverage within Wireless Sensor Networks," in *Proceedings of 16th Inter. Conf. on Computer Communications and Networks*, 2007.
- [13] D. B. Jordan and O. L. d. Weck, "Layout Optimization for a Wireless Sensor Network Using a Multi-Objective Genetic Algorithm," in *IEEE 59th Vehicular Technology Conf.*, 2004.
- [14] M. Dhanaraj and C. S. R. Murthy, "On Achieving Maximum Network Lifetime Through Optimal Placement of Cluster-heads in Wireless Sensor Networks," in *IEEE Inter. Conf. on Communications 2007*, 2007.
- [15] Q. Wang, K. Xu, G. Takahara and H. Hassanein, "Device Placement for Heterogeneous Wireless Sensor Networks: Minimum Cost with Lifetime Constraints," *IEEE trans. on wireless communications*, pp. 2444-2453, 2007.
- [16] S. Pandey, S. Dong, P. Agrawal and K. Sivalingam, "A Hybrid Approach to optimize Node Placements in Hierarchical Heterogeneous Networks," in *IEEE Wireless Communications and Networking Conf.*, 2007.
- [17] S. Chaudhry, V. Hung and R. Guha, "Optimal Placement of Wireless Sensor Nodes with Fault Tolerance and Minimal Energy Consumption," in *IEEE Inter. Conf. on Mobile Adhoc and Sensor Systems*, 2006.
- [18] M. Patel, R. Chandrasekaran and S. Venkatesan, "Energy Efficient Sensor, Relay and Base Station Placements for Coverage, Connectivity and Routing," in *IEEE 24th Performance, Computing, and Communications Conference*, 2005.
- [19] S. Dhillon and K. Chakrabarty, "Sensor Placement for Effective Coverage and Surveillance in Distributed Sensor Networks," *IEEE Wireless Communications and Networking*, vol. 3, pp. 1609-1614, 2003.
- [20] R. Stolkin and I. Florescu, "Probability of Detection and Optimal Sensor Placement for Threshold Based Detection Systems," *IEEE Sensors Journal*, vol. 9, no. 1, pp. 57-60, 2009.
- [21] L. Vickers, R. Stolkin and J. Nickerson, "Computational Environmental Models Aid Sensor Placement Optimization," in *MILCOM*, 2006.
- [22] Lin, F.Y.S. and P. Chiu, "A Near-Optimal Sensor Placement Algorithm to Achieve Complete Coverage-Discrimination in Sensor Networks," *IEEE Communications Letters*, vol. 9, no. 1, pp. 43-45, 2005.
- [23] S. Barrett, "Optimizing Sensor Placement for Intruder Detection with Genetic Algorithms," *IEEE Intelligence and Security Informatics*, pp. 185-188, 2007.

- [24] R. Mattikalli, R. Fresnedo, P. Frank, S. Locke and Z. Thunemann, "Optimal Sensor Selection and Placement for Perimeter Defense," in *IEEE Inter. Conf. on Automation Science and Engineering*, 2007.
- [25] Y. Chen, C.-N. Chuah and Q. Zhao, "Network Configuration for Optimal Utilization Efficiency of Wireless Sensor Networks," *Ad Hoc Networks*, vol. 6, no. 1, pp. 92-107, 2008.
- [26] T. Clouqueur, V. Phipatanasuphorn, P. Ramanathan and K. Saluja, "Sensor Deployment Strategy for Target Detection," in *Proceedings of the 1st ACM international workshop on Wireless sensor networks and applications*, 2002.
- [27] Q. Wang, K. Xu, G. Takahara and H. Hassanein, "Deployment for Information Oriented Sensing Coverage in Wireless Sensor Networks," in *IEEE Global Telecommunications Conference*, 2006.
- [28] N. Ahmed, S. S. Kanhere and S. Jha, "Probabilistic Coverage in Wireless Sensor Networks," in *Proc. IEEE Conf. on Local Computer Networks*, 2005.
- [29] Y. Yang and R. Blum, "Sensor Placement in Gaussian Random Field Via Discrete Simulation Optimization," *IEEE Signal Processing Letters*, vol. 15, p. 729 – 732, 2008.
- [30] M. Younis and K. Akkaya, "Strategies and techniques for node placement in wireless sensor networks: A survey," *Ad Hoc Networks*, vol. 6, no. 4, pp. 621-655, 2008.
- [31] S.-J. Park and R. Sivakumar, "Quantitative Analysis of Transmission Power Control in Wireless Ad-Hoc Network," in *Proc. Of Inter. Conf. on Parallel Processing*, 2002.
- [32] B. Chen, K. Jamieson, H. Balakrishnan and R. Morris, "Span: An Energy Efficient Coordination Algorithm for topology Maintenance in Ad Hoc Wireless Networks," *Wireless Networks*, vol. 8, no. 5, pp. 481-494, 2002.
- [33] W. Heinzelman, A. Chandrakasan and H. Balakrishnan, "Energy-efficient communication protocols for wireless sensor networks," in *Proc. 33rd Hawaii Int. Conf. Syst. Sciences*, 2000.
- [34] i. Bertsekas and R. Gallager, *Data Networks*, New Jersey: Prentice-Hall, 1992.
- [35] J. A. Manrique, J. S. Rueda-Rueda and J. M. T. Portocarrero, "Contrasting Internet of Things and Wireless Sensor Network from a Conceptual Overview," in *IEEE International Conference on Internet of Things (iThings) and IEEE Green Computing and Communications (GreenCom) and IEEE Cyber*,

*Physical and Social Computing (CPSCoM) and IEEE Smart Data (SmartData)*, Chengdu, 2016.

- [36] A. Konstantinidis and K. Yang, "Multi-objective energy-efficient dense deployment in Wireless Sensor Networks using a hybrid problem-specific MOEA/D," *Applied Soft Computing*, vol. 11, no. 6, pp. 4117-4134, 2011.
- [37] J. Tang, B. Hao and A. Sen, "Relay node placement in large scale wireless sensor networks," *Computer Communications*, vol. 29, no. 4, pp. 490-501, 2006.
- [38] A. Bari, A. Jaekel and S. Bandyopadhyay, "Optimal Placement of Relay Nodes in Two-Tiered, Fault Tolerant Sensor Networks," in *IEEE Symposium Computers and Communications*, 2007.
- [39] S. Misra, S. D. Hong, G. Xue and J. Rang, "Constrained relay node placement in wireless sensor networks: formulation and approximations," *IEEE/ACM Transactions on Networking*, vol. 18, no. 2, pp. 434-447, 2010.
- [40] F. Dai and J. Wu, "On constructing k-connected k-dominating set in wireless ad hoc and sensor networks," *Journal of Parallel and Distributed Computing*, vol. 66, no. 7, pp. 947-958, 2006.
- [41] M. T. Thai, N. Zhang, R. Tiwari and X. Xu, "On approximation algorithms of k-connected m-dominating sets in disk graphs," *Theoretical Computer Science*, vol. 385, no. 1-3, pp. 49-59, 2007.
- [42] X. Bai, D. Xuan, Z. Yun, T. Lai and W. Jia, "Complete optimal deployment patterns for full-coverage and k-connectivity ( $k \leq 6$ ) wireless sensor networks," in *Proceedings of the 9th ACM Inter Symposium on Mobile ad hoc networking and computing*, Hong Kong, 2008.
- [43] D. Li, J. Cao, D. Liu, Y. Yu and H. Sun, "Algorithms for the m-coverage problem and k-connected m-coverage problem in wireless sensor networks," *Network and Parallel Computing, Lecture Notes in Computer Science*, vol. 4672, pp. 250-259, 2007.
- [44] C. Huang, Y. Tseng and H. Wu, "Distributed Protocols for Ensuring Both Coverage and Connectivity of a Wireless Sensor Network," *ACM Trans. Sensor Networks*, vol. 3, no. 1, 2007.
- [45] X. Chen, H. Bai, L. Xia and Y.-C. Ho, "Design of a randomly distributed sensor network for target detection," *Automatica*, vol. 43, no. 10, pp. 1713-1722, 2007.
- [46] P. Medagliani, J. Leguay, G. Ferrari, V. Gay and M. Lopez-Ramos, "Energy-Efficient Mobile Target Detection in Wireless Sensor Networks with Random

- Node Deployment and Partial Coverage," *Pervasive and Mobile Computing*, vol. 8, no. 3, pp. 429-447, 2012.
- [47] S. Kumar, T. Lai and J. Balogh, "On k-Coverage in a Mostly Sleeping Sensor Network," *Wireless Networks*, vol. 14, no. 3, pp. 277-294, 2008.
- [48] H. Ammari and S. Das, "A Study of k-Coverage and Measures of Connectivity in 3D Wireless Sensor Networks," *IEEE Trans. Computers*, vol. 59, no. 2, pp. 243-257, 2010.
- [49] P. Balister, B. Bollobas, A. Sarkar and S. Kumar, "Reliable Density Estimates for Coverage and Connectivity in Thin Strips of Finite Length," in *Proc. 13th ACM Int'l Conf. Mobile Computing and Networking*, 2007.
- [50] M. Donmez, R. Kosar and C. Ersoy, "An Analytical Approach to the Deployment Quality of Surveillance Wireless Sensor Networks Considering the Effect of Jammers and Coverage Holes," *Computer Networks*, vol. 54, no. 18, pp. 3449-3466, 2010.
- [51] A. Hossain, S. Chakrabarti and P. K. Biswas, "Impact of Sensing Model on Wireless Sensor Network Coverage," *Wireless Sensor Systems, IET*, vol. 2, no. 3, pp. 272-281, 2012.
- [52] M. Karakaya and H. Qi, "Coverage Estimation for Crowded Targets in Visual Sensor Networks," *ACM Trans. Sensor Networks*, vol. 8, no. 3, 2012.
- [53] L. Lazos, R. Poovendran and J. Ritcey, "Analytic Evaluation of Target Detection in Heterogeneous Wireless Sensor Networks," *ACM Trans. Sensor Networks*, vol. 5, no. 2, pp. 1-38, 2009.
- [54] Y.-T. Lin, S. K.K. and M. S., "Adaptive cost efficient deployment strategy for homogeneous wireless camera sensors," *Ad Hoc Networks*, vol. 9, no. 5, pp. 713-726, 2011.
- [55] T. Liu, Z. Li, X. Xia and S. Luo, "Shadowing Effects and Edge Effect on Sensing Coverage for Wireless Sensor Networks," in *Proc. 5th Int'l Conf. Wireless Communications, Networking and Mobile Computing*, 2009.
- [56] R. Machado, W. Zhang, G. Wang and S. Tekinay, "Coverage Properties of Clustered Wireless Sensor Networks," *ACM Trans. Sensor Networks*, vol. 7, no. 2, 2010.
- [57] A. Newell, K. Akkaya and E. Yildiz, "Providing Multi-Perspective Event Coverage in Wireless Multimedia Sensor Networks," in *In Proceedings of 35th Conference on Local Computer Networks*, 2010.



- [58] C. Qian and H. Qi, "Coverage Estimation in the Presence of Occlusions for visual sensor networks," in *Proc. 4th IEEE Int'l Conf. Distributed Computing in Sensor Systems*, 2008.
- [59] P. Wan and C. Yi, "Coverage by Randomly Deployed Wireless Sensor Networks," *IEEE Trans. Information Theory*, vol. 52, no. 6, pp. 2658-2669, 2006.
- [60] G. Xing, R. Tan, B. Liu, J. Wang, X. Jia and C. Yi, "Data Fusion Improves the Coverage of Wireless Sensor Networks," in *Proc. 15th ACM Int'l Conf. Mobile Computing and Networking*, 2009.
- [61] X. Xing, G. Wang, J. Wu and J. Li, "Square Region-Based Coverage and Connectivity Probability Model in Wireless Sensor Networks," in *Proc. 5th Int'l Conf. Collaborative Computing: Networking, Applications and Worksharing*, 2009.
- [62] X. Xu, Z. Dai, A. Shan and T. Gu, "Connected Target  $\epsilon$ -probability Coverage in WSNs With Directional Probabilistic Sensors," *IEEE Systems Journal*, vol. 14, no. 3, pp. 3399-3409, 2020.
- [63] N. Rai and R. Daruwala, "Node density optimisation using composite probabilistic sensing model in wireless sensor networks," *IET Wireless Sensor Systems*, vol. 9, no. 4, pp. 181-190, 2019.
- [64] P. Sun and A. Boukerche, "Modeling and Analysis of Coverage Degree and Target Detection for Autonomous Underwater Vehicle-Based System," *IEEE Transactions on Vehicular Technology*, vol. 67, no. 10, pp. 9959-9971, 2018.
- [65] X. Li, D. Hunter and S. Zuyev, "Coverage Properties of the Target Area in Wireless Sensor Networks," *IEEE Trans. Information Theory*, vol. 58, no. 1, pp. 430-437, 2012.
- [66] N. Mohamed, J. Al-Jaroodi and I. Jawhar, "Modeling the Performance of Faulty Linear Wireless Sensor Networks," *Int'l Journal of Distributed Sensor Networks*, 2014.
- [67] S. He, J. Chen and Y. Sun, "Coverage and Connectivity in Duty-Cycled Wireless Sensor Networks for Event Monitoring," *IEEE Trans. Parallel and Distributed Systems*, vol. 23, no. 3, pp. 475-482, 2012.
- [68] C. Komar, M. Donmez and C. Ersoy, "Detection Quality of Border Surveillance Wireless Sensor Networks in the Existence of Trespassers' Favorite Paths," *Computer Communications*, vol. 35, no. 10, pp. 1185-1199, 2012.

- [69] R. Tan, G. Xing, B. Liu, J. Wang and X. Jia, "Exploiting Data Fusion to Improve the Coverage of Wireless Sensor Networks," *IEEE/ACM Trans. Networking*, vol. 20, no. 2, pp. 450-462, 2012.
- [70] L. Liu, X. Zhang and H. Ma, "Localization-Oriented Coverage in Wireless Camera Sensor Networks," *IEEE Trans Wireless Communications*, vol. 10, no. 2, pp. 484-494, 2011.
- [71] F. Xue and P. Kumar, "The Number of Neighbors Needed for Connectivity of Wireless Networks," *Wireless Networks*, vol. 10, no. 2, pp. 169-181, 2004.
- [72] C. Bettstetter and C. Hartmann, "Connectivity of Wireless Multihop Networks in a Shadow Fading Environment," *Wireless Networks*, vol. 11, no. 5, pp. 571-579, 2005.
- [73] H. Ammari and S. Das, "Integrated Coverage and Connectivity in Wireless Sensor Networks: A Two-Dimensional Percolation Problem," *IEEE Trans. Computers*, vol. 57, no. 10, pp. 1423-1434, 2008.
- [74] H. Ammari and S. Das, "Critical Density for Coverage and Connectivity in Three-Dimensional Wireless Sensor Networks Using Continuum Percolation," *IEEE Trans. Parallel and Distributed Systems*, vol. 20, no. 6, pp. 872-885, 2009.
- [75] S. Carruthers and V. King, "Connectivity of Wireless Sensor Networks with Constant Density," in *Proc. Ad-hoc, Mobile, and Wireless Networks*, 2004.
- [76] T. Kim, D. Tipper and P. Krishnamurthy, "Connectivity and Critical Point Behavior in Mobile Ad Hoc and Sensor Networks," in *Proc. IEEE Symp. Computers and Communications*, 2009.
- [77] L. Guo, H. Xu and K. Harfoush, "The Node Degree for Wireless Ad Hoc Networks in Shadow Fading Environments," in *Proc. 6th IEEE Conf. Industrial Electronics and Applications*, 2011.
- [78] V. A. Aalo and C. Mukasa, "Impact of interference on the coverage and connectivity of Ad hoc networks in a fading environment," *AEU-Int'l Journal of Electronics and Communications*, vol. 69, no. 8, pp. 1094-1101, 2015.
- [79] K. M. Mridula and P. M. Ameer, "Connectivity at wireless network borders under superimposed fading-shadowing effects," in *TENCON 2017 - 2017 IEEE Region 10 Conference*, 2017.
- [80] K. M. Mridula and P. M. Ameer, "Three-dimensional sensor network connectivity considering border effects and channel randomness with

- application to underwater networks," *IET Communications*, vol. 12, no. 8, pp. 994-1002, 2018.
- [81] X. Ta, G. Mao and B. Anderson, "On the Connectivity of Wireless Multihop Networks with Arbitrary Wireless Channel Models," *IEEE Communications Letters*, vol. 13, no. 3, pp. 181-183, 2009.
- [82] B. Xu, Q. Zhu and H. Hu, "Analysis of Connectivity in Ad-hoc Network Based on Interference and Fading Channel," *The Journal of China Universities of Posts and Telecommunications*, vol. 19, no. 5, pp. 77-82, 2012.
- [83] S. Bermudez and S. Wicker, "Connectivity of Finite Wireless Networks with Random Communication Range Nodes," in *Proc. IEEE Int'l Conf. Communications*, 2009.
- [84] F. Al-Turjman, H. Hassanein and M. Ibnkahla, "Quantifying Connectivity in Wireless Sensor Networks with Grid-based Deployments," *Journal of Network and Computer Applications*, vol. 36, no. 1, pp. 368-377, 2013.
- [85] Z. Sun, I. Akyildiz and G. Hancke, "Dynamic Connectivity in Wireless Underground Sensor Networks," *IEEE Trans Wireless Communications*, vol. 10, no. 12, pp. 4334-4344, 2011.
- [86] N. Saeed, A. Celik, M. Alouini and T. Y. Al-Naffouri, "Performance Analysis of Connectivity and Localization in Multi-Hop Underwater Optical Wireless Sensor Networks," *IEEE Transactions on Mobile Computing*, vol. 18, no. 11, pp. 2604-2615, 2019.
- [87] S. Pang, X. Hu, Q. Gao, Y. Li and Y. Xia, "Accurate Analysis of Connectivity and Resilience for a Class of Wireless Sensor Networks," *Chinese Journal of Electronics*, vol. 29, no. 2, pp. 208-219, 2020.
- [88] S. Khasteh, S. Shouraki, N. Hajiabdorahim and E. Dadashnialehi, "A New Approach for Integrated Coverage and Connectivity in Wireless Sensor Networks," *Computer Communications*, vol. 36, no. 1, pp. 113-120, 2012.
- [89] J. Li, L. Kang, Y. h. Zhang, X. Li and C. Wang, "On Critical Density for Coverage and Connectivity in Directional Sensor Network Using Continuum Percolation," in *IEEE 82nd Vehicular Technology Conference*, 2015.
- [90] M. Khanjary, M. Sabaei and M. R. Meybodi, "Critical density for coverage and connectivity in two-dimensional fixed-orientation directional sensor networks using continuum percolation," *Journal of Network and Computer Applications*, vol. 57, pp. 169-181, 2015.

- [91] H. P. Gupta, S. Rao and T. Venkatesh, "Analysis of stochastic coverage and connectivity in three-dimensional heterogeneous directional wireless sensor networks," *Pervasive and Mobile Computing*, vol. 29, pp. 38-56, 2016.
- [92] M. H. e. al., "A Wireless Sensor Network Border Monitoring System: Deployment Issues and Routing Protocols," *IEEE Sensors Journal*, vol. 17, no. 8, pp. 2572-2582, 2017.
- [93] S. N. Alam and Z. J. Haas, "Coverage and connectivity in three-dimensional networks with random node deployment," *Ad Hoc Networks*, vol. 34, pp. 157-169, 2015.
- [94] L. Vieira, M. G. Almiron and A. Loureiro, "Link probability, node degree and coverage in three-dimensional networks," *Ad Hoc Networks*, vol. 37, pp. 153-159, 2016.
- [95] C. Khatri, "Distributions of Order Statistics for Discrete Case," *Annals of the Institute of Statistical Mathematics*, vol. 14, no. 1, pp. 167-171, 1962.